1994

The Roles Ofmrna Stability And Secondary Structure In The Differential Expression Of The Escherichia Coliunc Genes

Ashok M. Patel

THE ROLES OF mRNA STABILITY AND SECONDARY STRUCTURE IN THE DIFFERENTIAL EXPRESSION OF THE *ESCHERICHIA COLI unc* GENES

by

Ashok M. Patel

Department of Biochemistry

Submitted in partial fulfilment
of the requirements for the degree of
Doctor of Philosophy

Faculty of Graduate Studies
The University of Western Ontario
London, Ontario
August 1994

ISBN 0-315-93202-3

ABSTRACT

The genes of the *Escherichia coli unc* operon are differentially expressed according to the subunit requirements in the mature F_1F_0-ATPase complex. The experiments described in this thesis were designed to elucidate how mRNA processing, degradation, and structure regulate the differential expression of the *unc* genes. Studies were focused on the *uncBE* region, near the 5′ end of the transcript, and the *uncDC* region at the 3′ end of the transcript.

Northern blot analysis of *uncC* mRNA, the last gene of the operon, suggested that the *unc* transcription terminator protected the *uncC* message against exonucleolytic degradation, and that this stabilization was important in adequate synthesis of its gene product, the ϵ subunit.

Northern blot and primer extension analysis of plasmid-encoded *uncDC* mRNA identified an RNase E-dependent endonucleolytic cleavage site 11 bases into the *uncC* coding region. This cleavage led to functional inactivation of the *uncC* mRNA and the upstream *uncD* mRNA, and consequently does not contribute to the differential relative expression of these genes.

A potential stem-loop structure 16 bases downstream of the *uncC* initiation codon, and 6 bases downstream of the aforementioned RNase E site, was subjected to site-directed mutagenesis to explore its significance in the RNase E-dependent cleavage, and in regulating the *uncC* expression. Results indicated that the structure was indispensable to the cleavage by RNase E, while the bases around the actual site were not so crucial. The expression studies uncovered a critical dependence of the stem-loop position in modulating the expression of *uncC*. The *uncC* expression was enhanced when the stem-loop was shifted downstream from the *uncC* ribosome binding site while moving it closer resulted in reduced expression of *uncC*. The

results imply that the stem-loop provides steric hindrance to the binding of the ribosome and hence limits *uncC* expression.

Northern blot analysis of chromosomally-encoded *unc* mRNA indicated that its 5′ region also underwent RNase E-dependent processing. Northern blots of mRNA expressed from a plasmid carrying the *uncBE* genes from the 5′ region of the operon revealed that the *uncB* message was rapidly degraded by multiple internal cleavages, some dependent on functional RNase E. Primer extension analysis showed that the cleavages were made either in the *uncB* coding region or in the intercistronic region between *uncB* and *uncE*, the latter being the most 3′ cleavage. The rapid degradation of *uncB* message through cleavages at these sites provides a mechanism for segmental decay of *unc* mRNA to contribute to the differential expression of the *unc* genes.

ACKNOWLEDGEMENTS

It is a great pleasure for me to express my personal gratitude and heartfelt thanks to Dr. S. D. Dunn for his inspiring guidance, unflagging optimism, constructive criticism, and unending encouragement throughout the course of this work.

I offer my special thanks to Dr. G. A. Mackie for his help and interest in my project. I also extend my sincere thanks to Dr. Ebisuzaki for his participation in my advisory committee. I would also like to thank all the faculty members of the biochemistry department, especially to Dr. B. D. Sanwal for his encouragement.

I thank Garry Dallmann and Faye Males for their help and friendship. I also thank the past and present members of this lab: Jia, Hans, and Eileen for putting up with me. I dearly appreciate the cooperation of the staff members, Maureen, Barb, Ruth and Ted.

I thank my friends Natubhai & Ramaben, Ravi & Bhawana, Sudhir & Usha, Vijay & Ragina for making my stay in London enjoyable.

The single largest contribution in shaping what I am today comes from the faith, hope, and pride of my father, brothers & sister in-laws, sisters and my wife, Asha. It is their love which kept me going and words would fail to express my feelings of indebtness to them. I, therefore, offer my sincere silent words of acknowledgement to them.

This thesis is dedicated to my father

&

In the sweet memories of my mother

TABLE OF CONTENTS

LIST OF FIGURES

LIST OF TABLES

LIST OF APPENDICES

LIST OF ABBREVIATIONS

ADP	Adenosine 5'-diphosphate
ATP	Adenosine 5'-triphosphate
bp	base pair
BSA	Bovine serum albumen
°C	Degree Celsius
CTP	Cytidine 5'-triphosphate
DEPC	Diethyl pyrocarbonate
DNA	Deoxyribonucleic acid
dNTP	deoxynucleotide triphosphate
DTT	Dithiothreitol
EDTA	Ethylenediaminetetraacetic acid
F_1 or F_1-ATPase	The peripheral portion of the proton translocating ATPase
F_0	The integral membrane portion of the translocating ATPase
GTP	Guanosine 5'-triphosphate
IPTG	Isopropyl β-D-thiogalactopyranoside
kb	Kilo base
LB medium	Luria-Bertani medium
M-MLV	Moloney-Murine Luekemia virus
mRNA	messenger ribonucleic acid
NTP	deoxynucleotide triphosphate
RBS	Ribosome binding site
rRNA	ribosomal ribonucleic acid
RNA	Ribonucleic acid
RNase	Ribonuclease
S-D	Shine-Dalgarno
SDS	Sodium dodecyl sulphate
SDS-PAGE	SDS-polyacrylamide gel electrophoresis
TBE buffer	Tris-Borate-EDTA buffer
TIR	Translation initiation region
Tris	Tris(hydroxymethyl) aminomethane
Tricine	N-tris(hydroxymethyl)-methyglycine

CHAPTER 1

GENERAL INTRODUCTION

1.1 OVERVIEW

The proton-translocating ATP synthase (F_1F_0 - ATP synthase) of *Escherichia coli* plays a pivotal role in the process of oxidative phosphorylation. It couples the translocation of protons across the membrane to ATP synthesis/hydrolysis. Structurally similar proton translocating ATPases are also found in the mitochondrial inner membranes and chloroplast thylakoid membranes (Senior, 1988; Boyer, 1989; Walker *et al.*, 1990; Penefsky and Cross, 1991; Boyer, 1993). These enzymes catalyse the terminal reaction in oxidative phosphorylation, the synthesis of ATP from ADP and inorganic phosphate, coupled to the H^+ gradient generated by respiratory or light-driven electron transport. The reaction catalyzed by the ATPases is reversible so that ATP can be hydrolysed to create an electrochemical proton gradient, which can be used for other cellular processes such as active transport and flagellar rotation.

The ATP produced by the F_1F_0-ATPase of *E. coli* is the main source of ATP under aerobic conditions The enzyme produces one ATP molecule per three protons transferred across the membrane (review by Cross *et al.*, 1984). *E. coli* strains which are defective in F_1F_0 activity cannot grow on non-fermentable carbon sources such as succinate and acetate since they are incapable of oxidative phosphorylation (Cox *et al.*, 1979). Such strains, however, are capable of growing on glucose since it can undergo glycolysis which generates ATP.

The *E. coli* F_1F_0-ATP synthase is composed of two distinct sectors (Fig. 1.1). The F_0 sector, which acts as a proton channel, is composed of three integral membrane proteins. These three subunits, designated *a*, *b*, and *c*, are present in a

Figure 1.1 A model for the arrangement of subunits in *E. coli* F_1F_0-ATPase. The diagram represents a side-view of the ATPase embedded in the inner membrane. This model was taken from the Ph.D. thesis of Garry Dallmann, University of Western Ontario (1993).

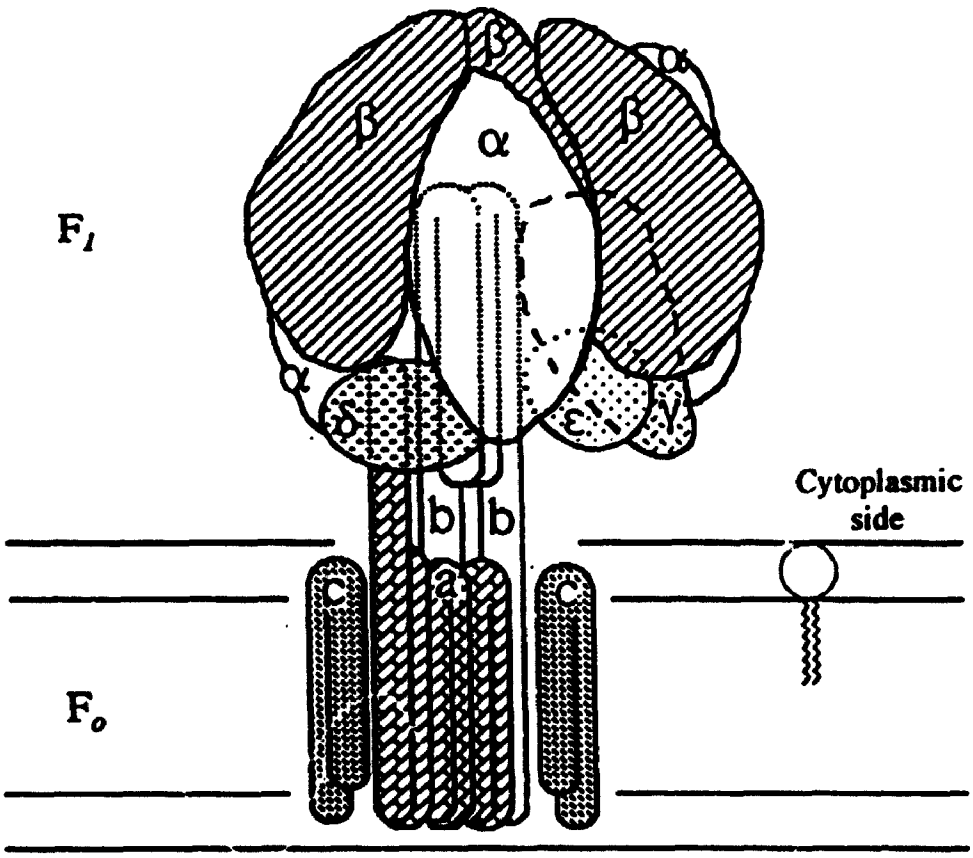
β
α
β
α
β
α
F_1
δ
ε
γ
Cytoplasmic side
b
b
c
a
c
F_o

stoichiometry of $a_1 b_2 c_{9\text{-}15}$ (Foster and Fillingame, 1982) in a mature ATPase complex. The F_1 sector of the enzyme which has the catalytic site for ATP synthesis/hydrolysis is peripheral to the membrane and is comprised of five types of subunits, α, β, γ, δ, and ϵ. These subunits are named according to their size, and are present in a stoichiometry of $\alpha_3\beta_3\gamma\delta\epsilon$ (Foster and Fillingame, 1982). The enzymes from all the sources are similar in the subunit composition and in the overall structure (reviewed by Walker *et al.*, 1990).

The *E. coli* F_1 sector can be removed from the membrane under conditions of low ionic strength, and this soluble form has uncoupled cytoplasmic ATPase activity. The β subunit is believed to contain the catalytic site for ATP synthesis and hydrolysis, although α can also bind nucleotides. The *E. coli* γ subunit is required for *in vitro* reconstitution of a minimal functional ATPase unit consisting of $\alpha_3\beta_3\gamma$ (Dunn and Futai, 1980). Both the δ and ϵ subunits are required for binding of F_1 to the F_0 sector in the membrane. The smallest subunit, ϵ, is also known to be a noncompetitive inhibitor of soluble F_1-ATPase (Sternweis and Smith, 1980).

Subunits *a* and *c* are essentially hydrophobic and are embedded in the membrane, and play roles in proton conduction. A polar loop region of the *c* subunit extends into the cytoplasm and is believed to interact with F_1 (Fraga *et al.*, 1994). The *b* subunit has a small membrane-spanning hydrophobic domain, while a large hydrophillic region interacts with the F_1 sector, forming a part of the stalk attaching F_1 and F_0 (Dunn, 1992).

The structure of the *E. coli* F_1F_0-ATPase is being extensively investigated in various laboratories (Abrahams *et al.*, 1993). In a postulated model of F_1, the α and

β subunits alternate in a hexagonal array around the γ subunit. The δ and ϵ subunits are positioned asymmetrically on the surface of the hexagonal array.

1.2 Organization of the *unc* Operon

In *E. coli* all the eight subunits of the F_1F_0-ATP synthase are encoded by the genes in the *unc* operon, where *unc* stands for uncoupled (Fig. 1.2). The *unc* operon is also referred to as the *atp* operon. The *unc* genes were mapped at about 83 min on the *E. coli* chromosome (Downie *et al.*, 1979; Gibson, 1983). The operon, which is about 7-kb in length, has a constitutive promoter, nine unique open reading frames, and a *rho*-independent transcription terminator. The operon has been sequenced and the order of genes has been established as *uncIBEFHAGDC* (Fig. 1.2) (Walker *et al.*, 1984).

The product of the first gene, *uncI*, is not a part of the ATP complex and is not essential to the assembly and function of the H^+-ATPase (von Meyenburg *et al.*, 1982; Gay, 1984, Schneppe *et al.*, 1991). Its precise function is still unknown. The next three genes, namely *uncBEF*, encode the subunits of the membrane-embedded F_0 sector, *a*, *c*, and *b*, respectively. The last five genes, *uncHAGDC*, encode the F_1 subunits in the order δ, α, γ, β, ϵ. An interesting feature of the *unc* operon is that the genes are grouped according to their function. For example, all the genes for the subunits of F_0 sector are grouped, and all the genes for the subunits of F_1 sector are grouped. This type of organization into F_0 and F_1 groups is to a large extent conserved in other bacteria which contain F_1F_0-like ATPases (Cozens and Walker, 1987).

Figure 1.2 Organization of genes in the *Escherichia coli unc* operon. The nine open reading frames are shown by the boxes. The genes are labeled on the top of the boxes, and the corresponding subunits encoded are shown within the boxes. The relative amounts of each subunit synthesized is shown at the bottom. Abbreviations: P, *unc* promoter; T, *unc* transcription terminator.

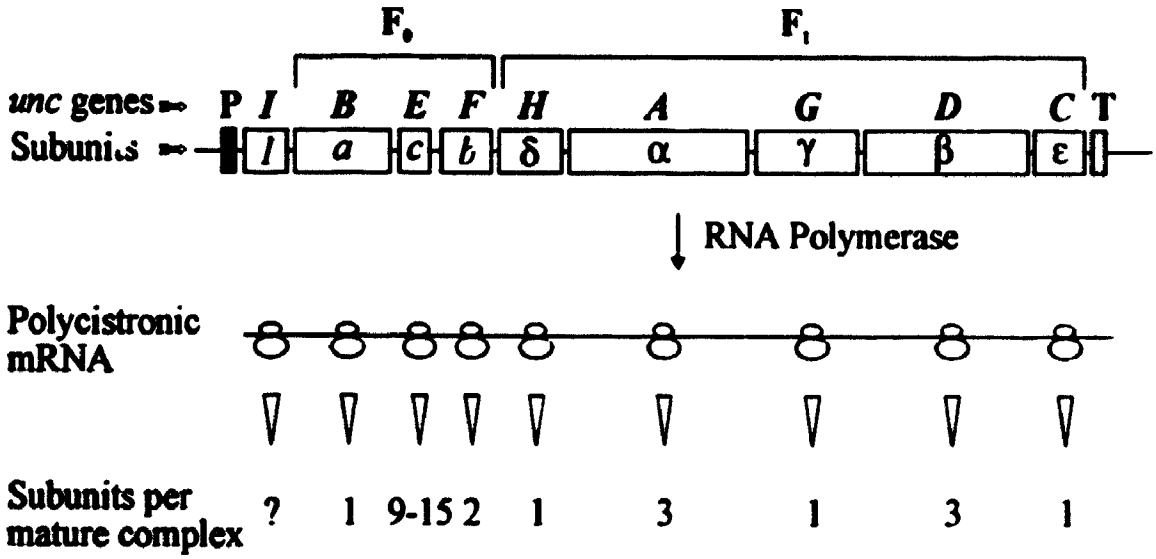
F0
F1
unc genes
P I B E F H A G D C T
Subunits
I a c b δ α γ β ε
RNA Polymerase
Polycistronic mRNA
Subunits per mature complex
? 1 9-15 2 1 3 1 3 1

The *unc* operon is interesting because its gene products interact functionally to form a complex with an irregular subunit stoichiometry. As described earlier, the stoichiometry of the subunits in a mature ATPase complex ranges from 1 to 9-15. The relative molar quantities of the subunits in *E.coli* F_1F_0-ATPase were estimated by labelling cells carrying *unc* genes on a λ transducing phage with [^{35}S]-sulfate and were found to be $ab_2c_{9-15}\alpha_3\beta_3\gamma\delta\epsilon$ (Foster and Fillangame, 1982). Thus, we have a situation where the genes are present only in single copies and are transcribed as a unit, but their gene products are required in different amounts. Studies by Brusilow *et al.* (1982) and Nielsen *et al.* (1981) have demonstrated that the subunits are in fact synthesized in relative amounts according to their final stoichiometry in the mature complex. Therefore, an important question is: **what regulates the apparent differential expression of the *unc* genes?**

Since all the genes are transcribed as a unit in a single polycistronic message, the rate of transcription cannot be responsible for the differential expression of the genes. Furthermore, there is no evidence of any significant internal promoters or premature termination of transcription within the operon. Porter *et al.* (1983) did detect two weak promoters between the major *unc* promoter and the *uncB* gene, but their importance, if any, is not known. If there was premature termination of transcription, one would then expect the earlier genes to be expressed better than the distal genes. This is not the case with the *unc* genes, rather, the genes alternate between those that are efficiently expressed and those that are poorly expressed (Fig. 1.2). One could argue that the polypeptides are made in equimolar amounts, assembled in the appropriate ratio, and the rest of the polypeptides are degraded.

However, the gene products were found to be similar in stability from *in vitro* experiments (Brusilow *et al.*, 1982), suggesting that the unequal synthesis of *unc* polypeptide cannot be explained by differential degradation of certain subunits. In addition, this type of regulation would be a waste of valuable energy for the cells, and is atypical of *E. coli*.

It is important to produce the appropriate subunits in the respective amounts; otherwise it could be harmful to the cells. For example, cells producing too much of the F_0 subunits could allow protons to leak across the membrane. Overproduction of the *a* subunit was shown to result in the inhibition of cell growth due to the increased proton conduction (Kanazawa *et al.*, 1984; von Meyenburg *et al.*, 1985). An excess of F_1 subunits on the other hand will hydrolyse the cytoplasmic ATP. The adequate expression of every gene has been shown to be important for proper function of the enzyme. Solomon and Brusilow (1988) have reported that a mutation in the ribosome binding site of *uncE* (*c* subunit) which lowers its expression affects the function of the F_0 sector. Similarly, a mutation (*uncC424*) in the *uncC* gene (ϵ subunit) which lowered its expression was shown to alter the growth properties and the enzymatic activity of the cells (Gibson *et al.*, 1977; Cox *et al.*, 1987).

These results, taken together, suggest that post-transcriptional regulation is responsible for the differential expression of the *unc* genes and that a controlled expression of the genes is essential.

1.3 Post-transcriptional Regulation

The regulation of gene expression at any stage after RNA synthesis is referred

to as post-transcriptional regulation. Over the past few years, post-transcriptional regulation of gene expression has been intensively studied, including genes that are present in operons. Although post-transcriptional regulation in *E. coli* can occur at many levels, translation initiation and mRNA stability are the two most important determinants of gene expression for genes that are located in polycistronic messages. In this thesis and related work from other laboratories, both of these factors have been shown to be important in regulating the differential expression on the *unc* genes. I shall describe these two aspect of post-transcriptional regulation first and then summarize how they have been implicated in the regulation of the *unc* genes.

1.4 Translation Initiation

Numerous studies have indicated that the intrinsic translational efficiency of the *unc* cistrons is the primary mode for achieving the differential expression of the *unc* genes (review by McCarthy, 1990). The efficiency with which a given species of mRNA is translated in *E. coli* is generally determined at the stage of translation initiation rather than elongation (Gualerzi and Pon, 1990; Jacques and Drefus, 1990). Initiation of protein synthesis in prokaryotes involves interaction of the 30S ribosomal subunit with the 5′ end of the mRNA, and the subsequent synthesis, elongation and termination of polypeptide chains. The efficiency of ribosome binding to mRNA is primarily determined by the primary and secondary structures of the mRNA in the translation initiation region (TIR) (Gold, 1988).

The rate of translation initiation to a large extent depends on variables such as the nature of the Shine-Dalgarno (S-D) sequence (Shine and Dalgarno, 1974),

initiation codon, the space between them and the choice of second codon (Gold, 1988; Ringquist *et al.*, 1992). Approximately 35 to 40 nucleotides of mRNA are bound to the ribosome (Hartz *et al.*, 1988) and this region of mRNA is called the ribosome binding site (RBS). The S-D sequences base pair with the 3' end of the 16S ribosomal RNA (rRNA) during the complex formation between the ribosome and mRNA. The affinity of the 30S subunit for the ribosome binding site (RBS) in general depends on the complementarity of the S-D sequences and the 16S rRNA, although nucleotides ranging in position from -20 to 15 could be involved in determining the overall affinity of the ribosome for RBS. Reduced complementarity of S-D sequences with the 16S rRNA has been shown to reduce expression of various genes (Gold, 1988).

Studies have indicated that AUG is the preferred initiation codon over GUG or UUG (Gold, 1988, Ringquist *et al.*, 1992). Since most *E. coli* messages have AUG as a start codon, the translation initiation is not regulated by the choice of a start codon. The relative positions of the start codon and the S-D sequences is important in positioning the anticodon with the codon. The spacing of nine nucleotides is considered to be the optimal distance for efficient translation (Gold, 1988). Other primary sequences on both sides of the S-D sequences have also been found to affect the binding of ribosomes, primarily by modulating the interaction of rRNA sequences with the mRNA (Gold, 1988).

Secondary structures within the TIR can have large effects on the rate of translation initiation. Such structures could limit the accessibility of the initiation codon for base-pairing with the initiator tRNA and the S-D sequences for base

pairing with 3' end of 16S *r*RNA (de Smit and van Duin, 1990). The presence of secondary structures has been shown to reduce the expression of genes such as the phage MS2 coat protein gene (de Smit and van Duin, 1990) and *lacZ* (Schutz and Reznikoff, 1990). Secondary structures are even more important in regulating the differential expression of genes encoded by polycistronic messages through a phenomenon called translational coupling.

1.5 Translation Coupling

Translation coupling is a phenomenon where efficient translation of a downstream gene depends on the translation of the adjacent upstream gene. Since most genes in *E. coli* are present in polycistronic mRNA, translational coupling is widely used as a mean to regulate expression of adjacent genes (McCarthy and Gualerzi, 1990). Two different types of translational coupling have been reported with respect to the translation of downstream genes by ribosomes. In the first case, the translation initiation site of the distal gene is sequestered in some kind of mRNA secondary structure and translation of the upstream gene disrupts such a structure, allowing independent translation initiation of the distal gene. Translational coupling of *E. coli rpmI* and *rplI* genes was shown to involve this type of mechanism (Lesage *et al.*, 1992). The second possibility is that the translation initiation site of the distal gene is intrinsically inefficient or masked in such a way that the translation can be achieved only by the ribosome that translated the upstream gene. This type of mechanism is generally seen for genes that have short intercistronic regions or in cases where the stop codon of the upstream gene overlaps with the start codon of a

downstream gene. The latter type of mechanism has been demonstrated to explain the translational coupling of coat gene and the lysis gene in the MS2 phage (Adhin and van Duin, 1990).

1.6 Translation Initiation and Coupling of *unc* Genes

As shown in Table 1.1, the initiation codons of all the nine genes in the *unc* operon are preceded by their own Shine-Dalgarno sequences, and the intercistronic region between each pair of genes varies. All except the *uncI* and *uncF* genes utilize AUG as a initiation codon. Although translation initiation as a means of achieving differential expression of the *unc* genes has been studied in various laboratories, most of the understanding in this field comes from the laboratories of McCarthy (Germany) and Brusilow (Wayne State University,Detroit).

The affinity of the *unc* RBS for ribosomes was studied by Schaefer *et al.* (1989) using toeprinting analysis. Toeprinting is a technique used to measure the affinity of a RBS for ribosomes by the ability of bound ribosomes to inhibit synthesis of cDNA in the primer extension analysis. These authors showed that the efficiency of ribosome binding could account for some of the differences seen in the expression of *unc* genes. The *uncI*, *uncG* and *uncC* genes, all of which are poorly expressed, did not give a toeprint signal. The authors suggested that this could be due to translational coupling in the case of *uncG* and low stability of the mRNA in the cases of *uncI* and *uncC*. In addition, Lang *et al.* (1989) also reported that the affinity of 30S ribosomal subunits correlates with the efficiency of translation initiation of the *uncE*, *uncB* and *uncG* genes. Solomon and Brusilow (1988) have characterized a

Table 1.1 Translation initiation regions of the *unc* genes. The regions from −20 to 17 are shown. The start codons are shown in bold and the most likely Shine-Dalgarno sequences are boxed. Wherever possible the stop codon of the preceding gene is also underlined. The intergenic space between the stop codon of the upstream gene and the start codon of the distal gene is also shown.

Table 1.1. Translation Initiation Regions of *unc* Genes

Genes	TIR	Intergenic Space
uncI	AUACCUCGAAGGGAGCAGGAGUGAAAAACGUGAUGUCU	
uncB	AACAAAGGGUAAAAGGCAUCAUGGCUUCAGAAAAUAUG	8
uncE	GAAACAAACUGGAGACUGUCAUGGAAAACCUGAAUAUG	46
uncF	CUAAAUAGAGGCAUUGUGCUGUGAAUCUUAACGCAACA	58
uncH	CGUUAAGGAGGGAGGGGCUGAUGUCUGAAUUUAUUACG	13
uncA	AGUCUUAAGGGGACUGGAGCAUGCAACUGAAUUCCACC	12
uncG	AAGGCAUUGAGGAGAAGCUCAUGGCCGGCGCAAAAGAG	51
uncD	UAUUUCGUAGAGGAUUUAAGAUGGCUACUGGAAAGAUU	26
uncC	CGCCUUAAUCGGAGGGUGAUAUGGCAAUGACUUACCAC	20

mutation in the *uncE* S-D sequence (G to A) which lowered the expression of *uncE* by a factor of 2-3. Mutations in the *uncC* RBS have also been demonstrated to lower expression (Gibson *et al.*, 1977; Cox *et al.*, 1987). These results reveal the significance of proper ribosome binding sites in efficient expression of the genes.

mRNAs having relatively unstructured TIRs appear to be expressed efficiently, while those having secondary structures in or around the RBS are generally less efficiently expressed (de Smit and van Duin, 1990; 1994). The importance of unstructured translation initiation regions in efficient translation was provided by McCarthy and Co-workers (1985; 1986; 1988) for the *uncE* gene. It was shown that the translation initiation region of *uncE* allows efficient translation initiation of *uncE* relative to the other *unc* genes. It was found that at least 30 bases upstream of the *uncE* initiation codon were required for efficient translation and it was suggested that this high efficiency of translation was due to relatively unstructured TIR of the *uncE* (McCarthy *et al.*, 1985). The unstructured region allows efficient 30S ribosome binding and thus better expression. When the *uncE* TIR (50 bases upstream of the initiation codon) was placed in front of the other *unc* genes or unrelated genes they observed that this region promoted efficient translation initiation (McCarthy *et al.*, 1988; Schauder and McCarthy, 1989). The *c* subunit, the gene product of the *uncE*, is the most highly expressed subunit of the ATPase complex. The above studies demonstrated that high expression of *uncE* was intrinsic to its TIR.

Formation of RNA secondary structures is energetically favourable, but the presence of secondary structures in TIR of mRNA can reduce the efficiency of translation initiation by preventing the binding of ribosomes. Some of the earlier

work done on translation of *unc* genes suggested the presence of potential mRNA secondary structures involving the *uncF*, *uncH* and *uncG* genes (Brusilow *et al.*, 1982). Klionsky *et al.* (1986) showed that the presence of a secondary structure in the *uncEF* intergenic region lowers the expression of *uncF* (*b* subunit) because the secondary structure sequesters the S-D sequence and the initiation codon of *uncF*. They demonstrated that destabilization of the stem-loop preceding *uncF* resulted in a 3-fold increase in *uncF* expression and a 1.6-fold increase in expression of the downstream *uncH* gene. These results indicated translational coupling between *uncF* and *uncH*.

Since then, potential mRNA structures have been implicated in the regulation of a number of pairs of *unc* genes. Pati *et al.* (1992) demonstrated that *uncH* (*δ* subunit) expression is controlled by a secondary structure which masks the *uncH* S-D sequence and its expression is coupled to the preceding *uncF* gene (*b* subunit). Translation of the final few codons of *uncF* opens the structure and, due to the short intergenic region, allows the terminating ribosome to re-bind and translate *uncH*. Similar results were also reported earlier by Hellmuth *et al.* (1991) where *uncH* translation was found to be more efficient if the two upstream genes, *uncE* and *uncF*, were present.

Recently, Dallmann and Dunn (1994) and Rex *et al.* (1994) reported physically mapped secondary structure in the *uncDC* and *uncHA*, respectively. Dallmann and Dunn (1994) suggested that a secondary structure that sequesters the *uncC* S-D sequence lowers the expression of *uncC* relative to *uncD*, and that these two genes are coupled through this structure. They reported that translation of *uncD* opens the

secondary structure for a limited time in which the *uncC* translation initiation can proceed. Rex *et al.* (1994) stated that the translation of *uncH* (δ subunit) and *uncA* (α) is coupled through a structure which sequesters the TIR of *uncA*. These authors suggested that the translation of *uncH* induces formation of an alternative mRNA secondary structure which is less inhibitory to the translation of *uncA*. The new structures allowed better access to *de novo* ribosomal initiation.

1.7 mRNA Stability

The steady-state concentration of mRNA is directly proportional to the rate of its synthesis and inversely proportional to its rate of decay. Therefore, mRNA degradation plays an important role in the control of gene expression. Most *E. coli* mRNAs are very unstable, having a half-life of about 2-3 minutes (Donovan and Kushner, 1986), although some species are considerably more stable. The stability of a given message is often measured in terms of the chemical and functional stability. A functional stability refers to the average time in which a given species of mRNA is active in directing synthesis of a complete and functional polypeptide, whereas the chemical stability reflects the rate of loss of mRNA mass. Although the two are related, chemically stable species are not always functional in directing protein synthesis. Alternatively, a part of a message may be physically lost before its functional inactivation occurs, presumably as a result of cleavage in the untranslated region of mRNA. Even though a number of enzymes that carry out the degradation of RNAs are characterized, the structural determinants of mRNA that make them stable or prone to degradation are poorly understood.

The degradation of RNA is carried out by a combination of exo- and endoribonucleases (Belasco and Higgins, 1988; Petersen, 1992). RNase II and polynucleotide phosphorylase, the gene products of the *rnb* and *pnp* genes, respectively, are the two major exonucleases that are implicated in exonucleolytic degradation (Donovan and Kushner, 1986). These enzymes degrade RNA that is not base-paired at the 3′ end. Their activity is often impeded by stable 3′ stem-loops or by RNA binding proteins (Petersen, 1992). There are no known exonucleases in bacteria that carry out degradation of RNA from the 5′ to 3′. Endonucleases cleave RNAs internally and thus expose new 3′ termini to exonucleases. Endonucleolytic cleavages are believed to be the rate-determining step in the degradation of a number of specific *E.coli* mRNA (Belasco and Higgins, 1988; Patersen, 1992). The three major endonucleases that have been identified are RNase E, RNase K and RNase III.

RNase E is believed to be the most important endonuclease that is known to play a general role in the degradation of mRNA. RNase E, encoded by the *rne* gene, was initially identified as an enzyme which is responsible for processing the 9S ribosomal RNA into the 5S ribosomal RNA (Apirion, 1978; Misra and Apirion, 1979). Ono and Kuwano (1979) previously characterized a strain which had increased stability of the bulk mRNA at the nonpermissive temperature. Later these authors (1980) showed that the locus of this mutation, termed *ams* (for altered mRNA stability) maps to 24 min on the *E. coli* chromosome. Recently, the *ams* and *rne* were shown to be alleles of the same gene, encoding RNase E (Mudd *et al.*, 1990b; Babitzke and Kushner, 1991).

Several specific mRNA have now been identified which contain RNase E cleavage sites, including the gene 32 from T4 related bacteriophage (Mudd *et al.*, 1988; Loayza *et al.*, 1991), phage f1 (Kokoska *et al.*, 1990), the *rpsO-pnp* operon (Regnier and Hajnsdore, 1991) and *rpsT* gene (Mackie, 1991). In a number of cases, cleavages by RNase E have been demonstrated as rate limiting steps in the chemical decay and the functional inactivation of mRNA (Mudd *et al.*, 1988; Regnier and Hajnsdorf, 1991; Nilsson and Uhlin, 1991).

The cleavage specificity of RNase E is very poorly defined. RNase E preferentially cleaves single-stranded A-U rich sequences that are located next to secondary structures (Ehretsmann *et al.*, 1992; Cormack and Mackie, 1992). It appears that the position of the secondary structure is a more critical factor than the sequence of the secondary structure. The mechanism by which RNase E cleaves or recognizes its substrate is also unknown, but is under intensive study in various laboratories. It is believed that the enzyme binds the secondary structure while performing the cleavage (Ehretsmann *et al.*, 1992).

RNase III was the first endonuclease that was identified as being involved in mRNA degradation. It was initially reported as one of the enzymes involved in the maturation of ribosomal RNA (Kindler *et al.*, 1973). Cleavages by RNase III have been implicated in initiating degradation of some specific-mRNAs (Bardwell *et al.*, 1989; Regnier and Grubberg-Manago, 1989; Takata *et al.*, 1989). It is not clear how RNase III recognizes its substrate, but an extensive double-stranded region is required (Belasco and Higgins, 1988).

A partially purified preparation of RNase K was found to cleave *ompA* and

bla mRNA *in vitro* (Nilsson *et al.*, 1988; Lundberg *et al.*, 1990). But it is not clear if this enzyme is distinct from RNase E, because some of the sites in *ompA* mRNAs that are cleaved by RNase K *in vitro* are also affected by *rne* mutations *in vivo*. Thus, it is imperative to determine whether RNase K is regulated by RNase E or if the purified RNase K is just a functional proteolytic fragment of the RNase E.

Elements that determine the relative stability of mRNA are not well understood. Double-stranded structures are believed to protect mRNAs against exonucleolytic decay (Petersen, 1992). Stem-loops are also believed to be important in targeting the endonucleses to the cleavage sites. The role of nonnucleolytic processes such as translation or RNA-binding proteins in determining the stability of mRNA is not yet resolved. In particular, the role of translation in regulating degradation is controversial (review by Petersen, 1992). Some messages are stabilized by efficient translation, possibly due to the density of ribosome protecting the message against nucleases (Klug and Cohen, 1990). For other messages, translation does not affect degradation (Emory and Belasco, 1990).

It has been shown that the degradation of polycistronic messages is not concerted, but in fact occurs segmentally (Belasco *et al.*, 1985; Newbury *et al.*, 1987). This segmental decay which is largely controlled by endonucleolytic cleavage events could give rise to mRNA transcripts with unequal stability. The more stable of the resulting transcripts would then be expected to synthesize more of their gene product, if they are still translationally active. The first evidence of the segmental stability regulating differential expression of genes in polycistronic messages was obtained for the *puf* operon of *Rhodobacter capsulatus* (Belasco *et al.*, 1985). Various reports have

since indicated that segmental differences are important in regulating the differential expression genes in operons including *malEFG* (Newbury *et al.*, 1987), *pap* (Baga *et al.*, 1988), and *lac* (Cannistraro *et al.*, 1986).

1.8 *unc* mRNA Stability

Although the intrinsic translational efficiency of the *unc* cistrons is the major determinant of the differential expression of the *unc* genes, the role of mRNA processing and stability cannot be overlooked. This aspect of the regulation had received little attention until recently, and is often avoided because it is difficult to study.

There are various reports indicating that the *unc* mRNA undergoes extensive endonucleolytic processing but the precise details are not known. McCarthy (1990) reported that the mRNA for the first two genes of the operon, *uncIB*, are relatively unstable. The remaining seven genes are similar in functional and chemical stability. Schaefer *et al.* (1989) also reported that the 5′ region of the *unc* mRNA is unstable and that the *unc* primary transcript undergoes significant endonucleolytic processing. However, the locations of the processing sites and the mechanism of processing was not determined by the authors.

1.9 Purpose of the Thesis

The *unc* operon offers an attractive system to study post-transcriptional regulation as its genes are expressed in unequal amounts. The experiments described in this thesis are designed to gain more insight into the regulatory mechanisms that

govern the differential expression of the *unc* genes. In particular, the roles of mRNA processing, degradation, and structure, all of which are interrelated, in regulating the expression of the *unc* genes was studied. I have used small segments of the *unc* operon cloned into expression plasmids to analyze the degradative events, and to study the expression of some of the *unc* genes. The results were confirmed with the constitutively expressed *unc* mRNA, whenever possible.

Chapter 2 looks at the role of the *unc* transcription terminator in stabilizing the transcript of the last gene, *uncC*. The importance of the terminator in ensuring adequate expression of *uncC*, and its use in purification of the *uncC* gene product, ϵ, is also discussed.

In Chapter 3, I have identified a RNase E-dependent processing site in the initial coding sequences of the *uncC* mRNA. This cleavage led to functional inactivation of *uncC* and the upstream *uncD* gene. Analysis of chromosomally-encoded mRNA from an RNase E-deficient strain revealed that the 5′ region of the *unc* message also underwent RNase-dependent processing.

Chapter 4 describes a series of site-directed mutagenesis experiments that were designed to investigate the potential roles of a secondary structure in the *uncC* coding region, just downstream of the RNase E cleavage site that was identified in Chapter 3. In this chapter I have examined the effects of mutations in this potential regulatory secondary structure on the expression of *uncC*, and on the processing by RNase E. To examine the effects of the above mutations on translation of *uncC*, each of the mutant plasmids were exploited as templates to direct synthesis of *uncC* *in vivo*, and the expression of *uncC* was quantitated by Western blot analysis. The

effect of the mutations on the processing was studied by Northern blot analysis.

Having established in Chapter 3 that the 5′ region of the *unc* mRNA undergoes RNase E-dependent processing, I have in Chapter 5 taken up the task of finding the mechanism of inactivation of the early *unc* genes. Earlier results are enhanced by a more rigorous investigation which demonstrated that the *uncIB* part of the *unc* message is rapidly inactivated by multiple endonucleolytic cleavages, some of which are dependent on functional RNase E.

CHAPTER 2

ROLE OF THE *ESCHERICHIA COLI unc* TRANSCRIPTION TERMINATOR IN EFFICIENT EXPRESSION OF *uncC*

2.1 INTRODUCTION

The major interest in the Dunn laboratory is to study the structure, mechanism and regulation of synthesis of the *E. coli* ATP synthase whose subunits are encoded by the *unc* operon. In particular the role of the ϵ subunit, encoded by the *uncC* gene, is being explored in great detail. The ϵ subunit is required for binding the peripheral, catalytic F_1 sector to the membrane-bound F_o sector (Sternweis, 1978) and inhibits the ATPase activity of soluble F_1 (Sternweis and Smith, 1980). Thus in mutants defective in ϵ, the remainder of F_1 behaves as an uncoupled, cytoplasmic ATPase, causing severe growth impairment (Klionsky *et al.*, 1984). Adequate production of the ϵ subunit is therefore essential.

Schaefer and co-workers (1989) have suggested, based on Northern blots and ribosome-binding studies, that the *uncC* message encoding ϵ is less abundant than other parts of the *unc* transcript. A number of factors may shorten the lifetime of the *uncC* message relative to the messages for the other subunits. First, as *uncC* is the final gene in the operon, it is transcribed last. Second, the 3'-exonucleases polynucleotide phosphorylase and RNase II are involved in the degradation of *E. coli* mRNAs (Donovan and Kushner, 1986), and the *uncC* message is at the 3'-end of the transcript. Thus, its coding sequences are easily accessible to exonucleases. Third, it has been previously reported that endonucleolytic cleavage of the *uncC* mRNA at processing sites may functionally inactivate the message (McCarthy *et al.*, 1988; Schaefer *et al.*, 1989). In fact I have mapped a endonucleolytic cleavage site (discussed in Chapter 3) in the early coding region of the *uncC* message which functionally inactivates the message (Patel and Dunn, 1992). Finally, Dallmann and

Dunn (1994) have recently shown that the presence of a secondary structure in the intercistronic region between *uncD* and *uncC* limits its expression.

Because of the importance of adequate ϵ production, I am investigating the mechanism of decay of the *uncC* message using expression vectors carrying small portions of the *unc* operon. In the studies described here, the effects of the *unc* transcription terminator on ϵ expression and on the *uncC* mRNA level and half-life were determined.

2.2 MATERIALS AND METHODS

(I) Chemicals and Enzymes

All chemicals were of reagent grades. Chemicals used in the preparation of RNA, proteins and the probes were from either BDH (Toronto) or Sigma (St. Louis). Radiochemicals were from either Amersham (Oakville) or Dupont (Mississauga). Agarose and polyacrylamide were of ultra pure quality from Bio-Rad (California). The restriction enzymes used in the subcloning were obtained from various suppliers including Pharmacia (Montreal, Que), New England Biolabs (Mississauga, Ont) and Boehringer-Mannheim (Dorval, Que). The T7 RNA polymerase was purchased from Pharmacia. Tryptone and yeast extract used for bacterial growth were obtained from either Difco (Detroit, Mich) or BDH. Carbenicillin, isopropyl-β-D-thiogalactoside (IPTG), and nucleoside triphosphates were from Sigma.

(ii) Bacterial Strains and Growth

The *E.coli* strain used in this study was JM103 (*Δlacpro*, F'*tra*D36, *proAB*, *lacI*^{q}*ZΔM15*), described by Messing *et al.* (1981). All strains, unless otherwise indicated, were grown in LB medium (Sambrook *et al.*, 1989) containing 40 ug/ml carbenicillin at 37°C with shaking. During early logarithmic growth IPTG was added to a concentration of 1mM to induce expression from the promoter. For the turnover studies the initiation of transcription was prevented by addition of rifampin to a concentration of 100 μg/ml of culture after 10 min of induction. Samples were taken for RNA preparation at various time interval after the addition of rifampin.

(iii) Plasmid Constructions

Recombinant DNA procedures were carried out by standard methods (Sambrook *et al.*, 1989). Plasmids bearing *uncC* were constructed from the expression vector pKK223-3 (Brosius and Holy, 1984), and plasmid pAP55 (Brusilow *et al.*, 1983), which bears the *unc* operon. The plasmids pSD15, pTK1 and pSD37 were from our laboratory stock and have been described previously (Patel *et al.*, 1990). Dr. Dunn had originally prepared pSD15 by cloning the 1.2-kbp *Pst*I fragment of pAP55 bearing part of *uncD*, all of *uncC*, and the *unc* transcription terminator, into pUC8 (Vieira and Messing, 1982) which had been cut with *Pst*I, and selecting a clone-bearing plasmid with the insert in the orientation of expression. pTK1 was constructed by inserting the 0.63-kbp *Mnl*I-*Pst*I fragment of pSD15 into pKK223-3 which had been cut with *Sma*I and *Pst*I. pSD37 was constructed by inserting the 0.44-kbp *Mnl*I-*Hpa*II piece from pSD15 into pKK223-3 which had been cut with *Sma*I

and *Acc*I. The only difference in the plasmids pTK1 and pSD37 is that pTK1 contained the *unc* transcription terminator (Fig. 2.1). Plasmid pHN3 which was used to prepare *in vitro* transcribed RNA to make the *uncC*-specific antisense riboprobe was constructed by cloning the *Mnl*I-*Hpa*II fragment of the *uncC* gene into pTZ18U (Mead *et al.*, 1986), in the opposite direction of expression. Constructs were verified by restriction endonuclease mapping.

The plasmids were maintained and expressed in *E. coli* strain JM103. Transformed derivatives of this strain were streaked on minimal medium plates supplemented with thiamine and carbenicillin to ensure maintenance of both the F' factor and the expression vector. The transformation of cells were carried out by the standard calcium chloride procedures adapted from Mandel and Higa (1970) as described by Sambrook *et al.* (1989).

(iv) Induction and Analysis of Cellular ϵ Content

Cells containing either pTK1 or pSD37 were grown at 37°C until reaching an A_{600} of 0.2 at which point IPTG was added to a concentration of 1 mM to induce expression. Control flasks received no inducer. After 10 min, samples were removed, chilled, sedimented, and extracted for 5 min at 100°C with electrophoresis sample buffer containing 2% sodium dodecyl sulfate (SDS). Equivalent amounts of cell extract were run on 15% polyacrylamide gels using the buffer system of Laemmli (1970) and electroblotted onto nitrocellulose as described previously (Dunn, 1986). ϵ was detected by probing the blot with 50,000 dpm/mL ^{125}I-ϵ-1 monoclonal antibody (Dunn *et al.*, 1985) and radioautography. A portion of culture was taken at the time

Figure 2.1 Structures of the *uncC* expression plasmids. A schematic diagram of pKK223-3 with the relevant genes, including the gene encoding β-lactamase (*amp*), the hybrid *trp-lac* promoter (P_{tac}) and the *rrnB* transcriptional terminator(T_{rrnB}). The fragments cloned in pTK1 and pSD37 are shown below the vector. pTK1 contained the *Mnl*I to *Pst*I fragment, whereas pSD37 contained *Mnl*I to *Hpa*II fragment, lacking the natural *unc* transcriptional terminator (T_{unc}). Transcription in pTK1 terminates at the *unc* terminator and in pSD37 it continues until the *rrnB* terminator (T_{rrnB}). The relevant transcripts and the *uncC*-specific probe used in the studies are also shown.

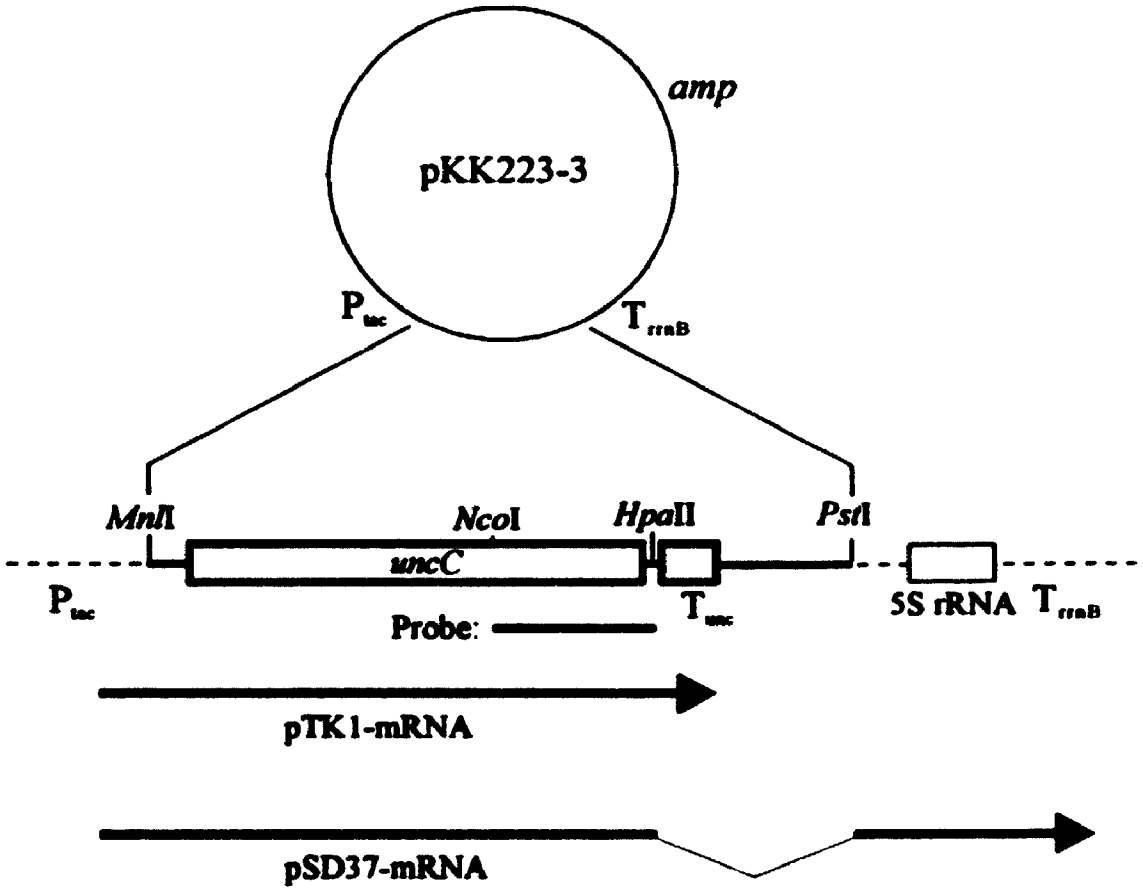
amp
pKK223-3
P tac
T rrnB
MnlI
NcoI
HpaII
PstI
uncC
P tac
T unc
5S rRNA
T rrnB
Probe:
pTK1-mRNA
pSD37-mRNA

of induction for toluene treatment and determination of β-lactamase activity (Ross and O'Callaghan, 1975).

(v) Purification of RNA

RNA for the Northern blot analysis was prepared according the procedure developed by Dennis and Nomura (1975) with subsequent modification by Mackie (1989). In this method 2 mL of liquid culture (at A_{600}=0.2) was added to 1 mL of 1.5% SDS, 30 mM EDTA, 300 mM sodium acetate in a boiling water bath and extracted at that temperature for 1 min. After cooling, the samples were extracted successively with aqueous phenol, phenol/chloroform, and ether, then the RNA was precipitated with 70% ethanol. After washing and drying the pellets, each was dissolved in 0.1 mL of DEPC-treated water. The concentration of nucleic acids was measured by taking absorbance at 260 nm on Bausch & Lomb Spectronic 1001 spectrophotometer.

(vi) Northern Blot Analysis of RNA

Samples of the extracted RNA were run on a 6% polyacrylamide gel containing 8 M urea in 1X Tris-Borate buffer (0.09 M Tris, 0.09 M Borate, 2.5 mM EDTA, Sambrook et al., 1989) for 60 min at 150 V. Gels were soaked in 1X TBE for 10 minutes to remove urea, thus preventing it from interferring with the blotting procedure. The RNA was then electophoretically transferred onto Zeta-probe membrane (Bio-Rad) using 0.5X TBE buffer for 60 min at 80 V in a Bio-Rad Mini Trans-Blot Cell with a chilled ice pack within the apparatus. Current was maintained

below 0.35 amp. RNA was fixed to the membrane by illumination of the blot with ultraviolet light for 3 min (Stratagene Stratalinker 1800) and drying *in vacuo* for 60 min at 80°C. Pre-hybridization and hybridization with the *uncC*-specific ribo-probe were carried out at 55°C as described by Mackie (1989). Basically, the blots were prehybridized in a standard hybridization buffer (50% formamide, 5X SSC, 5X Denhardt's solution (Denhardt, 1966), 0.1% SDS, 40mM Na_2HPO_4/NaH_2PO_4 (pH 7.0), and 250 ug/ml of yeast RNA) at 42°C for 1 hr. The membranes were subsequently hybridized at 55° in 10 mls of fresh hybridization buffer with 10^5 cpm/ml of the ^{32}P-labeled *uncC*-specific probe. The hybridized membranes were washed with 2X SSC (0.30 M sodium chloride, .03 M sodium citrate) and 0.1% SDS at 60°C for 1 hr, with a change of solution every 15 min. The blots were then dried and exposed to X-ray film.

(vii) Labelling of Hybridization Probe

Plasmid pHN3 was linearized with *Nco*I and used as a template for *in vitro* transcription by T7 RNA polymerase to prepare *uncC*-specific probe. The antisense probe would be complementary to the region between the *Hpa*II site following *uncC* and the *Nco*I site 138 bases upstream (Fig.2.1). *In vitro* transcription was carried out using 2 μg of the appropriate linearized template with 40 U of T7 RNA polymerase at 37°C for 60 min in the presence of 1mM ATP, CTP and GTP, and 100 μM [α-^{32}P]UTP which provided the label. The reaction buffer included 40 mM Tris-HCl, pH 8.0, 6 mM $MgCl_2$, 10 mM DTT and 2 mM spermidine. The reaction was stopped with 2M ammonium-acetate and extracted once with phenol/choloroform/isoamyl

alcohol (P/C/I 24:24:1) and the RNA was precipitated by addition of 2.5 volume of 95% ethanol. RNA was recovered by centrifugation, reprecipitated, washed with 70% ethanol and the dried pellet was taken up in 100 μl of DEPC-treated water and stored at -20°C until required.

(viii) Quantification of Northern Blots

The relative levels of mRNA were estimated by scanning the blots with an LKB ultrascan-XL Enhanced Laser Densitometer. The area under each peak was measured by weight, and a plot of % of the original mRNA remaining vs time was prepared to determine the half-lives.

2.3 RESULTS

(i) Effect of Transcription Terminator on *uncC* Expression

Two different plasmids, pSD37 and pTK1, were constructed using pKK223-3 as the vector (Brosius and Holy, 1984). The inserted sequence in each plasmid begins at the *MnlI* site 7 bp upstream from the Shine-Dalgarno sequence, and extends through the *uncC* structural gene, but pSD37 lacks the downstream *unc* transcription terminator (Fig. 2.1). Transcription from pSD37 continues to the *rrnB* terminator (Brosius *et al.*, 1981) provided by the vector.

The effectiveness of these two plasmids in directing the synthesis of the *uncC* gene product, ϵ, was detected by immunoblot analysis of cultures which had been induced for 10 min with 1 mM IPTG (Fig. 2.2 A). The strain carrying pTK1 made far more ϵ than the strain carrying pSD37. The trace of ϵ in the strain carrying the

Figure 2.2 Induction of ϵ in derivatives of *E. coli* JM103 bearing pSD37 and pTK1. Cultures were induced with IPTG when the A_{600} reached 0.2. (A) Ten min after induction cells were extracted and their ϵ content was analyzed by immunoblotting using ^{125}I-labeled anti-ϵ. Each lane received proteins extracted from the cells in 20 μL of culture. The left lane received purified F_1-ATPase as a standard. Only the portion of the blot near ϵ is shown; no other bands were present. (B) Two hours after induction cells were extracted and analyzed by SDS-polyacrylamide gel electrophoresis. Each lane received proteins extracted from 20 μL of culture. The gel was stained with Coomassie blue R-250.

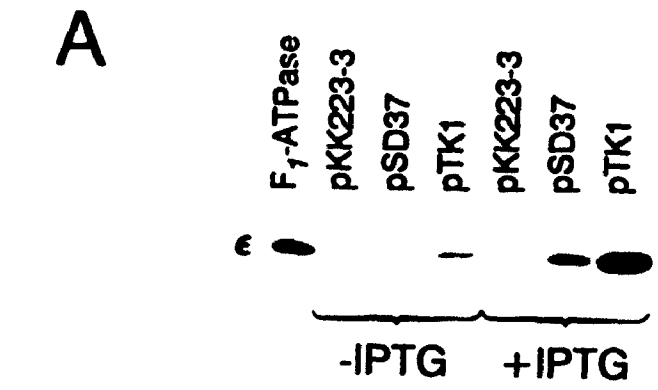
A
F1-ATPase
pKK223-3
pSD37
pTK1
pKK223-3
pSD37
pTK1
ε
-IPTG
+IPTG

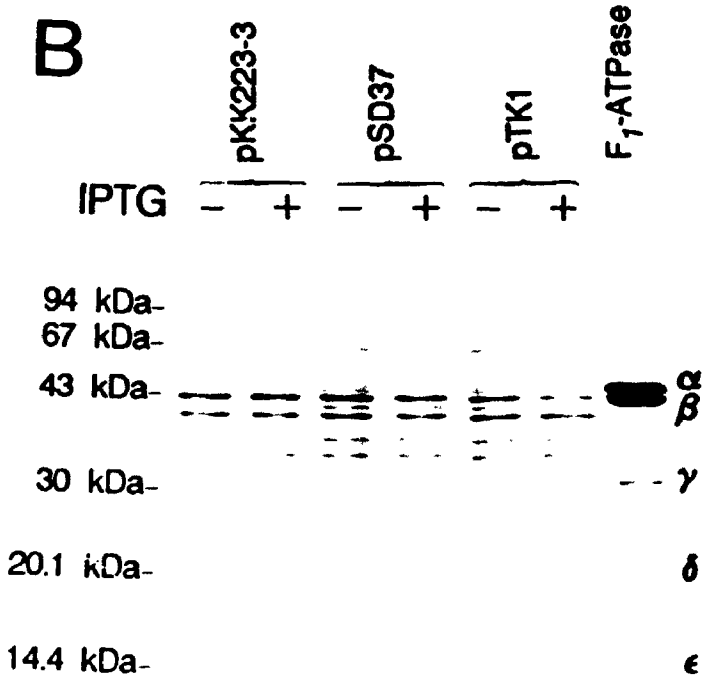
B
pKK223-3
pSD37
pTK1
F1-ATPase
IPTG
– + – + – +
94 kDa-
67 kDa-
43 kDa-
30 kDa-
20.1 kDa-
14.4 kDa-
α
β
γ
δ
ε

parental vector pKK223-3 indicates the normal level of ϵ produced from the chromosomal *unc* operon. The production of ϵ in the uninduced pTK1 sample reflects incomplete repression of the *tac* promoter in pKK223-3 by the *lac* repressor (Brosius and Holy, 1984). A quantitative comparison of the induced cultures, made by blotting various amounts of the extracts (data not shown), revealed that pTK1 was ten-fold more efficient that pSD37 in directing the synthesis of ϵ. After two hours of induction, the ϵ present in the strain bearing pTK1, but not the strain bearing pSD37, was visible on a polyacrylamide gel stained with Coomassie blue (Fig. 2.2 B). Overproduction of ϵ was not inhibitory to cell growth.

(ii) Comparison of Steady-State Levels of *uncC* mRNA Transcribed from pTK1 and pSD37

The differential production of ϵ from pSD37 and pTK1 could arise through a number of mechanisms. First, it could be due to difference in the plasmid copy number. One would expect that the copy number for both plasmids to be similar since they have the same origin of replication. To confirm this, the relative plasmid copy numbers were measured by determining β-lactamase (encoded by the *amp* gene) activities in the cultures just before induction. The strain bearing pSD37 had about 50% more β-lactamase than the strain bearing pTK1 (data not shown), implying that the copy number of pSD37 was higher than that of pTK1, rather than lower. Next the *uncC* mRNA in extracts of induced cultures were compared by Northern blots (Fig. 2.3 A) using an *uncC*-specific ribo-probe. The message from pSD37 is larger in size (745 bases) because it contains an additional 210 nucleotides that includes the

Figure 2.3 Analysis of mRNA species transcribed from plasmids pSD37 and pTK1. Derivatives of *E. coli* strain JM103 carrying pSD37 or pTK1 were grown and induced as described in the Materials and Methods. Ten min after induction, samples of culture were removed and the RNA was extracted for comparison of steady-state levels. Rifampin was then added to the remaining cultures to a final concentration of 0.1 mg/mL. Samples were taken at the indicated times for extraction of RNA. Northern blots of the RNA samples using the *uncC*-specific probe were performed as described in Materials and Methods. N, non-induced sample. (A) Comparison of steady-state message levels. The lanes received 1.46 μg of RNA (pTK1) or 1.74 μg of RNA (pSD37). (B) Degradation of the message transcribed from pSD37. Each lane received between 5.1 and 5.6 μg of the RNA sample extracted at the indicated time after addition of rifampin. (C) Degradation of the message transcribed from pTK1. Each lane received between 1.3 and 1.5 μg of the RNA extracted at the indicated time after addition of rifampin.

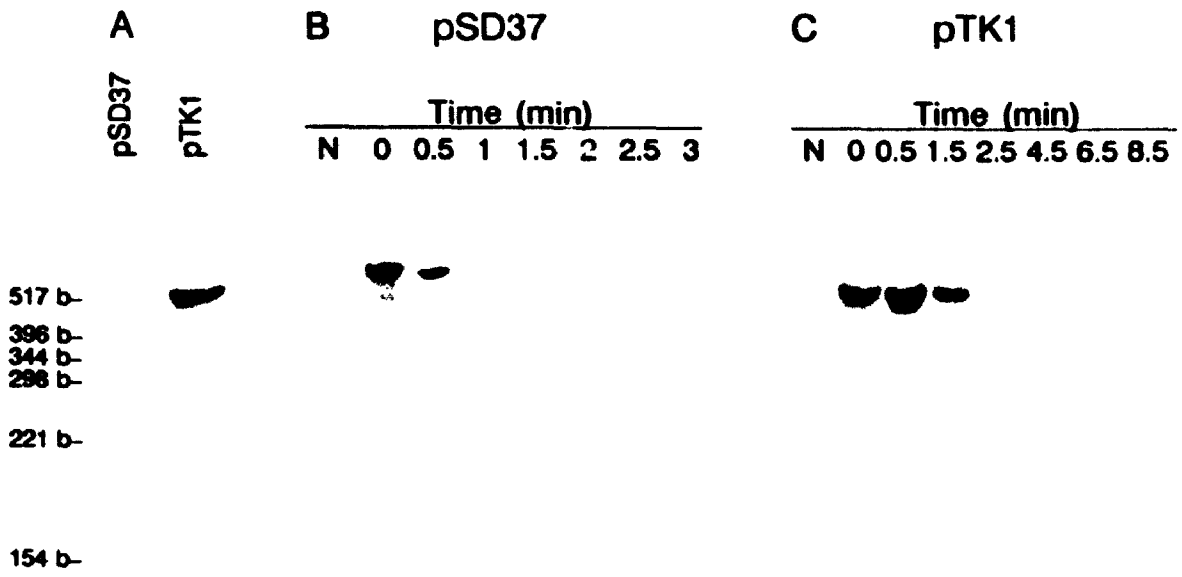
A
B pSD37
C pTK1
pSD37
pTK1
Time (min)
N 0 0.5 1 1.5 2 2.5 3
Time (min)
N 0 0.5 1.5 2.5 4.5 6.5 8.5
517 b-
396 b-
344 b-
298 b-
221 b-
154 b-

immature 5S rRNA, between the cloning region and the *rrnB* T_1 terminator, while in pTK1 (message length 531 bases) the *unc* terminator begins just seven bases beyond the stop codon. The pTK1 message was much more abundant than the pSD37 message. The levels were quantified on another blot which received various amounts of the extracted RNA (data not shown). The difference in abundance of full-length message was about eleven-fold, consistent with the difference in expression of ϵ.

(iii) Turnover of the *uncC* Messages Transcribed from pTK1 and pSD37

As the copy numbers of pSD37 was two fold higher than pTK1, and the *uncC* genes on these plasmids were transcribed from the same promoter, it seemed unlikely that different rates of synthesis would be responsible for the different steady state levels of the transcripts. I therefore analyzed the degradation of the two messages. The half-lives were determined after treating induced cells with rifampin to inhibit initiation of transcription by RNA polymerase. The decay of message was analyzed by Northern blots (Fig. 2.3 B and C.) In comparing these blots, note that in the experiment with pSD37 (Fig. 2.3 B) the time points were taken at just 30 s intervals, and that each lane received three times more RNA extract than in the experiment with pTK1 (Fig. 2.3 C). The signals were quantified by scanning and plotted to determine the half-lives (Fig. 2.4). The message encoded by pSD37 had a half-life of just 25-30 s while the pTK1 message had a half-life of 90-100 s. This result indicates that the message encoded by pSD37 is more susceptible to nuclease attack. A truncated form of the pSD37 message, apparent on the blot in Fig. 2.3 B, migrates

Figure 2.4 Semilogarithmic plots of the decay of the mRNA transcribed from pTK1 or pSD37. The relative amount (to 0 time point) of mRNA at each time point was determined by densitometer scanning of the autoradiogram shown in Fig. 2.3. The results were plotted versus time after rifampin addition (●, pSD37; ▽, pTK1). The measured half-life for the mRNA transcribed from pTK1 and pSD37 were 90-100 sec and 30 sec, respectively.

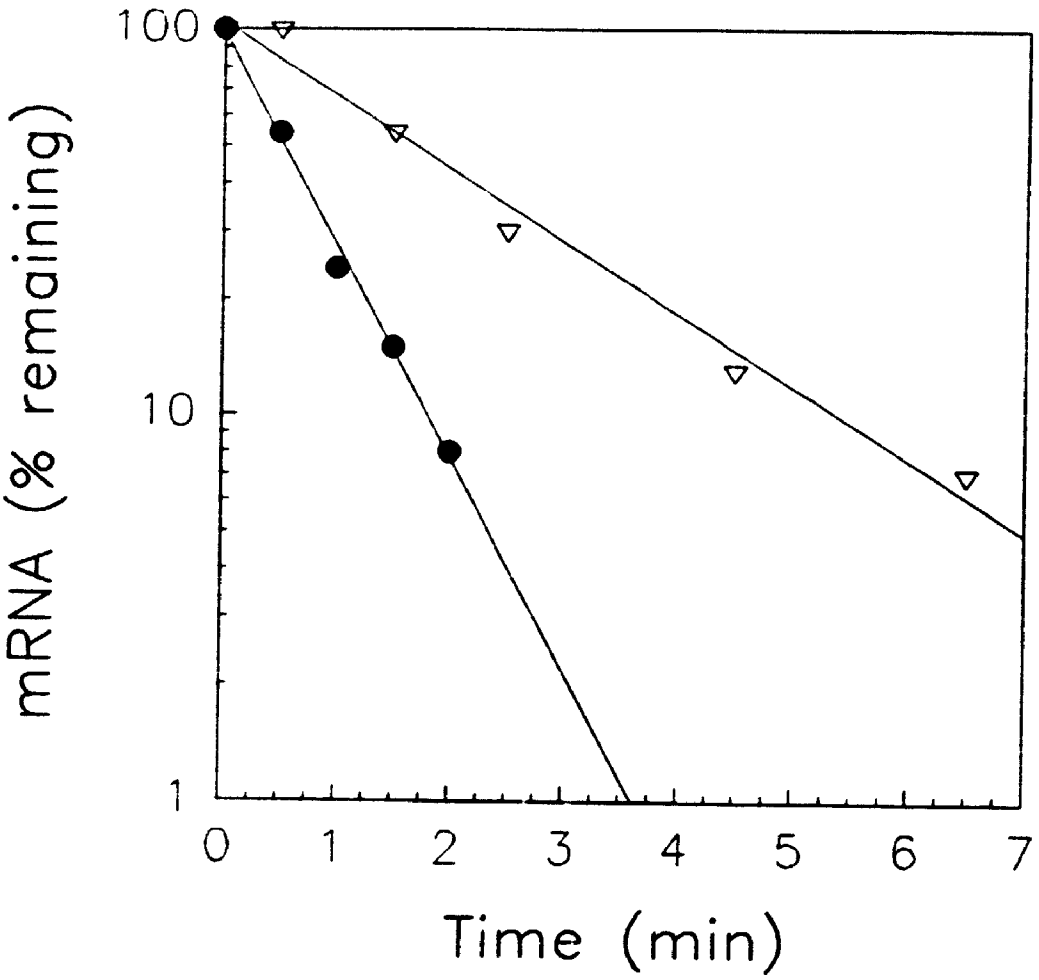
100
10
1
mRNA (% remaining)
0
1
2
3
4
5
6
7
Time (min)

similarly to the pTK1 message. It cannot be the same species, however, as it lacks the *unc* terminator sequence.

2.4 DISCUSSION

In prokaryotes, mRNA stability is an important factor in the regulation of gene expression. Protection of mRNA sequences against exonucleolytic attack is important for efficient expression of genes that are located in the 3′ end of polycistronic messages because of their easy access to polynucleotide phosphorylase and ribonuclease II which degrade RNA from 3′ ends (Donovan and Kushner, 1986). Sequences that have the potential to form stem-loop structures are known to stabilize mRNAs by impeding the action of 3′-exonucleases (Belasco and Higgins, 1988). Rho-independent terminators usually contain a palindromic sequence (followed by poly(U)) which forms a stem-loop that is energetically favourable. The predicted secondary structure of the *unc* transcription terminator is shown in Fig. 2.5. The *unc* terminator has GAAA in the loop and 13 potential base-pairs in the stem which could be formed. Differential stability among terminator structures may arise from the intrinsic stabilities of the base-paired structure, or from the sequence-dependent binding of trans-acting factors to the stem or loop. It has previously been shown that RNA hairpins containing GNRA loop (where N=any nucleotide and R=purine) sequences are substantially more stable over other tetranucleotide loops (Woese *et al.*, 1990; Anato and Tinoco, 1992; SantaLucic *et al.*, 1992). Heus and Pardi (1991) showed that this unusual stability was due to novel base pairing between the G and A residues in the loop, extensive base stacking, and two uncommon hydrogen bonds.

Figure 2.5 The predicated secondary structure of the *unc* transcriptional terminator. The bases are numbered according to Walker *et al.* (1984) and the *uncC* stop codon is underlined.


A A
G A
G C
U A
C G
7550 U A
G C
A U
C G
C G
G C
A U
7530 A U
7570
A U
A U
5'-UAACACCGGCUUGAAAAGCAC UUUU-3'

We believe that the long stretch of base-paired region and the GAAA loop gives the *unc* terminator a high stability.

Transcripts ending with the *unc* terminator exhibited a half-life of 90-100 s, which is typical of *E. coli* messages (Donovan and Kushner, 1986). It appears that the hairpin structure formed by the *unc* terminator is important in protecting the message against exonucleases, and that this stabilization is essential for adequate production of ϵ. The *uncC* message could be inactivated, then, either through slow exonucleolytic attack, or by endonucleolytic cleavage. The faint band visible just below the major transcript from pTK1 on the Northern blots shown in Fig. 2.3 A suggested a possible processing site which will be the subject of investigation in the next chapter. Although the *rrnB* terminator sequence provided by pKK223-3 can also form a hairpin structure, it did not protect the message. Thus even a strong terminator does not guarantee a stable message. The hairpin may be removed by endonucleolytic cleavage at an RNase E processing site (Misra and Apirion, 1979) involved in the maturation of the 5S rRNA sequence located between the cloning region and the *rrnB* terminator. Such a cleavage would be consistent with the smaller message seen in extracts of cells bearing pSD37 (Fig. 2.3). Decay of this smaller message would then occur by exonucleolytic attack, unimpeded by RNA secondary structure.

The rapid degradation of messages ending at the *rrnB* terminator of pKK223-3 clearly detracts from the usefulness of this vector for obtaining high-level expression. In particular, the presence of RNase E-dependent processing site 5′ to the terminator would make this vector ineffective in achieving high expression of proteins.

Cloned sequences which include endogenous terminators, such as that in pTK1, should be expressed much more effectively than those from the beginning or middle of an operon, or cDNAs, which are likely to be expressed poorly due to rapid degradation of their messages. Our laboratory has constructed a derivative of pKK223-3 with the *unc* terminator and demonstrated its use in overexpressing either individual *unc* genes or number of unrelated proteins in *E. coli* (unpublished data, personal communication Dr. Shaw, Department of Biochemistry, University of Western Ontario)

The highly efficient overproduction of ϵ attained in strains carrying pTK1 allowed Dr. Dunn to develop a simple and rapid method of purifying large amounts of the subunit (Patel *et al.*, 1990). Some earlier methods required denaturants to dissociate ϵ from F_1-ATPase (Smith and Sternweis, 1977) or from antibodies (Dunn, 1986b). Dreyfus and Satre (1984) developed a method of purifying ϵ from membrane extracts that included a trichloroacetic acid extraction. In contrast all of the steps in the new procedure are less harsh to the structure of the protein.

CHAPTER 3

RNase E-DEPENDENT CLEAVAGES IN THE 5′ AND 3′ REGIONS OF THE *ESCHERICHIA COLI unc* mRNA

3.1 INTRODUCTION

The 7-kb *unc* operon of *Escherichia coli* contains nine cistrons, last eight of which encode the subunits of F_1F_0-ATPase. The order of the genes in the operon has been established as *uncIBEFHAGDC* (Gunsalus *et al.*, 1982). *uncI*, the first gene in the operon, encodes a small polypeptide whose function is not known. The next three genes, *uncBEF*, encode the three subunits of the membrane-embedded F_0 sector, namely *a*, *c* and *b*, respectively. The last five genes encode δ, α, γ, β, and ϵ, the subunits of the F_1 sector which has the catalytic site for the ATP synthesis and hydrolysis. The stoichiometry of these subunits in the mature ATPase complex is $ab_2c_{9\text{-}15}\alpha_3\beta_3\gamma\delta\epsilon$ (Foster and Fillingame).

As indicated in the general introduction, previous studies have shown that the subunits are produced in the appropriate relative amounts from a single polycistronic mRNA. Any differential expression must therefore occur at the post-transcriptional level. The organization of the *unc* operon seems to bear no relationship to their rate of expression. Rather, the genes generally alternate in order between those that are expressed more and less efficiently, and are grouped functionally.

Several studies have implied that different intrinsic efficiencies of translation initiation among the *unc* genes provide a major contribution to the disparity in the levels of synthesis. Another potential mechanism of posttranscriptional regulation is the differential processing and degradation of mRNA. This mechanism has been demonstrated to function in regulating the differential gene expression of a number of *Escherichia coli* operons (Baga *et al.*, 1988; Newbury *et al.*, 1987), but the generality of this mechanism is not yet established. In this chapter, I investigated the

relationship between *unc* mRNA processing and differential expression of the *unc* cistrons.

Most *E. coli* mRNAs are short lived (Donovan and Kushner, 1986), and their turnover is carried out by exonucleases and endonucleases (Belasco and Higgins, 1988). RNase II and polynucleotide phosphorylase have been shown to be the two major enzymes involved in the exonucleolytic degradation of *E. coli* mRNA in a 3′ to 5′ direction (Donovan and Kushner, 1986). Polycistronic mRNAs have been shown to be endonucleolytically processed into monocistronic units prior to further degradation (reviews by Ehretsmann *et al.*, 1992; Petersen, 1992). It is now generally believed that internal cleavages by endonucleases are the critical first step in the degradation of some *E. coli* mRNA. The cleavages by endonucleases expose new 3′ ends which can be attacked by the exonucleases. Although, three different endonucleases, RNase E , RNase III and RNase K, have been identified, cleavages by RNase E (encoded by *rne* gene) for most mRNAs appears to initiate instantaneous degradation of mRNA (Mudd *et al.*, 1988; 1990; Babitzke and Kushner, 1991; Melefors and von Gabain, 1991). Ehretsmann *et al.* (1992) proposed that RNase E cleavages occur within a single-stranded consensus, G/A′A′UUA/U (the primes indicate sites of cleavage), adjacent to a region of double-stranded structure.

In this chapter I report evidence of RNase E-dependent processing in the 5′ and 3′ region of the *unc* mRNA and discuss its implications on the overall degradation of the *unc* message, and on the differential expression of some of the *unc* genes.

3.2 MATERIALS AND METHODS

(i) Enzymes and Chemicals

Sources of most chemicals have been described in the previous Chapter (section 2.2). The restriction enzymes used to carry out the studies described in this chapter were from New England Biolabs (Mississauga, Ont.) or Pharmacia (Montreal, Quebec). T7 DNA polymerase, T4 nucleotide kinase, RNA guard, ribonucleotides and deoxyribonucleotides were from Pharmacia. The "sequencing kit" was from Boehringer Mannheim (Dorval, Quebec). The M-MLV reverse transcriptase was purchased from New England Biolabs and [α-^{35}S]ATP used in DNA sequencing was from either Amersham (Oakville, Ont.) or ICN (Mississauga, Ont.).

(ii) Bacterial Strains

The *E. coli* strains used in this study are listed in Table 3.1.

(iii) Plasmid Construction

Recombinant DNA procedures were carried out by standard methods (Sambrook *et al.*, 1989). The *unc* fragments contained in the various plasmids that were used to carry out the experiments described in this chapter are shown diagrammatically in Fig. 3.1, and a brief description of their construction is given below.

Expression plasmids bearing the *uncC* gene (pSD38, pSD39, pSD44, pGD2, and pTK1) constructed using the vector pKK223-3 (Brosius and Holy, 1984) have been described previously (Dunn and Dallmann, 1990). Basically, these plasmids

TABLE 3.1 Bacterial Strains

Strain	Genotype	References
JM103	*Δlac-pro* F' *traD36 proAB lacI*^{q} Z*ΔM15*	Messing *et al.* (1981)
SK5003	*thr leu pnp-7 rnb-500*	Donovan and Kushner (1986)
SK5004	*thr leu pnp-7*	Donovan and Kushner (1986)
SK5005	*thr leu rnb-500*	Donovan and Kushner (1986)
SK5006	*thr leu*	Donovan and Kushner (1986)
SK5665	*thyA715 ams-1*(Ts)[a]	Arraiano *et al.* (1988) and Babitzke and Kushner (1991)
MG1693	*thyA715*	Arraiano *et al.* (1988) and Babitzke and Kushner (1991)
N3431	*lacZ43 thi-1 relA1 spoT1 rne-3071*(Ts)	Goldblum and Apirion (1981)
N3433	*lacZ43 thi-1relA1 spoT1*	Goldblum and Apirion (1981)
1100	*bglR thi-1 rel-1* HfrP01	Klionsky *et al.* (1984)
DK8	1100 Δ(*uncB-uncC*)*ilv*::Tn*10*	Klionksy *et al.* (1984)

[a]Babitzke and Kushner (1991) have proposed renaming the *ams-1* allele as *rne-1*.

Figure 3.1 Construction of plasmids containing fragments of the *unc* operon. The *unc* operon, segments of the operon cloned in expression plasmids or used as antisense RNA probes, and the restriction endonuclease sites defining the ends of these segments are shown. P, promoter; T, terminator.

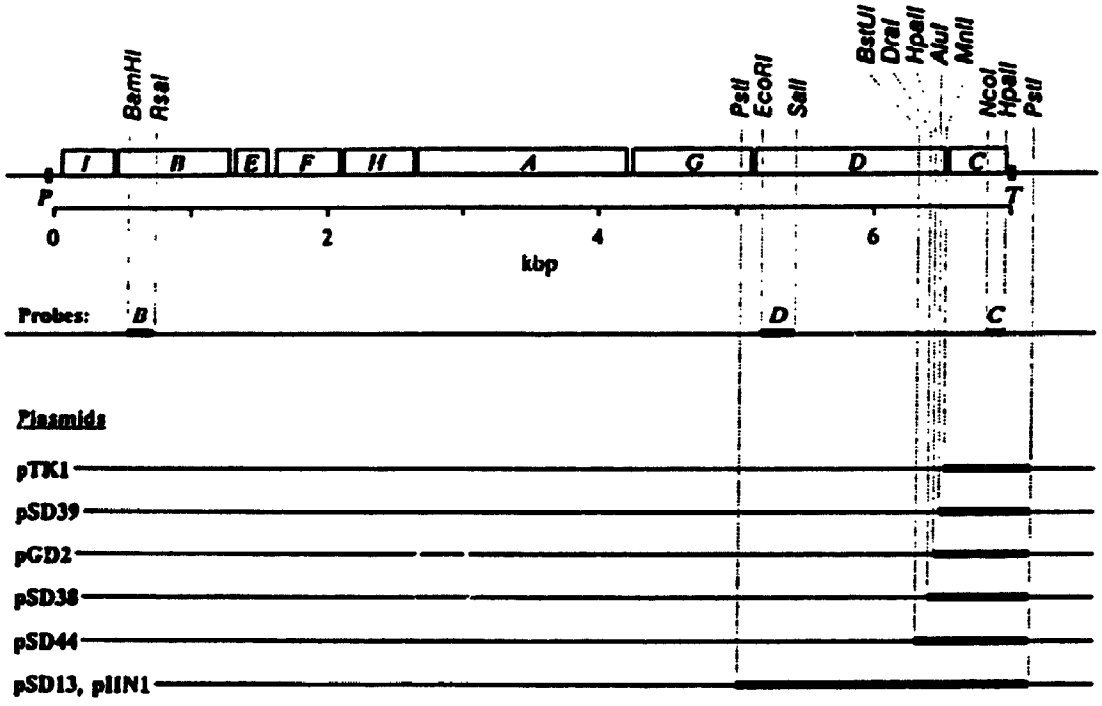
BamHI
AsaI
PstI
EcoRI
SalI
BstUI
DraI
HpaII
AluI
MnlI
NcoI
HpaII
PstI
I
B
E
F
H
A
G
D
C
P
T
0
2
4
6
kbp
Probes:
B
D
C
Plasmids
pTK1
pSD39
pGD2
pSD38
pSD44
pSD13, pIIN1

contained a nested set of *unc* fragments starting at various sites in the *uncD* and ending at the *Pst*I site following the *unc* transcription terminator (Fig. 3.1). Plasmid pSD13, which carries the 3'-end of *uncG*, all of *uncDC*, and the *unc* transcription terminator was constructed by inserting the 2.1-kb fragment produced by partial digestion of pAP55 (Brusilow *et al.*, 1982) with *Pst*I into the *Pst*I site of pUC8 (Vieira and Messing, 1982) and selecting a clone bearing a plasmid with the insert in the proper orientation for expression. pHN1 was constructed by transferring the insert from pSD13 into pEX1 (Passador and Linn) using the *Hind*III and *Sma*I sites. pHN6 was constructed by transferring the insert from pSD38 (Dunn and Dallmann, 1990) into pTZ18U (Mead *et al.*, 1986) using *Eco*RI and *Hind*III sites.

The plasmids pHN3, pHN7 and pHN8 carried the inserts described below in the direction opposite to that for expression, producing the antisense RNA to be used as *uncC*-, *uncD*-and *uncB*-specific probes, respectively. pHN3 contained the 0.4-kb *Mnl*I-*Hpa*II fragment of the *uncC* gene cloned into the vector pTZ19U (Mead *et al.*, 1986) which bears a promoter for T7 RNA polymerase. pHN7 was constructed by inserting the 0.25-kb *Eco*RI-*Sal*I (early *uncD* coding region) fragment of pSD13 into pTZ19U which had been cut with *Sal*I and *Eco*RI. pHN8 carried the 0.2-kb *Bam*HI-*Rsa*I (early *uncB* coding region) fragment of *uncB* gene cloned into pTZ18U (Mead *et al.*, 1986). All constructs were verified by restriction endonuclease mapping.

(iv) Site-Directed Mutagenesis

Site-directed mutagenesis (Carter, 1987) was used to introduce a stop codon

mutation in the *uncD* gene, 129 bases upstream of the normal stop codon. Single-stranded phage DNA derived from phage M13GD9 (Dallmann and Dunn, 1994) was prepared and annealed to the mutagenic primer, 5'-AGGGAGACTTATTTACCC-3' (mutated base is underlined). The primer was then extended using T4 DNA polymerase and all 4 dNTPs in presence of T4 DNA ligase. Transformation of *E. coli* strain JM103 was carried out as described by Sambrook *et al.* (1989). The resulting plaques were screened for presence of mutation by plaque hybridization using ^{32}P-end labeled mutagenic primer. Single-stranded DNA from positive plaques was prepared and the region of interest was sequenced. The introduction of mutation was 129 bases upstream of the normal *uncD* stop codon, and thus shortened the β subunit by 43 amino acids.

In order to construct a derivative of pHN1 (containing same sequences as pHN1 but having the stop codon mutation), I used the following strategy. The 1.2-kb *EcoR*I-*Aat*II fragment from a phage that contained the desired mutation was cloned into the 6.2-kb *EcoR*I-*Aat*II fragment of pHN1. This resulted in an intermediate plasmid, pHN13, containing the entire *uncC* but lacking the 5' end of *uncD*. The 5' *uncD* region was restored by ligating the 1.9-kb *Xma*III fragment of pHN1 into the 5.8-kb *Xma*III fragment of pHN13. The resulting plasmid pHN14 was identical to pHN1 with the mutation C6953A (bases numbered according to Walker *et al.* (1984)).

pGD12, a derivative of pHN1, containing a stop codon 27 bases upstream of the normal *uncD* stop codon was kindly provided by Garry Dallmann (Dallmann and Dunn, 1994).

(v) Sequencing of Single Stranded DNA

Single-stranded DNA from the M13 plaques were prepared as described by Sambrook *et al.* (1989). The sequence between the *Xma*III site in *uncD* and the *Aat*II site in *uncC* was confirmed by the dideoxy sequencing method of Sanger *et al.* (1977). The sequencing reaction was carried out using 1-2 μg of single-stranded DNA, 1 pmol of a primer and [α-^{35}S]ATP by following the protocol provided with the "sequencing kit" from Boehringer Mannheim.

(vi) Bacterial Growth

Cells were grown at 37°C with shaking in Luria-Bertani broth (Sambrook *et al.*, 1989). Selective media for the strains carrying expression plasmids contained 40 μg/ml carbenicillin. During early logarithmic growth isopropyl-β-D-thiogalactoside (IPTG) was added to a concentration of 1 mM to induce expression. After 10 min of induction, samples were removed and RNA was extracted by the method described in the previous chapter, originally published by Mackie (1989).

(vii) Temperature Shift Experiments

The temperature sensitive RNase E mutant strains and their respective wild type isogenic strains carrying pHN1 were grown at 30°C to early log phase (A_{600}=0.2). Half of the culture was then shifted to 43°C and the other half kept at 30°C. After incubation for 30 min at the two temperatures, expression was induced by addition of IPTG to 1mM. RNA was extracted from samples taken after 10 min of induction to compare steady-state pHN1 mRNA levels. Rifampicin was then

added to a final concentration of 0.1 mg/ml and RNA was extracted from samples taken at various times.

(viii) Northern Analysis

Samples of the extracted RNA were run on either polyacrylamide or agarose gels. In polyacrylamide gel Northern blot analysis, RNA was size fractionated on a 6% polyacrylamide gel containing 8 M urea in 1X TBE (0.09M Tris, 0.09 M Borate, 2.5 mM EDTA) buffer at 180 V for 90 minutes. The RNA was electroblotted to Zeta-probe membrane as described in Chapter 2. Agarose Northern blot analysis was performed by fractionation of RNA samples on a 1.25% agarose gel in 10 mM sodium phosphate buffer, pH 7.0, for 3 hrs at 80 V after treatment of RNA with glyoxal at 55°C for 60 min in the presence of dimethyl sulfoxide. The RNA was then vacuum blotted to an Amersham Hybond-N filter with 3 M NaCl, 0.3 M sodium citrate (20X SSC) as transfer buffer for 2.5 hrs. RNA was fixed to the membrane by illumination of the blot with ultraviolet light for 3 min and drying *in vacuo* for 60 min at 80°C. Pre-hybridization and hybridization with the appropriate probe were carried out at 55°C as described by Mackie (19886). The procedure is described in more detail in Chapter 2 (section 2.2).

Probes were detected using two different methods. Filters hybridized with ^{32}P-labelled probes were subjected to autoradiography for 16-24 hrs. Alternatively, hybridization was detected using the digoxygenin-UTP (DIG-UTP) system marketed by Boehringer Mannheim Biochemica. Filters hybridized with probes labelled with DIG-UTP were blocked with 2% "Blocking reagent for nucleic acid hybridization and

detection" at room temperature for 3 hrs and then incubated with high-affinity anti-DIG Fab fragments conjugated to alkaline phosphatase for 30 min. The membrane was washed in 100 mM Tris-HCl, 150 mM NaCl, pH 7.0 at room temperature for 1 hr, with two changes of wash solution. The membrane was then incubated with the Lumi-Phos 530 substrate for 30 min at 37°C and exposed to X-ray film to record the chemiluminescent signal for 1 to 30 min.

(ix) Labelling of Hybridization Probes

For Northern analysis, antisense RNA transcribed *in vitro* using T7 RNA polymerase was used as a probe. The *unc*C probe was prepared by the *in vitro* transcription of pHN3 linearized with *Nco*I producing antisense RNA to the region between *Hpa*II and *Nco*I sites in the *unc*C gene. pHN7 linearized with *Eco*RI and pHN8 linearized with *Bam*HI were used to prepare the *uncD* and *uncB* probes, respectively. The *uncD* probe was directed to the region between the *Sal*I and *Eco*RI sites in the *uncD* gene and the *uncB* probe was directed to the region between the *Bam*HI and *Rsa*I sites in the *uncB* gene. *In vitro* transcription was carried out as described in Chapter 2 (section 2.2 (vii)).

(x) 5'-end Mapping of the Processed Transcript by Primer Extension

A synthetic oligonucleotide primer, 5'-TTAATGGCGGTGAGCAGC-3', complementary to a region 122-139 bases into the *unc*C coding sequence, was radioactively end-labelled with [γ-^{32}P]ATP using T4 polynucleotide kinase as described by Sambrook *et al.* (1989). RNA was hybridized to the labelled primer by

treatment for 2 min at 90°C, 10 min at 40°C and 10 min on ice and then the primer was extended for 45 min at 50°C by 200 U of M-MLV reverse transcriptase (New England Biolabs) in the presence of 50 mM Tris-HCl, pH 8.3, 75 mM KCl, 10 mM DTT, 3 mM $MgCl_2$ and 0.5 mM of each dATP, dCTP, dGTP, and dTTP. Products were denatured and analyzed on a 6% polyacrylamide/8 M urea sequencing gel, along with the pSD38-based sequencing ladder.

3.3 RESULTS

(i) Processing in the 3′ End of the *unc* mRNA Derived From Various *uncC* Expression Plasmids

It is often difficult to analyze degradation of *E. coli* mRNA because of its rapid turnover. Efforts to understand the degradation of the constitutively expressed *unc* mRNA is even more difficult because of its length. Therefore, smaller segments of the *unc* operon were cloned into expression plasmids under the control of the *tac* promoter so that expression could be induced by addition of IPTG.

The portions of *unc* operon carried by plasmids used in expression studies, and the locations of the antisense probes, are shown in Figure 3.1. Plasmids pSD44, pSD38, pGD2, pSD39, and pTK1 constitute a nested set of *uncC* expression plasmids containing inserted sequences beginning at various restriction sites in the *uncD* gene, and extending through the *uncC* gene and the *unc* transcription terminator, as previously described (Dunn and Dallmann, 1990). RNA from induced cultures of strains carrying these plasmids was analyzed by Northern blots using an antisense RNA probe complementary to the 3′-end of the *uncC* sequence (Fig. 3.2). The

Figure 3.2 Analysis of *unc* message transcribed *in vivo* from various plasmids. Northern blot analysis of mRNA transcribed from a set of *uncC* expression plasmids. Equal total RNA (1 μg) from the induced *E. coli* strain JM103 carrying various plasmids was size-fractionated on a 6% polyacrylamide/8M urea gel, and Northern blot analyses were performed using the [^{32}P]-labelled *uncC* probe as described in the *Materials and Methods*. RNA was from *E. coli* strains bearing recombinant plasmids pSD39 (lane 1), pKK223-3 (lane 2), pSD44 (lane 3), pSD38 (lane 4), pGD2 (lane 5), pSD39 (lane 6), pTK1 (lane 7). All samples except that in lane 1 were from induced samples. The size markers are shown on the left.

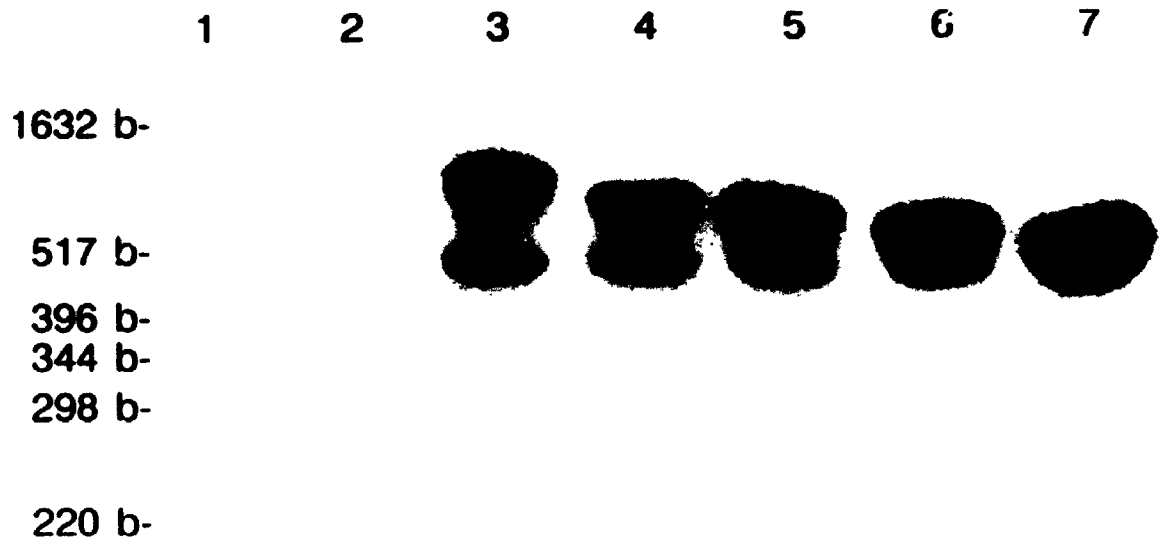
1
2
3
4
5
6
7
1632 b-
517 b-
396 b-
344 b-
298 b-
220 b-

controls, an induced culture carrying pKK223-3 (lane 2) and non-induced culture carrying pSD39 (lane 1) gave no signal. All the induced strains (lanes 3-7) carrying recombinant plasmids contained two species that hybridized with the *uncC* probe. Both of these species appeared only after induction, excluding the possibility that they arose from different promoters. The upper band in each case was of the expected size for the full length message; one can see that as the size of the cloned fragment increased, the size of the upper band also increased. The smaller species of mRNA, about 0.5 kb, was the same size in all the induced strains. This band was likely the 3′ end of each full length message, since all the constructs had a common 3′ end and the probe was directed toward the 3′ end of the message. This suggested that the smaller species arose from the full length messages by some process of nucleolytic decay. One can estimate from the size of the smaller band that its 5′ end is near the beginning of the *uncC* gene, which encodes the ϵ subunit of the F_1-ATPase. There appeared to be little or no effect of the amount of upstream *uncD* sequence on the efficiency of the processing.

(ii) Processing of Message Derived From a Plasmid Containing *uncDC*

Messages transcribed from pSD13 (Fig. 3.1), which carries the entire *uncDC* region, were analyzed to determine the fate of the sequence upstream from the processing site and to determine the role of *uncD* translation on the processing event. RNA samples from a strain carrying pSD13 were analyzed by Northern blots using either *uncD*- or *uncC*-specific antisense RNA probes (Fig. 3.3A). The high molecular weight bands (larger than 2.0-kb) detected with both probes were due to presence

Figure 3.3 Analysis of the *uncDC* mRNA. (A) Northern blot analysis of mRNA transcribed from plasmid pSD13. One μg of RNA from strain JM103 bearing the plasmid pSD13, induced (lanes 1), pSD13, non-induced (lanes 2), and pUC8, induced (lanes 3) was separated on a 1.25% agarose gel and Northern hybridization with the [^{32}P]-labelled *uncD* and *uncC* probe was carried out as described in the *Materials and Methods*. (B) A schematic representation of the pHN1 derivatives containing *uncD* stop-codon mutations. The open boxes represent the *uncD* and *uncC* coding region, and the shaded box shows the *unc* transcription terminator. The bases are numbered as defined by Walker et al. (1984). (C) Effects of *uncD* translation on the processing. Northern blot analysis of pHN1 and its mutant derivatives containing the *uncD* stop-codon mutations (pGD12 and pHN14) was carried out using DIG-labeled *uncC*-specific probe as described in the *Materials and Methods*. Only the part of the blot near the 2.0-kb and 0.5-kb band is shown.

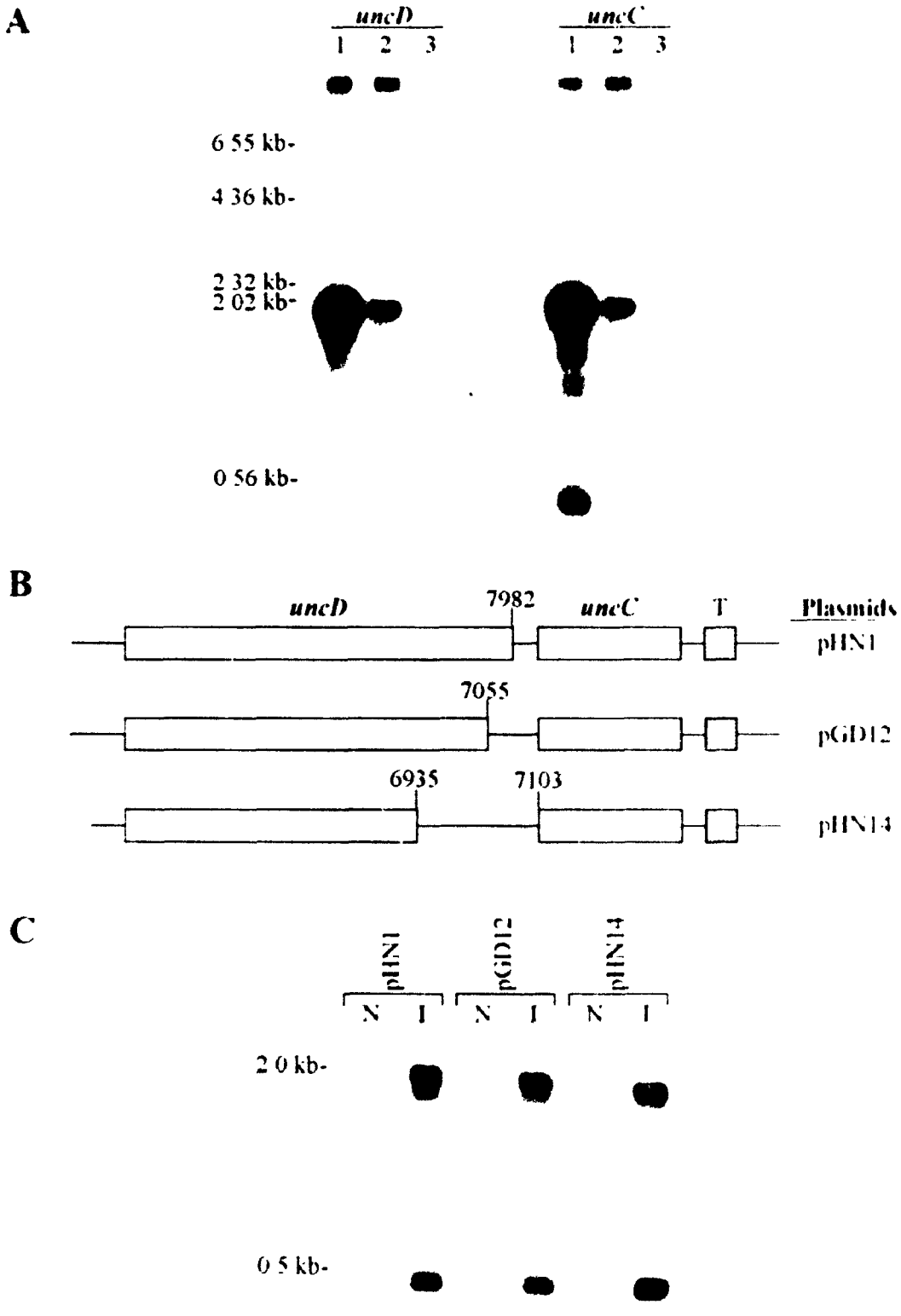
A
uncD
1 2 3
uncC
1 2 3
6 55 kb-
4 36 kb-
2 32 kb-
2 02 kb-
0 56 kb-
B
uncD
7982
uncC
T
Plasmids
pHN1
7055
pGD12
6935
7103
pHN14
C
pHN1
pGD12
pHN14
N I N I N I
2 0 kb-
0 5 kb-

of the plasmid DNA that sometimes copurifies during RNA preparations as DNAse I treatment of the RNA samples resulted in disappearance of these bands (data not shown). Some of the bands at the top are seen irrespective of induction (lanes 1 and 2) but are not seen in lanes 3 which received RNA from a strain containing the parental vector, pUC8. These must be the pSD13 plasmid DNA which contains sequences that can hybridize to the *unc*-specific probes.

The *uncC* probe recognized both the 2-kb full length message and the expected 0.5-kb processed message, but the *uncD* probe recognized only the 2-kb message (Fig. 3.3A, compare lanes 1). One might expect the *uncD* probe to recognize a 1.5-kb species, corresponding to the message upstream of the processing site. The failure to detect such a product implies that, upon processing, the sequences upstream of the cleavage site were degraded quickly.

The full length (2.0-kb) and the processed (0.5-kb) transcripts were also present in the uninduced control (lanes 2), suggesting that expression from the *tac* promoter is not completely repressed under normal condition. This could be due to pUC8 being a high copy number plasmid. Therefore, a new plasmid pHN1, containing the same insert as pSD13, was constructed using pEX1 as the parental vector (Passador and Linn). pEX1 is a derivative of pKK223-3 (Brosius and Holy,1984) bearing a *lacI*^{q} gene so that expression can be regulated in any strain.

To investigate whether the translation of the 3'-end of the *uncD* message just upstream from *uncC* has any effect on the processing, stop codons were introduced upstream of the normal *uncD* stop codon. Site-directed mutagenesis (Carter, 1987) was used to introduce stop codons 27 or 129 bases upstream of the normal *uncD* stop

codon. The pHN1 derivatives containing the mutations are shown in Fig. 3.3B. The mutations in pGD12 and pHN14 changed the intercistronic region between the *uncD* and the *uncC* genes from 20 to 40 and 149, respectively. The resulting β subunits, encoded by *uncD*, would be shortened by 9 (pGD12) and 43 (pHN14) amino acids.

Comparison of the steady state levels of mRNA from a strain carrying the wild type *uncDC* and the mutated *uncDC* showed no significant difference in the levels of the full length and the processed message (Fig. 3.3C). Thus, it seems that the translation of the 3'-region of the *uncD* message has no effect on the processing.

(iii) Processing in the chromosomally-encoded *unc* mRNA

To determine whether the observed processing also takes place on the chromosomally-encoded *unc* message, total RNA from various strains without any expression plasmid was analyzed also by Northern blots (Fig. 3.4). Because the chromosomally-encoded messages are far less abundant than those from induced multi-copy plasmids, much larger amounts of RNA were used in this experiment, compared to the experiments described in the earlier figures. RNA from an *unc* deletion strain, DK8 (lanes 2), was included in the experiment to distinguish *unc* transcripts from non-specific signals. The *uncC* probe exhibited considerable affinity for the abundant ribosomal RNA species at 2.9 and 1.5 kb, while the *uncD* probes faintly recognized only the 2.9-kb species. RNA from strain 1100 (lanes 1), the *unc*$^+$ parent of DK8, contained a major *unc*-specific species of about 6 kb recognized by both probes. Several less-abundant intermediate species were also recognized by both probes, while only the *uncC* probe recognized a 0.5-kb species. These fragments

Figure 3.4 Northern blot analysis of chromosomally-encoded mRNA from various strains. RNA from various strains was subjected to Northern blot analysis using the [^{32}P]-labelled *uncD* and the *uncC* probes. Lanes 1, 1100 (*unc*$^+$); lanes 2, DK8 (*unc*$^-$); lanes 3, SK5006 (*pnp*$^+$, *rnb*$^+$); lanes 4, SK5005 (*pnp*$^+$, *rnb*$^-$); lanes 5, SK5004 (*pnp*$^-$, *rnb*$^+$); lanes 6, SK5003 (*pnp*$^-$, *rnb*$^-$); lanes 7, JM103/pSD13, induced sample. Lanes 1-6 received 15 μg and lane 7 received 1 μg of total RNA.

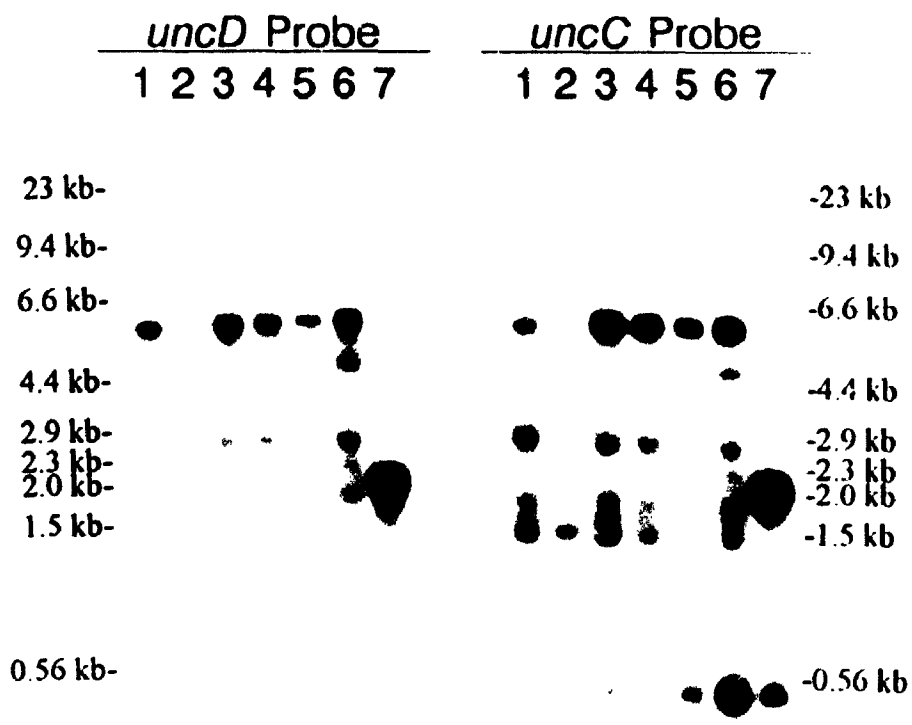
uncD Probe
1 2 3 4 5 6 7
uncC Probe
1 2 3 4 5 6 7
23 kb-
9.4 kb-
6.6 kb-
4.4 kb-
2.9 kb-
2.3 kb-
2.0 kb-
1.5 kb-
0.56 kb-
-23 kb
-9.4 kb
-6.6 kb
-4.4 kb
-2.9 kb
-2.3 kb
-2.0 kb
-1.5 kb
-0.56 kb

of *unc* transcript apparently constitute a nested set with a common 3′ end, presumably the normal 3′ end of the complete transcript, as they are all recognized by the *uncC* probe which is complementary to the 3′ end of operon. The 0.5-kb species comigrated with the processed message from plasmid pSD13 (lane 7), implying that the processing event described above for plasmid-encoded message also occurs in the chromosomally-encoded *unc* message. RNA samples prepared from a set of 3′-exonuclease-deficient mutants were also analyzed (lanes 3-6). Compared to the wild-type control strain (lane 3), mutations in either ribonuclease II (lane 4) or polynucleotide phosphorylase (lane 5) had no apparent effect on the level of the 0.5-kb *uncC*-specific band, but the double mutant (lane 6) had strongly elevated levels of this species. This result implies that ultimate degradation of the processed fragment is mediated by exonucleolytic decay.

(iv) Determination of the 5′-end of the processed transcript

The 5′ end of the processed message was mapped precisely by extension of a primer complementary to the mRNA sequence about 100 bases into the *uncC* gene. cDNA synthesis was carried out by M-MLV reverse transcriptase and the products were electrophoresed alongside the products of dideoxy nucleotide sequencing reactions on a sequencing gel (Fig.3.5).

Primer extension products obtained using RNA from strains carrying various recombinant plasmids are shown to the right of the sequencing ladder. Extension products representing the full length pSD38 message (F) and the processed message (P) are indicated. Note that the processed message from the strain carrying pSD13

Figure 3.5 Primer extension analysis of RNA from strains carrying plasmids pSD38 and pSD13. An end-labelled primer was used to prime cDNA synthesis using total cellular RNA from *E. coli* JM103 bearing the indicated plasmid as a template. The products were analyzed on a 6% polyacrylamide sequencing gel along with pSD38-based dideoxy-sequencing ladder. A control (lane labelled *in vitro* RNA) in which the primer was extended on a message transcribed *in vitro* from pHN6 was used to determine reverse transcriptase stops that were due to secondary structure. The bands corresponding to the full length (F) transcript of pSD38 and the processed message (P) are indicated on the right. Also shown is a band (S) representing a reverse transcriptase stop. I, induced; N, non-induced samples.

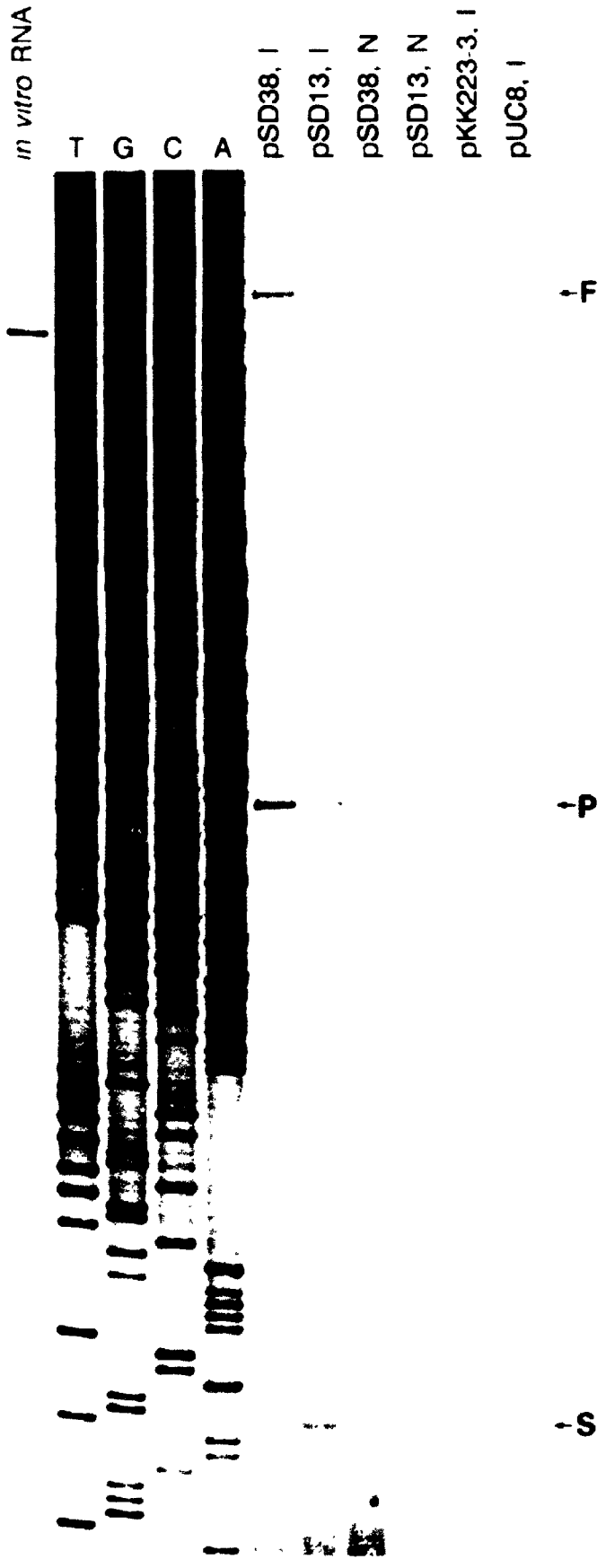
in vitro RNA
T
G
C
A
pSD38, I
pSD13, I
pSD38, N
pSD13, N
pKK223-3, I
pUC8, I
F
P
S

(contained complete *uncD*) has the same 5' end as that from the strain carrying pSD38 (contained 3'-end of *uncD*). A shorter product (S) present in both of these samples corresponds to a site previously noted by Schaefer *et al.*(1989). Primer extension by RNA transcribed *in vitro* using T7 RNA polymerase also produced the S band, implying that it represents a stop site for reverse transcriptase due to secondary structure. The P band was not seen in this sample, implying that it arose from extension of transcripts processed *in vivo*. The 5' end of the processed transcript was mapped to be 11 bases into the coding region of *uncC* gene. The sequence shown in Fig. 3.6 shows that the processing removes most of the *uncC* coding sequence from the initiating codon and the ribosomal binding site, and at the same time leaves the upstream *uncD* sequence accessible to exonucleolytic attack.

(v) Dependence of the *uncC* processing on RNase E

The recent work implicating RNase E in the processing and degradation of specific mRNA's in *E. coli* prompted us to examine the effect of temperature-sensitive mutations in this enzyme on the cleavage in the *uncC* message. Two RNase E mutant strains, SK5665 (*ams*-1, recently renamed *rne*-1 (Babitzke and Kushner, 1991) and N3431 (*rne*-3071), both of which have reduced RNase E activity at the restrictive temperature, were transformed with the plasmid pHN1. RNA was extracted from induced cells bearing pHN1 and Northern blot analyses were performed with the *uncC*-specific antisense RNA probe (Fig. 3.7A). Both mutants and their isogenic wild type strains produced low but detectable levels of the processed fragment at the permissive temperature of 30°C. However, at 43°C each

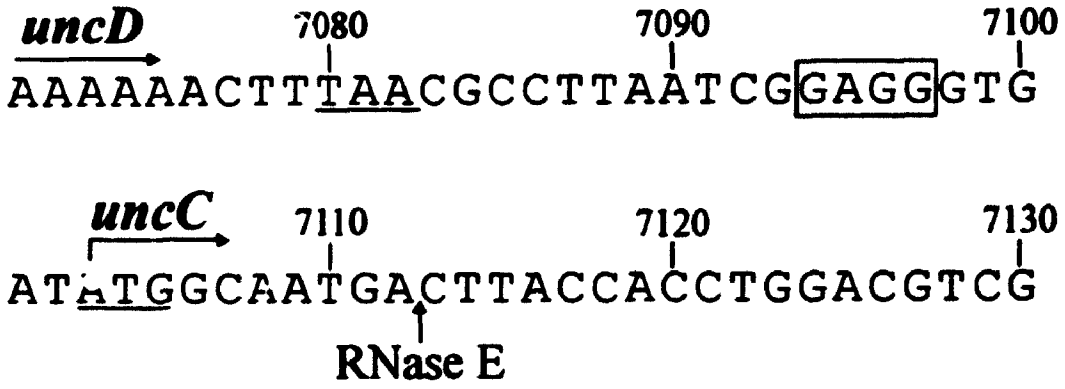

Figure 3.6 Nucleotide sequence of the intercistronic DNA regions between the *uncD* and the *uncC* gene. The *uncD* stop codon and the *uncC* initiation codon are underlined, and the *uncC* ribosome binding site is shown in a box. The position of the RNase E processing site is shown by an arrow. The bases are numbered according to Walker *et al.* (1984).

Figure 3.7 Analysis of mRNA species transcribed from plasmid pHN1 in various *E. coli* strains. *E. coli* strains MG1693 (*ams*$^+$), SK5665 (*ams-1*), N3433 (*rne*$^+$), and N3431 (*rne-3071*) bearing pHN1 were grown to early-log phase at 30°C, shifted to 43°C, and induced as described in the *Materials and Methods.* Ten min after induction, samples were taken for RNA extraction to compare steady state levels. Rifampicin was then added at time zero to block initiation of transcription and samples were collected for RNA extraction at the indicated time points. Northern blots of the RNA samples were performed using the DIG-UTP-labelled *uncC* probe as described in the *Materials and Methods.* N, non-induced samples. (A) Comparison of steady-state message levels. All lanes received 0.44 μg of RNA. (B) and (C) Degradation of the pHN1 message in MG1693 (*ams*$^+$) and SK5665 (*ams-1*) at 30°C and 43°C respectively.

A.

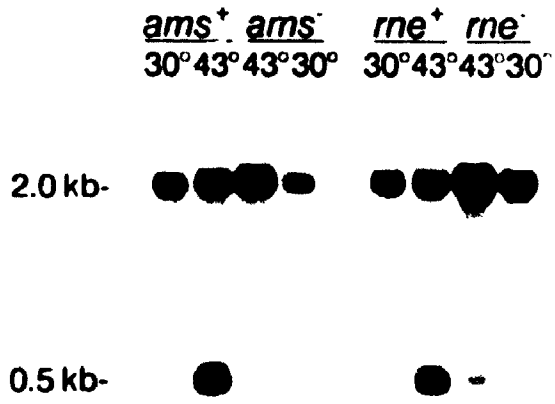
ams+ ams- rne+ rne-
30°43°43°30° 30°43°43°30°
2.0 kb-
0.5 kb-

B. 30°

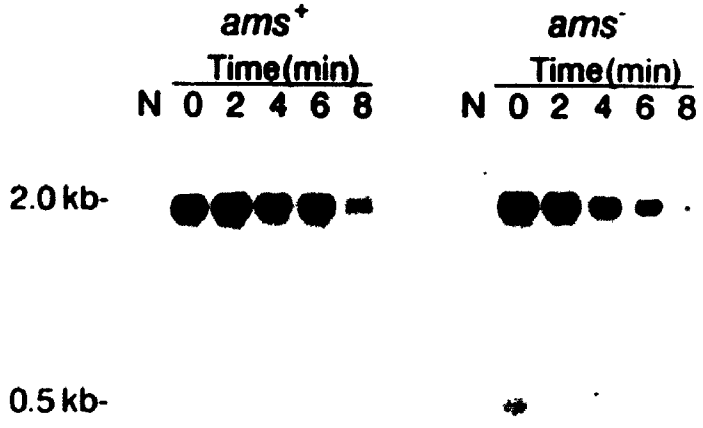
ams+
Time(min)
N 0 2 4 6 8
ams-
Time(min)
N 0 2 4 6 8
2.0 kb-
0.5 kb-

C. 43°

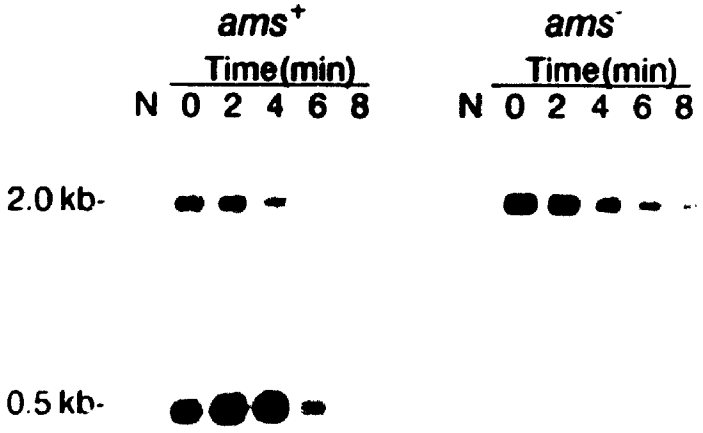
ams+
Time(min)
N 0 2 4 6 8
ams-
Time(min)
N 0 2 4 6 8
2.0 kb-
0.5 kb-

of the mutants contained f[illegible] lower levels of the 0.5-kb processed message and higher levels of the 2-kb intact message than the wild-type controls at that temperature. These results imply that RNase E is essential for the processing in the *uncC* message.

One surprising observation was the extreme elevation of the 0.5-kb product at 43°C compared to the 30°C in the RNase E wild type strains. There were no apparent differences in the levels of the full length message eliminating the possibility of variation in the processing. Thus, the observed differences imply an increased stability of the processed product at the higher temperature, but the reason for such a striking stabilization is not apparent.

The absence of 0.5-kb cleavage product at the restrictive temperature in the mutants can be most easily explained by an inhibition of the cleavage. An extreme destabilization of the processed product at the restrictive temperature could also explain the disappearance of the smaller product. However, if this were the case then the levels of the full length precursor message should be same in the mutants and in the wild type isogenic strains. As all the strains carried the same plasmid, it seemed unlikely that rates of synthesis would be responsible for the different steady state levels of the full length transcript. Analysis of the half-life of the pHN1 message in strains MG1693 (*ams*$^+$) and SK5665 (*ams*$^-$) grown at 30°C (Fig. 3.7B) or 43°C (Fig. 3.7C) supported a role for RNase E in the processing event. Cells were induced with 1 mM IPTG for 10 min, then rifampicin was added to inhibit further transcription. Northern blot analysis of RNA samples prepared at different time points after addition of rifampicin revealed that the 2.0-kb pHN1 message was degraded with a half-time of about 2 min at 30°C in both strains. At 43°C, the half-

life was 4 min in the *ams*$^-$ strain but just 2 min in the *ams*$^+$ strain. This stabilization in the mutant strain, and the lack of significant amounts of the 0.5-kb product, imply a role of RNase E in the cleavage. A similar difference in stability was found when the pHN1 transcript was compared in the *rne*$^-$ and *rne*$^+$ strains (data not shown). The residual degradation of the full length message in the mutant strains is apparently mediated by the exonucleases, as no stable intermediates can be detected.

(vi) Processing of the Chromosomally-encoded *unc* Message in the RNase E Mutants

To determine if the processing in the chromosomally-encoded *unc* message is also affected in the RNase E mutant, RNA samples extracted from strains MG1693 (*ams*$^+$) and SK5665 (*ams*$^-$) lacking plasmids were analyzed by Northern blots using the *uncC*-specific probe (Fig. 3.8, left panel). The expected 0.5-kb downstream cleavage product was detected at the restrictive temperature in the *ams*$^+$ strain (lane 3), but was not seen in the *ams*$^-$ strain (lane 2). Notice that the message was faintly visible in both strains at the permissive temperature (lanes 1 and 4). This implies that cleavage of the chromosomally-encoded *unc* message in the *uncC* coding region is also mediated by RNase E. As in the case of the plasmid-encoded message described above, levels of the 0.5-kb fragment is substantially elevated at the higher temperature in the wild-type strain (compare lanes 2 and 3). The probe did not detect any species in the *unc* deletion strain (lane 6) suggesting that all the bands seen in the other lanes are *unc*-specific.

One interesting observation was the appearance of a 7-kb species in the *ams*$^-$

Figure 3.8 Requirement of RNase E for the processing of the chromosomally-encoded *unc* message. Equal amounts of total cellular RNA (10 μg) from various *E. coli* strains were analyzed by Northern blot using the *uncC*- and the *uncB*-specific antisense RNA probes. Lanes 1 and 2, SK5665 (*ams-1*) at 30°C and 43°C respectively; lanes 4 and 3, MG1693 (ams^+) at 30°C and 43°C respectively; lanes 5, 1100 (unc^+); lanes 6, DK8 (unc^-).

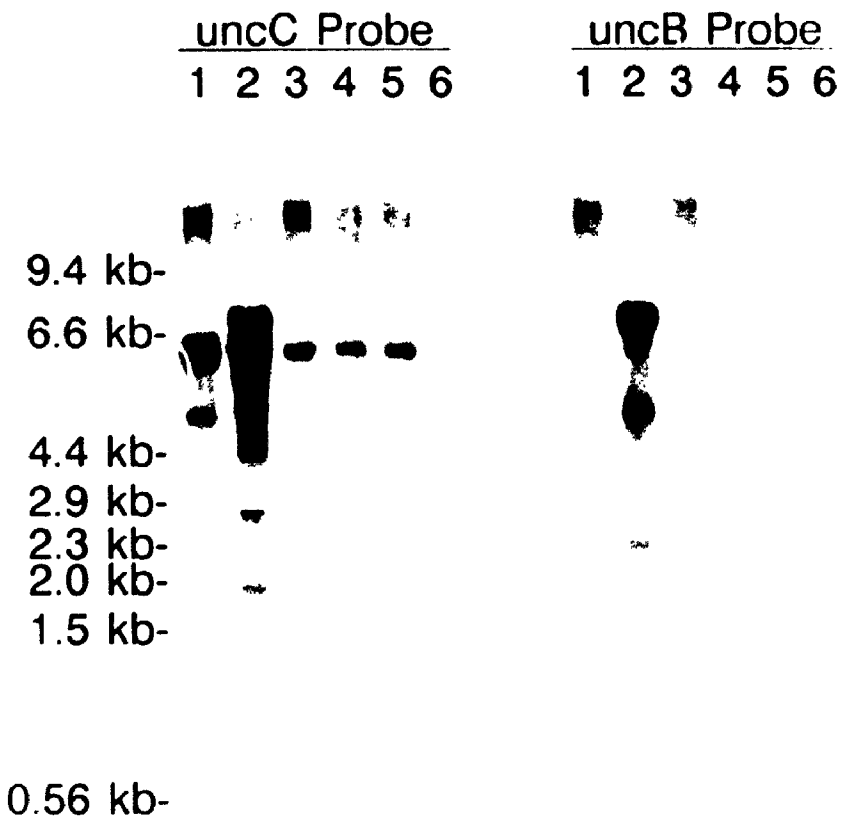
uncC Probe
1 2 3 4 5 6
uncB Probe
1 2 3 4 5 6
9.4 kb-
6.6 kb-
4.4 kb-
2.9 kb-
2.3 kb-
2.0 kb-
1.5 kb-
0.56 kb-

strain at 43°C (lane 2). This species was not present under conditions where RNase E was active. In the right-hand panel, note that the 7-kb species was also detected with a probe to the 5′ end of the *uncB* gene (lane 2). However, the *uncB* probe failed to recognize any such species in RNA extracted from cells having an active RNase E (lanes 1, 3-5). In particular, the major 6-kb species detected with the *uncC* probe did not hybridize with the *uncB* probe. This implied that the 6.0-kb species is lacking the 5′ region of the full length *unc* mRNA. Based on the size of the *unc* operon, and the data described above, the 7-kb species likely represents the intact message. The absence of this message in wild-type cells implies that nascent *unc* transcripts are cleaved in an RNase E-dependent reaction at one or more sites in the *uncB* region near the 5′ end before transcription of the operon is complete.

3.4 DISCUSSION

The results presented here demonstrate post-transcriptional endonucleolytic processing of the primary *unc* message to produce discrete mRNA species. It is unlikely that the products were derived by 5′ to 3′ exonucleolytic processing, as there is no known 5′ to 3′ exonuclease in *E. coli*. Furthermore, the appearance of the 7-kb band and the absence of the 0.5-kb *uncC* fragment in strains lacking the endonuclease RNase E implicate this enzyme in processing both ends of the message.

The role of RNase E in the processing of the *uncC* mRNA was indicated by the findings that the RNase E mutant (*ams-1* or *rne-1*) contained higher steady-state levels of the pHN1-derived 2-kb message, that this message had a longer half-life, and by the virtual absence of the 0.5-kb product. The nucleotide sequence around

the *uncC* cleavage site, AAUGA↓CUUAC, is also consistent with RNase E involvement (Ehretsmann *et al.*, 1992). Demonstration of a direct role of RNase E in the cleavage will require *in vitro* studies with a purified preparation of the enzyme.

The residual mechanism of degradation of the 2-kb message in the *ams* mutant produced no stable intermediates, suggesting the involvement of the 3'-exonucleases. In the previous Chapter it was shown that the *unc* terminator hairpin imparts substantial protection against exonucleolytic attack (Patel *et al.*, 1990, also Chapter 2); the present results suggest that this protection is not absolute.

The cleavage of the *uncC* message about 10 bases into the coding region has several implications. First, it leads to functional inactivation of the *uncC* message by removing the ribosome binding site and the initiating codon from the rest of the coding region. The cleavage is interesting because it occurs at a site that will minimize the stranding of ribosomes on a faulty message. It creates a truncated mRNA species which can not load ribosomes, and translationally inactive messages may be more prone to degradation (Belasco and Higgins, 1988). Secondly, the absence of any upstream product of the cleavage must reflect a very short half life.

In accordance with the subunit stoichiometry of F_1F_o-ATPase, *uncD* is more highly expressed than *uncC*. However, the processing has no apparent role in controlling the differential expression of the β and ϵ subunits as it leads to inactivation of both the *uncD* and *uncC* genes. More likely, this processing may be an important event in the overall degradation of the *unc* mRNA. In support of this idea, the total levels of *unc* message were markedly increased in the *ams* mutant. The relative importance of the *uncC* site to any others is not certain, but this site is

well situated to initiate the exonucleolytic degradation of the upstream *unc* message, as well as inactivating the final *uncC* cistron directly.

Using RNA extracted from the RNase E mutant, I have detected a 7-kb chromosomally-encoded species which I believe to be the full-length *unc* transcript. This message is of the expected size and hybridizes to probes to both the 5′ (*uncB*) and the 3′ (*uncC*) regions of the operon. The 7-kb species is barely detectable in *ams*$^+$ strains, implying that it is rapidly processed in wild-type cells to produce the 6.2-kb species that hybridizes with *uncC* but not with *uncB*. Based on the *in vivo* mRNA elongation rate of 42 nucleotides/s (Gotta *et al.*, 1991), transcription of the *unc* operon should require 2 to 3 minutes. This allows ample time for processing a site near the 5′ end before transcription of the 3′ end is completed.

Previously, chromosomally-encoded *unc* message has been studied by Jones *et al.* (1983), by McCarthy and coworkers (1988), and by Schaefer *et al.* (1989). The results reported here agree with those of the latter two groups in demonstrating the presence in wild-type cells of a major 6.2-kb message lacking the 5′ end of the operon. The studies with the *ams*$^-$ mutant extend their findings by demonstrating the existence of the precursor 7-kb message that includes *uncB*, and in implicating RNase E in its conversion to the 6.2-kb species. The full-length plasmid-borne *unc* message has been detected by McCarthy *et al.* (1991).

The processing in the 5′ end of the *unc* mRNA may be important in the differential expression of some *unc* genes. The upstream *uncIB* message is apparently degraded, as no species of the appropriate size was detected with the *uncB* probe. These results correlate well with those demonstrated by McCarthy and

coworkers (1991). These authors reported that the functional half-lives of the *uncI* and *uncB* messages are just one to two minutes, compared to five to twelve minutes for the third gene in the operon, *uncE*. The almost complete absence of the 7-kb transcript in *rne*$^+$ cells (Fig. 3.8) implies that the physical half-lives of *uncI* and *uncB* are short relative to the two to three minutes required to synthesize the complete message. The rapid degradation of the 5′ end can be expected to restrict the levels of proteins expressed from the first two genes. It should be noted in this regard that *uncB* gene product, the hydrophobic *a* subunit, occurs in just one copy per ATP synthase molecule and is known to be toxic if overexpressed (Eya *et al.*, 1989).

Two RNase E cleavage sites have recently been identified by Gross (1991) in the *uncBE* intercistronic region of hybrid plasmid-encoded messages. Experiments discussed in Chapter 5 identified the same sites in chromosomally-encoded *unc* message extracted from *rne*$^+$ cells. The 5′-ends produced by cleavage at these sites are located 27 and 45 bases upstream from the *uncE* initiation codon.

Some of the other species seen on Northern blots, such as the 5-kb species detected with the *uncC* probe, were not affected by the *ams*$^-$ mutation. If these arise through endonucleolytic processing, it seems likely that other nucleases are involved.

In conclusion, studies presented in this chapter demonstrate that both ends of the 7-kb *unc* message are subject to RNase E-dependent endonucleolytic processing. The 5′ processing events appear to be involved in reducing the half-lives of the first two genes, while we speculate that the 3′ event may initiate degradation of the major 6-kb message that remains. The functional implication of the processing in the *uncC* message is investigated in the next chapter , and the processing in the

5′ end of the *unc* message is analyzed further in the Chapter 5.

CHAPTER 4

SECONDARY STRUCTURE IN THE *uncC* mRNA LIMITS ITS EXPRESSION AND IS ESSENTIAL FOR RNase E-DEPENDENT CLEAVAGE

4.1 INTRODUCTION

As described in Chapter 1, the genes of *E. coli unc* operon, which encodes all the subunits of the F_1F_0-ATP synthase, are expressed in a such a way as to accommodate the subunit requirements. The gene order for the subunits of the synthase is *uncBEFHAGDC* and the stoichiometry of respective subunits is a_1c_{9-15} $b_2\delta_1\alpha_3\gamma_1\beta_3\epsilon_1$. Since the subunits are expressed from a single polycistronic message, the regulation of the relative expression of the *unc* genes must occur at the post-transcriptional level.

It has been shown that the control of the differential expression of the *unc* genes is primarily regulated at the point of translation initiation. In general the translational efficiency of a given message depends largely on the nature of primary and secondary structure of the translation initiation region (TIR) (de Smit, 1990; Gold, 1988). The ribosome binding site (Shine-Dalgarno sequence), initiation codon and the distance between the two are important factors in determining the efficiency of translation initiation (Dreyfus, 1988; Gold, 1988; Jacques and Dreyfus, 1990; Ringquist *et al.*, 1992). It has been well documented that secondary structures in the TIR of mRNA can interfere with the binding of ribosomes to the Shine-Dalgarno sequence (S-D), and therefore lower the rate of translation initiation (de Smit and van Duin, 1990). In particular, secondary structures located within polycistronic messages have been shown to regulate the relative expression of genes in some operons, primarily through translational coupling where translation of the downstream gene depends on the translation of the upstream gene (Adhin and van Duin, 1989; de Smit and van Duin, 1990; Oppenheim and Yanofsky, 1980; Schmidt

et al., 1987; Wikstrom *et al.*, 1992).

There is considerable evidence for involvement of secondary structures in the regulation of the *unc* genes. First, Klionsky *et al.* (1986) have shown that a putative stem-loop structure in the *uncEF* intergenic region down regulates the expression of the *b* subunit, the *uncF* gene product. Secondly, McCarthy and co-workers have reported that secondary structures play an important role in the efficiency of translation initiation of individual *unc* genes (McCarthy and Bokelmann, 1988; Gerstel and McCarthy, 1989; Hellmuth *et al.*, 1991). In particular, Hellmuth *et al.* (1991) clearly demonstrated that the translation of *uncHA* is coupled through a putative secondary structure which is found in the intercistronic region between the two genes. Recently, Rex *et al.* (1994) physically mapped the aforementioned structure and demonstrated that the coupling involves a conformational switch in the secondary structure of the *uncHA* mRNA, induced by translation of the upstream *uncH* message. They proposed that this "switch" in the conformation of the mRNA allows efficient translation initiation of the *uncA*. Thirdly, the role of secondary structure in controlling the expression of *uncH* (encoding δ) was well documented by Pati *et al.* (1992). They used an in-frame *lacZ* fusion to *uncH* to show that destabilizing the mRNA secondary structure preceding *uncH* resulted in a considerable increase in the expression of *uncH*, and that its expression is translationally coupled to the upstream *uncF* gene.

Recently, Dallmann and Dunn (1994) demonstrated that a stable mRNA secondary structure in the *uncDC* intercistronic region is involved in the differential expression of β and ϵ, the *uncD* and *uncC* gene products, respectively. This structure

(Fig. 4.1B) which sequesters the *uncD* stop codon and the *uncC* S-D sequence was the first structure in the *unc* mRNA to be physically mapped by chemical and enzymatic probes. In their physical determination of the structure, the authors also obtained evidence for the presence of another independent secondary structure in the early *uncC* coding region (Fig. 4.1B). This structure, which starts 14 bases from the *uncC* initiation codon, was also predicted by the RNA folding program FOLD of the University of Wisconsin Genetics Computer Group (Devereux *et al.*, 1984; Zuker and Stiegler, 1981). The 3' boundary of this structure corresponded to the stop of M-MLV reverse transcriptase in the primer extension analysis of *in vivo* and *in vitro* transcribed *uncDC* mRNA that was reported in the previous chapter (Patel and Dunn, 1992). The two independent stem-loops are separated by a 16 base single-stranded region containing the RNase E processing site which was mapped in the previous Chapter. The free energy of formation of the structure in *uncC* mRNA was calculated to be -23.6 Kcal/mol by the method of Freier *et al.* (1986).

In this chapter, I present the results of experiments designed to study roles of the secondary structure in the *uncC* mRNA (downstream of the RNase E cleavage) in the processing by RNase E and in controlling the synthesis of the ϵ subunit. This subunit, which is a competitive inhibitor of F_1 ATPase, plays an important role in the binding of F_1 to F_0 and thus its controlled expression is essential in the assembly and activity of the ATPase complex.

In this work I constructed a series of recombinant plasmids containing *uncDC* with various mutations either in the region close to the actual RNase E cleavage site or in the stem-loop downstream of the site. The influence of these mutations on the

Figure 4.1 (A) Schematic diagram of the *Pst*I-*Pst*I fragment of the *unc* operon containing the *uncDC* genes, encoding the β and ϵ subunits, respectively. The plasmid pHN1 carried the entire shown insert and the plasmid pES2 carried the *Mnl*I-*Pst*I fragment, both cloned into the expression vector pEX1. T, *unc* transcription terminator. (B) Previously mapped secondary structure of the *uncDC* mRNA surrounding the RNase E site in *uncC* (region shown by ⊔ in A). The *uncD* stop codon (UAA) and the *uncC* Shine-Dalgarno (GGAGG) are boxed and the *uncC* start codon (AUG) is underlined. The RNase E cleavage site is shown by an arrow. Bases are numbered according to Walker *et al.* (1984).

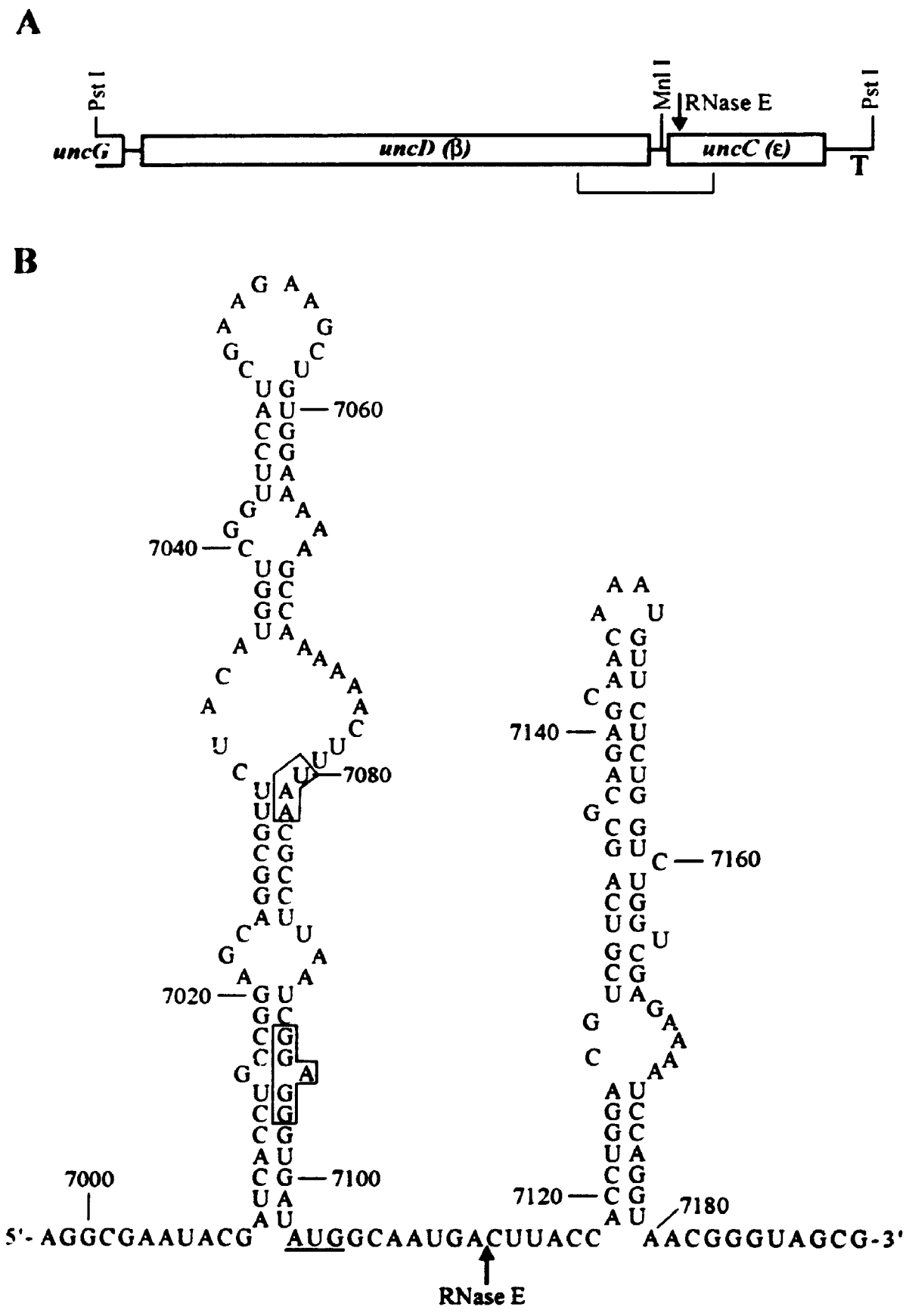
A
Pst I
MnI I
RNase E
Pst I
uncG
uncD (β)
uncC (ε)
T
B
7040
7060
7080
7020
7100
7140
7160
7120
7180
7000
5'- AGGCGAAUACG AUGGCAAUGACUUACC AACGGGUAGCG-3'
RNase E

processing by RNase E and on the translation efficiency of the *uncDC* mRNA which encodes β and ϵ, respectively, was investigated. The distance between the S-D sequence of the *uncC* and the base of the secondary structure downstream of the RNase E site in *uncC* was altered to examine its effect on the expression of the *uncC* gene product. The mechanism by which this structure limits the expression of *uncC* is discussed.

4.2 MATERIALS AND METHODS

(i) Enzymes and Chemicals

Taq DNA polymerase was from Promega, T7 DNA polymerase was from Pharmacia and T4 DNA polymerase was from New England Bio-Labs. Other reagents were described in Chapters 2 and 3.

(ii) Bacterial Strains and Growth

E. coli strains JM103, MG1693 and SK5665 have been described in earlier chapters. The *E. coli* strain MM294 (*supE44 hsdR endA1 pro thi*) (Meissner and Yuan, 1968) was used in an experiment involving ϵ expression. Strains carrying plasmids were grown at 37°C with shaking in LB medium (Sambrook *et al.*, 1989) containing 40 μg/mL carbenicillin. Temperature shift experiments performed to inactivate RNase E were carried out as described in Chapter 3.

(iii) Plasmid Construction

Recombinant DNA procedures were carried out by standard methods

(Sambrook *et al.*, 1989). The construction of plasmid pHN1 which contained *uncDC* was described in Chapter 3 (also see Fig. 4.1A). Plasmid pES2, constructed by Eileen Skakoon (Skakoon and Dunn, 1993a), contains the *Mnl*I-*Pst*I fragment (Fig. 4.1A) bearing the *uncC* gene and the *unc* transcription terminator. pHN3, which was used to make *in vitro* transcribed *uncC*-specific riboprobe, was described in Chapter 2. Plasmid pHN35 was constructed by digesting pSD13 (Patel and Dunn, 1992) with *Sma*I and *Sac*I followed by blunting the *Sac*I end by T4 polymerase and subsequently ligating the blunt ends with T4 DNA ligase. The difference between pSD13 and pHN35 is that the latter is missing the 5′ *uncD* sequences. Construction of the derivatives of pHN1 and pES2 having mutations at various sites in the *uncC* gene which were used to study RNase E processing and for the determination of relative β and ϵ expression is discussed below.

The position of nucleotide labeled through out the chapter is according to Walker *et al.* (1984). The complete nucleotide sequence of the *uncDC* is shown in the appendix.

Construction of pHN1 Derivatives Containing Mutations at the RNase E Cleavage Site—To study the effect of mutations at the RNase E site on the processing, the codon ACU, encoding Thr-4 of ϵ, was mutated by M13-based oligonucleotide-directed mutagenesis using the method of Carter (1987). The phage M13GD9 (Dallmann and Dunn, 1994) which contained the 1.7-kb *Sal*I-*Pst*I fragment (3′*uncD* and *uncC*) of the *unc* operon cloned into the M13mp8 (Messing *et al.*, 1981) was used as a template for mutagenesis. A degenerate oligonucleotide, 5′-

CCAGGTGGTARGNCATTGCCATATC-3' (R=C, G ; N=A, C, G, T) was used to introduce the change. Single-stranded DNA derived from M13GD9 was annealed to the mutagenic primer and extended using T4 DNA polymerase as described in Chapter 3 (Section 3.2). Plaques were screened using an oligonucleotide with the wild type sequences, 5'-GTGGTAAGTCATTGC-3', since the primer used for the mutagenesis was degenerate at two positions. Plaques which readily lost the radioactive label were selected as positives containing the desired mutations. Single stranded DNA was prepared from 25 positive plaques and sequenced by the dideoxynucleotide triphosphate method using T7 DNA polymerase (Sanger *et al.*, 1977) The sequencing primer, 5'-TTAATGGCGGTGAGCAGC-3', was complementary to a region 122 to 139 bases into the *uncC* coding sequence. Out of eight possible mutations only three were repeatedly obtained. They were T7113G(M13HN16), T7113C(M13HN17) and A7111C (M13HN18), with the M13GD9 derivative shown in parentheses. Subcloning of all these single mutations into pHN1 through the intermediate plasmids (pHN19, pHN20, pHN21) was carried out by the procedure described in Chapter 3. The corresponding pHN1 derivatives with the mutations were called pHN23 (T7117G), pHN24 (T7113C) and pHN25 (T7111C).

Double mutations in the plasmids pHN29 (ACU→CCG) and pHN30 (ACU → CCC) were created by the same method and strategy described above. To mutate ACU→CCG, the phage M13HN16 (T7113G) was used as a template with the mutagenic primer, GTGGTACGGCATTGCCAT (mutation is underlined). To mutate ACU→CCC, the phage M13HN17 (T7117C) was used as a template with the

mutagenic primer, GTGGTACCCCATTGCCAT (mutation is underlined).

Construction of pHN1 Derivatives with Mutations in the Stem-loop Structure—Mutations to alter the stability of the stem-loop were carried out by PCR. The plasmid pSD15 (Patel *et al.*, 1990) was used as a template in the PCR reaction. It contained the 1.2-kb *Pst*I fragment of the *unc* operon bearing part of *uncD* and all of *uncC* cloned into pUC8. The two mutations (C7121T, G7123A), both at sites near the base of the stem on the 5′ side (Fig. 4.1B) were constructed with the mutagenic primer 5′-GACGACGTCTARGTGGTAAGTC-3′ (R=G, A). The mutated bases are underlined and the *Aat*II restriction site used for subcloning the mutation is shown in bold. The PCR reaction using the mutagenic primer, the universal reverse sequencing primer (5′-CAGGAAACAGCTATGAC-3′) and pSD15 linearized with *Hind*III was carried out using Taq DNA polymerase as described by Sambrook *et al.* (1989). Basically, 100 pmol of each primer and 16 ng of the template plasmid was mixed with 0.2 mM of dNTPs, 5U of the enzyme, and 1X amplification buffer supplied with the enzyme by Promega in a total volume of 100 μl. The cycle for the reaction was 1 min denaturation at 94°C, 2 min annealing at 50°C and 3 min polymerization at 74°C. Thirty cycles were carried out. The products were digested with *Aat*II and *EcoR*I and cloned into the *EcoR*I and *Aat*II sites of pHN1, and the resulting intermediate plasmids were called pHN31(C7121T) and pHN32(C7121T, G7123A). The mutations were confirmed by sequencing before constructing the derivatives of pHN1 with the desired mutations (pHN33 and pHN34 carrying C7121T and C7121T, G7123A, respectively).

The pHN1 derivatives, pHN40 (C7174T, G7177A) and pHN41 (A7180G), which contained mutations near the base of the stem on the 3' side (Fig. 4.1B) were constructed by PCR using a similar approach. The mutations C7174T and G7177A was introduced with the primer, 5'-CTGGTCGAGAAAATTCAAGTAACGGG-3'. (the mutations are underlined and the *Taq*I site used for subcloning is shown in bold). The PCR reaction using *Hind*III cut pSD15 (as a template), the mutagenic primer and a second primer, 5'-CAGATAGATAAACTCTTCG-3' was carried out as described above. The PCR products was digested with *Taq*I and *Mam*I. The digested PCR product was then ligated into pHN35 which was partially digested with *Taq*I (so as to get about one cut per molecule) and digested to completion by *Mam*I. A preliminary screening of transformants with the insertion of the PCR product at the correct location was carried out by screening for production of ϵ using a colony-lift method (Helfman and Hughes, 1987). ^{125}I-labeled monoclonal antibody ϵ-1 (Dunn *et al.*, 1985) was used, followed by confirmation of the mutation by sequencing. The mutations were passed into pHN1 by the normal procedure and the resulting plasmid was named pHN40 (C7174T, G7177A).

Strengthening of the stem by mutation (A7180G) in pHN41 was performed using the primer, 5'-CTGGTCGAGAAAATCCAGGTGACGGGTAGCG-3' by following the procedure outlined above. The mutated base in the primer is underlined and the *Taq*I site is indicated in bold.

Construction of Deletion and Insertions Derivatives of pHN1—The deletion of the fourth codon of ϵ, AUG (Fig. 4.1B), and insertion of codons between third

and fourth codons of ϵ (Fig. 4.1B) was carried out by PCR using the method similar to that used to construct the stem-loop mutation in pHN33 and pHN34.

The primer for the deletion mutation was 5'-GACGACGTCCAGGTGGTAAG 'TTGCCATATCACCC-3' (site of deletion is shown by prime) and that for the insertionwas5'-GACGACGTCCAGGTGGTAAGTCATRGRTGCCATATCACCC-3' (R= T, A, codon inserted is underlined), with the *Aat*II site used for subcloning shown in bold. Three identified insertion derivatives of pHN1 were pHN48 (ACT), pHN49 (TCA) and pHN50 (TCT), with the inserted codon shown in parentheses. The deletion derivative of pHN1 was pHN39 (ΔAUG).

The hybrid derivatives of pHN1 containing the insertion mutations and the mutation A7180G were constructed by cloning the *Aat*II fragments of the insertions plasmids (pHN48, pHN49 and pHN50) into the large *Aat*II fragment of pHN41 (A7180G). The resulting derivatives with the insertion and A7180 were called pHN50, pHN52 and pHN53.

Construction of *uncC* Expression Plasmids Containing Mutations—In order to construct a set of plasmids containing only the *uncC* gene (with mutations), Dr. S.D. Dunn used the following procedures. Plasmids pHN34, pHN39, pHN41, pHN49 and pHN52 were initially digested with *Mnl* I, followed by filling of the overhangs by T4 DNA polymerase and then subsequent digestion with *Hind*III. The *Mnl*I-*Hind*III fragments which contain the mutations were cloned into the *Sma*I and *Hind*III sites of the vector pEX1, resulting in mutant forms of pES2, expressing only *uncC*. The resulting plasmids were named according to the source they were derived from. For

example pES2-34 was a mutant form of pES2 containing the same mutation that was present in pHN34.

The plasmids pES37 and pES137 which contained deletions in *uncC* were described earlier (Skakoon and Dunn, 1993b). pES37 contained the deletion of GACGTC, encoding amino acid residues Asp-7 and Val-8 of ϵ and pES137 contained deletion of a 24-base sequence encoding amino acid residues Asp-7 through Gln-14 of ϵ.

(iv) RNA and Protein Extraction

Expression was induced by addition of IPTG to a final concentration of 1 mM to early logarithmic phase cultures of strains carrying plasmids. Control cultures received no IPTG. After 10 min of induction, samples were taken for RNA and protein preparation. RNA was extracted from a 1 mL of culture as described in Chapter 2. For the protein preparations 1 mL samples were removed, chilled, sedimented, and extracted for 5 min at 100°C with electrophoresis sample buffer containing 2% SDS.

(v) Northern Blots and Primer Extension Analysis

Equal amounts of total mRNA were size-fractionated either on 1.25% agarose gels or on 6%polyacrylamide-8 M urea gels as indicated in earlier chapters. All the routine procedures used to process the blots were described in detail in Chapters 2 and 3. The riboprobe used to detect the *unc*-specific transcripts was produced by *in vitro* transcription of pHN3, linearized with *Nco*I. The label was provided by DIG-

UTP (refer to Chapter 3 for more detail).

Primer extension analysis of RNA extracted from strains carrying plasmids was performed as described in Chapter 3, using M-MLV reverse transcriptase and ^{32}P-labeled primer. The primer, 5'-TTAATGGCGGTGAGCAGC-3', complementary to a region 122 to 139 bases into the *uncC* coding sequence was radioactively end-labeled with [γ-^{32}P]ATP by using T4 polynucleotide kinase as described by Sambrook *et al.* (1989).

(vi) SDS-PAGE and Western Blots

SDS-PAGE was carried out on 15% gels using the buffer system of Laemmi (1970). Proteins were electroblotted to Immobilon-P PVDF transfer membranes (Millipore) using carbonate blot buffer as described by Dunn (1936) and analyzed immunochemically (Dunn *et al.*, 1985) using ^{125}I-labeled monoclonal antibodies β-6 and ϵ-4 (Dunn *et al.*, 1985). Iodination of the antibodies was carried out by the Iodo-Gen method (Fraker and Speck, 1978).

In the Western blot analysis signals for β were normally stronger compared to ϵ because of the differences in the amounts of the subunits, the specificity of the antibody and the labelling of the antibody. Therefore, in some of the experiments the signal for β was reduced by putting a red plastic film between the x-ray film and the intensifying screen. In the later experiments 0.5 mL of unlabeled β-6 hybridoma culture supernatant was included with the 10 mL of solution during the probing of the blots with radiolabeled antibodies.

(vii) Quantification of Relative Levels of β and ϵ Expression

Cultures of *E.coli* strains carrying derivatives of either pHN1(expressing β and ϵ) or pES2 (expressing ϵ) were grown in LB medium with constant shaking. IPTG was added to final concentration of 0.1 mM at A_{600} of 0.2. After 10 min of induction 1 mL of samples were taken, cells were precipitated by centrifugation and proteins were extracted by boiling in a electrophoresis buffer containing 2% SDS. Equal amounts of each whole cell culture extract along with known amounts of purified F_1-ATPase standards were subjected to SDS-PAGE on four 15% gels and blotted as described above. Blotting was done using a Bio-Rad Trans-Blot Cell at 1 Amp for 2 hours. The blot buffer was cooled during the transfer by water circulation through glass cooling coils inserted in the blot cell. Blocking and probing of the blots with ^{125}I-labeled MAbs β-6 and ϵ-4 (50,000 dpm/mL) was done according to Dunn (1986). To reduce the signal for β, 0.5 mL of unlabeled β-6 hybridoma culture medium supernatant was included during the probing. Blots were rinsed twice in 5 mL of 1X rinse buffer containing 0.1% BSA for 2 min, immediately stained in Amido black 10B (0.1% Amido black in 5% acetic acid, 45% methanol) for 10 min. Blots were then destained in 90% methanol and 2% acetic acid, and washed in water. They were exposed to x-ray films after drying them at room temperature. β and ϵ bands of each sample from all the four blots were cut and the radioactivity was counted in a Beckman Model Gamma 8000 gamma counter.

Known amounts of purified F_1-ATPase were used to calculate the absolute molar amounts of β and ϵ produced from each plasmid. A linear relationship between the amounts of F_1 standards and radioactive counts was obtained in all the

Western blots.

4.3 RESULTS

(i) Effect of Mutations at the RNase E Site on the Cleavage

Studies in the previous chapter identified an RNase E-dependent cleavage site in the early coding region of the *uncC* mRNA which functionally inactivates the *uncC* message and exposes the upstream message to exonucleolytic degradation. Cleavages by RNase E have been implicated in initiating decay of many *E. coli* mRNA (Mudd *et al.*, 1988; Yajnik and Godson, 1993; Petersen, 1992) and we wished to investigate if this cleavage is important in the overall degradation of the *unc* mRNA and if it contributes to the differential expression of the *unc* genes. At the time the studies were begun it was not clear what features of the mRNA are necessary for cleavage by RNase E. It was known that the cleavages occur in A-U-rich regions and that sequences adjacent to these sites have the potential to form secondary structures. Plasmid pHN1 (Fig. 4.1A) which contains the *uncDC* genes was used to elucidate the sequences and structures required for cleavage by RNase E. As indicated earlier the plasmid was constructed using the vector pEX1, a derivative of pKK223-3 carrying the $lacI^q$ gene. The constitutive expression of the $lacI^q$ gene product, the *lac* repressor, prevents significant expression from the *tac* promoter under non-inducing conditions.

Five mutations in the codon ACU, encoding Thr-4 of ϵ, (Fig. 4.2A) were introduced as described in the Materials and Methods. Northern analysis of mRNA extracted from induced cultures of strains carrying pHN1 and its mutant derivatives

Figure 4.2 (A) Point mutations constructed at the RNase E cleavage site in the *uncC* mRNA. The arrow indicates the position of the RNase E cleavage site and the box shows the codon that is mutated, with the mutations shown in bold below the box. The appropriate change in the amino acid and the names of the plasmids are also shown. All the plasmids are derivatives of pHN1. **(B) and (C)** Northern analysis of the point mutants shown in A. *E. coli* strain JM103 carrying the mutant derivatives of pHN1 were grown at 37° to A_{600} of 0.2, and subsequently induced with 0.1mM IPTG for 10 min, followed by RNA extraction. Equal amounts of total RNA (1μg) was size fractionated on a 1.25% agarose gel, blotted to nylon membrane, and hybridized with the *uncC*-specific probe. The 2.0-kb band is the full length transcript and the 0.5-kb band represents the processed species. N, un-induced sample; I, ir duced sample.

A

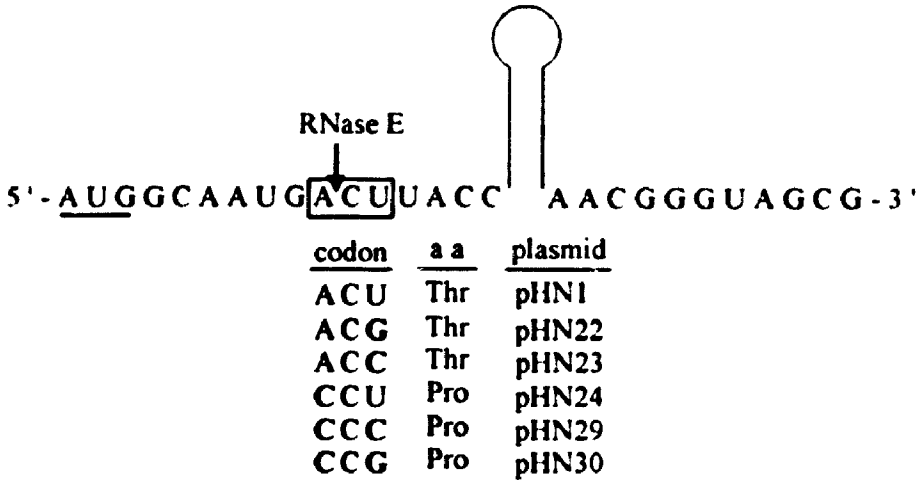

codon	a a	plasmid
ACU	Thr	pHN1
ACG	Thr	pHN22
ACC	Thr	pHN23
CCU	Pro	pHN24
CCC	Pro	pHN29
CCG	Pro	pHN30

B

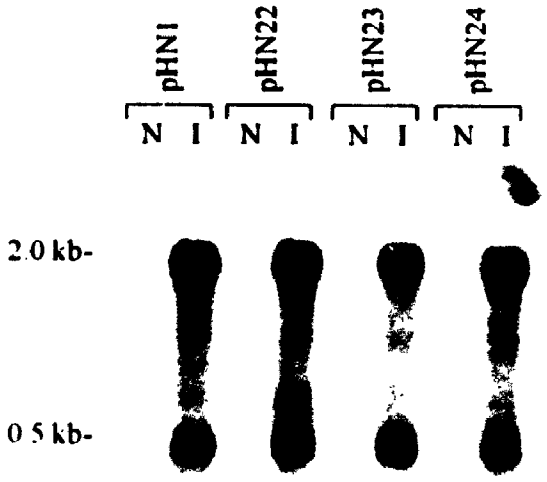

C

using the *uncC*-specific probe are shown in Fig. 4.2B and C. In the three single mutants (pHN22-24, Fig. 4B) the full length (2.0-kb) and the processed species (0.5-kb) were detected at levels similar to that of pHN1, indicating that these changes did not affect processing. Out of the two double mutants (Fig. 4.2C), the mutation CCG (pHN30) had somewhat reduced levels of the processed species compared to pHN1, but the levels of the full length message remained similar. The mutation in pHN29 had no effect on the apparent levels of the two species. These results suggested that alteration of the site in most cases did not change the efficiency of the cleavage, with only minor reduction in pHN30 and that the mutations had no affect on the stability of the full length primary transcript. The probe did not recognize any transcript in the un-induced samples (N), suggesting that expression from the IPTG inducible *tac* promoter was repressed well under normal conditions.

Transcripts containing the various mutations were mapped by primer extension to see if the 5' ends of the processed species in these mutants remained same as that seen in pHN1 (Fig. 4.3A). The cleavages were generally made in the same region but the precise positions were altered in pHN22, pHN29 and pHN30 as shown in Fig. 4.4.

(ii) Effect of Destabilizing mRNA Secondary Structure on the Cleavage

As seen in the above studies most mutations at the cleavage site did not result in a significant reduction in the cleavage. Therefore, two types of mutations were constructed to alter the stability of the mRNA structure downstream of the RNase E site in *uncC*.

Figure 4.3 Primer extension analysis of RNA from strains carrying pHN1 and its derivatives. (A and B) A ^{32}P-end-labeled primer was used to prime cDNA synthesis, using total RNA (5 μg) from induced cultures of *E. coli* JM103 bearing the indicated plasmid as a template. The products were analyzed on a 6% polyacrylamide sequencing gel along with a pHN1-based dideoxy-sequencing ladder. Only the bands corresponding to the RNase E processed species are shown. pHN1, N; un-induced control.

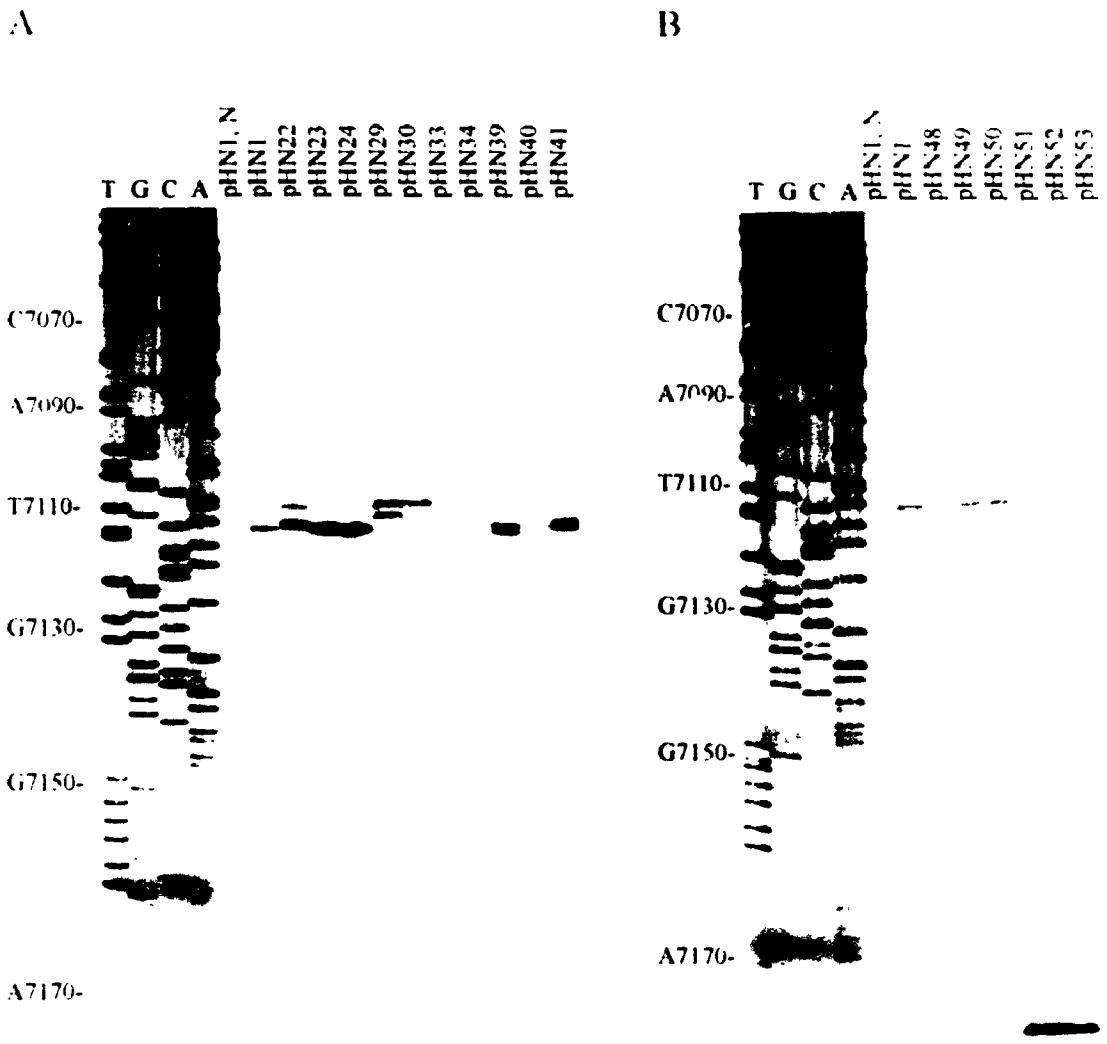
A
T G C A
pHN1, N
pHN1
pHN22
pHN23
pHN24
pHN29
pHN30
pHN33
pHN34
pHN39
pHN40
pHN41
C7070-
A7090-
T7110-
G7130-
G7150-
A7170-
B
T G C A
pHN1, N
pHN1
pHN48
pHN49
pHN50
pHN51
pHN52
pHN53
C7070-
A7090-
T7110-
G7130-
G7150-
A7170-

Figure 4.4 Positions of RNase E cleavage sites in the mutant derivatives of pHN1 as mapped in Fig. 4.3. Mutations in the region 5′ to the stem-loop are shown below the structure with the RNase E site shown by open triangles. pHN48-53 are derivatives with the insertion of a codon represented by NNN in the box. The exact insertion of the codon is shown in Fig. 4.7A. The filled circles indicate the position of extra bands seen in pHN51, pHN52 and pHN53. Cleavage in the derivatives which contain mutations in the base of the stem (pHN33, pHN34 and pHN40) is shown by the filled triangle.

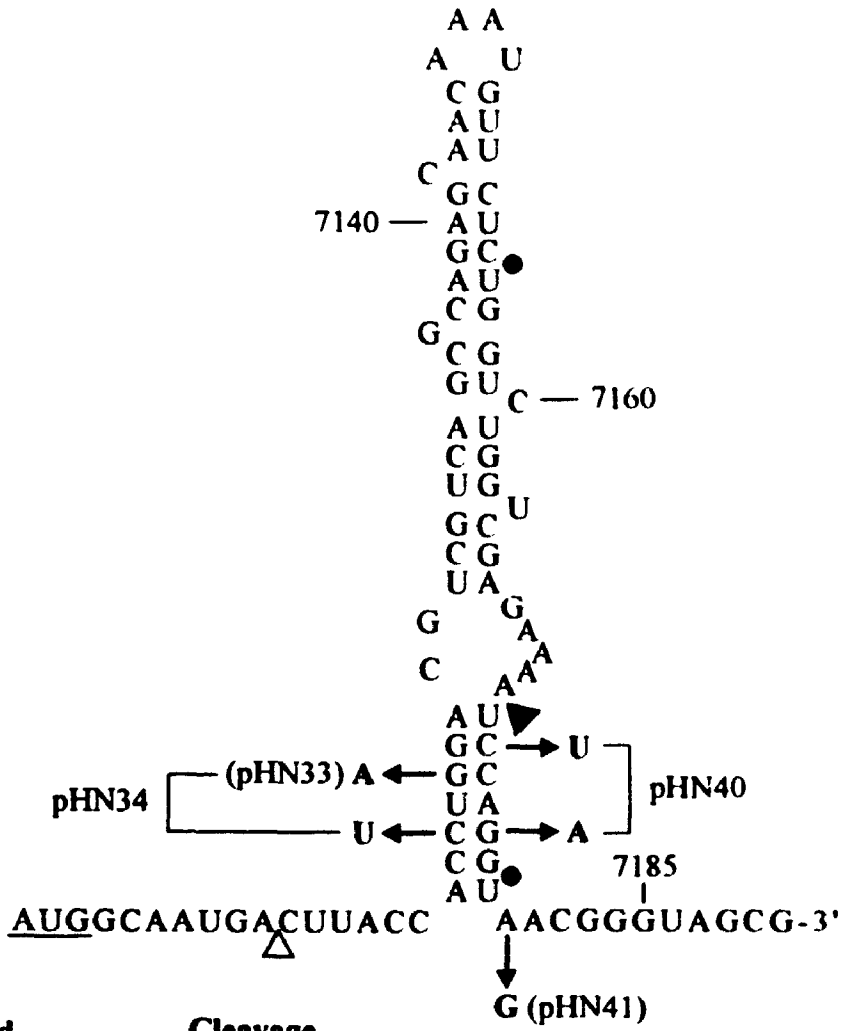

Plasmid	Cleavage
pHN22	GCAAUGACGUAC
pHN23	GCAAUGACCUAC
pHN24	GCAAUGCCUUAC
pHN29	GCAAUGCCCUAC
pHN30	GCAAUGCCGUAC
pHN39	GCA ACUUAC
pHN41	GCAAUGACUUAC
pHN48-53	GCAAUGNNNACUUAC

First, point mutations were made in the base of the stem without changing the encoded amino acid (Fig. 4.5A). The stem-loop was destabilized by mutating G7121 to A in pHN33 and was further destabilized by mutating C7121U in pHN34. Both of these plasmids are derivatives of pHN1. Northern blot analysis using the *uncC*-specific probe revealed that the single mutation in pHN33 caused some decrease in the 0.5-kb processed species, whereas the double mutation in pHN34 resulted in more drastic reduction in the levels of the processed species (Fig. 4.5B). However, levels of the full length transcript in both mutants remained similar to pHN1. The processed product in pHN33 and pHN34 ran somewhat faster than the species from pHN1. Primer extension mapping of the mRNA (Fig. 4.3A) showed that 5'-ends of the processed species in these mutants were different than in the wild type pHN1. The cleavages in pHN33 and pHN34 were mapped at T7173, about 60 bases downstream of the normal site (Fig. 4.4, see filled triangle). Thus blocking the processing at the natural site seemed to give rise to a new cleavage or caused an increase of a previously existing minor site. The levels of the full length message remained similar implying that there was no net affect of reduced cleavage on the levels of the primary transcript. One might argue that the lower levels of the processed species seen in the mutants is due to the species being less stable over the normal processed species.

Secondly, RNA extracted from strains carrying plasmids which had deletion of bases that are involved in forming the stem-loop was analyzed by Northern blotting (Fig. 4.5A). Both deletions would destabilize the structure greatly. These deletion mutations were in plasmids which only contained the *uncC* gene (like pES2),

Figure 4.5 (A) The *uncC* mRNA secondary structure downstream of the RNase E cleavage site, showing the stem-loop mutations. The nucleotides altered in the plasmids pHN33 and pHN34 (derivatives of pHN1) and the nucleotides deleted in the plasmids pES37 and pES137 (derivatives of pES2) are shown. The point mutations in pHN33 and pHN34 do not change the encoded amino acids and the deletions in pES37 and pES137 maintain the rest of the *uncC* reading frame intact. **(B)** Northern analysis of the stem-loop point mutants. Equal amounts of total RNA (1 μg) extracted from induced *E. coli* JM103 bearing the shown plasmid were separated on a 1% agarose gel, blotted to nylon membranes and probed with the *uncC*-specific probe as described in the Materials and Methods. (C) Northern analysis of the stem-loop deletion mutants. Equal amounts of total RNA (1μg) extracted from induced *E. coli* strain JM103 carrying the appropriate plasmids was size fractionated on a 6% polyacrylamide-8 M urea gel, blotted to Zeta-probe membrane and hybridized to *uncC*-specific probe. N, un-induced sample; I, induced sample.

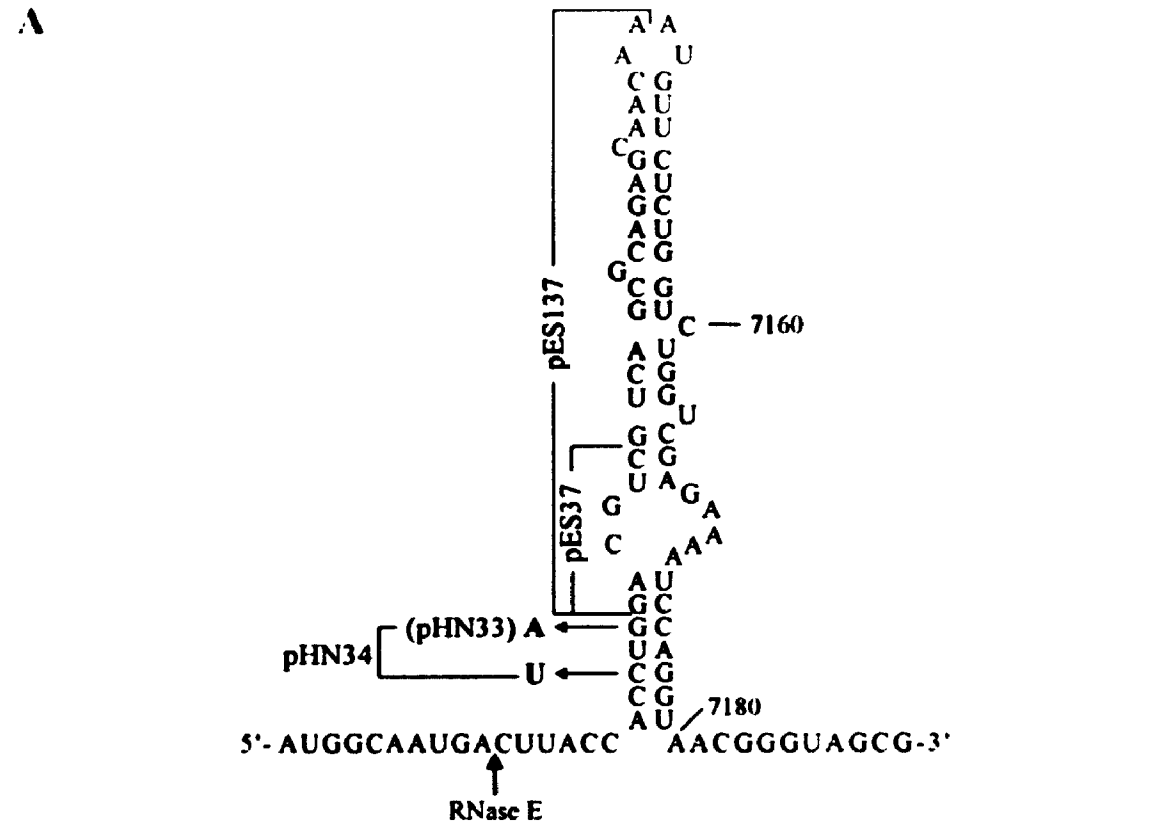
A
pES137
pES37
pHN34
(pHN33) A
U
7160
7180
5'- AUGGCAAUGACUUACC AACGGGUAGCG-3'
RNase E

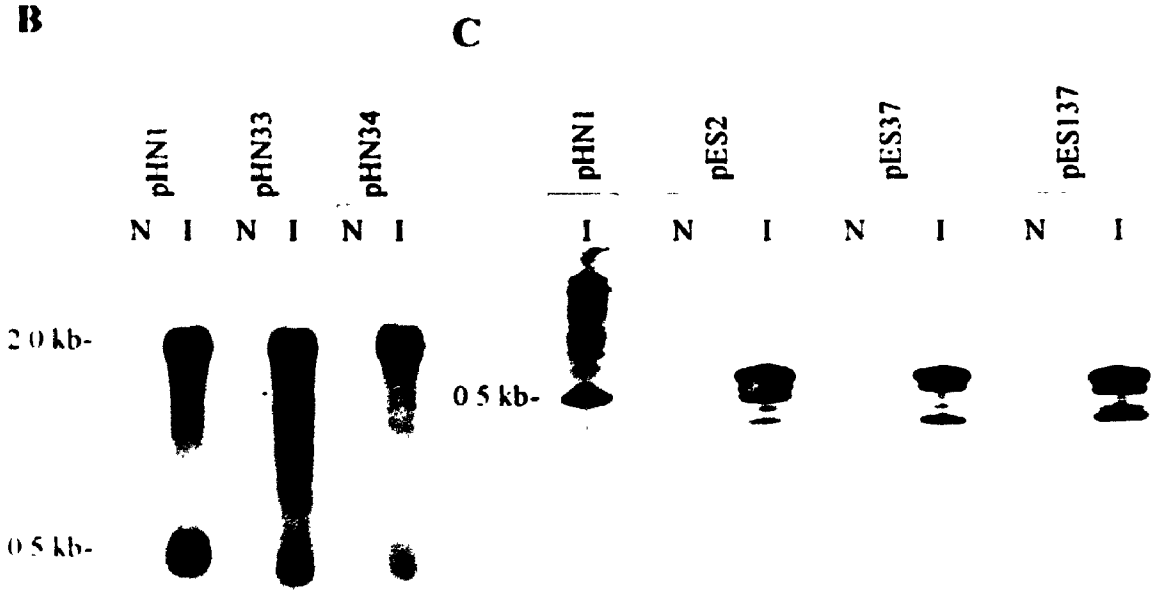
B
pHN1
pHN33
pHN34
N I N I N I
2.0 kb-
0.5 kb-
C
pHN1
pES2
pES37
pES137
I N I N I N I
0.5 kb-

thus Northern blots were performed on a polyacrylamide gels using *uncC*-specific probe (Fig. 4.5C). RNA from a strain containing pHN1 was included in the experiment to assign the position of 0.5-kb processed species usually seen (left lane). The probe detected a number of mRNA species in pES2 and its derivatives containing the deletions. The top band is the full length transcript which is present in similar amounts in all three plasmids. The second species probably arose from cleavage in the leader sequence provided by the vector. The third species, which comigrates with the processed species from pHN1, represents the RNase E cleavage product that is normally seen. This species is present in lower amounts in pES37 and in much lower amounts in pES137, compared to pHN1. This implies that the secondary structure is important for efficient processing. While the levels of the RNase E processed species were reduced, the levels of the two smallest fragments increased in the deletion mutants. This suggests that lowering cleavage at one site resulted in better cleavage at other sites which might normally be weaker sites.

(iii) Effect of Mutations on the Expression of ϵ

In order to investigate if the secondary structure in the *uncC* had any role in regulating the expression of the *uncC gene* product, proteins from strains carrying pHN1 and its mutant derivatives were analyzed for β and ϵ content. Proteins were extracted with boiling SDS sample buffer after 10 min and 1 hr of induction. The 1 hr induced samples were analyzed by SDS-PAGE (Fig. 4.6A, upper panel) and the 10 min induced samples by Western blots using labeled ^{125}I-ϵ-4 and ^{125}I-β-6 monoclonal antibodies (Fig. 4.6A, lower panel). Purified F_1-ATPase was loaded on

Figure 4.6 (A) Effects of mutations at the RNase E cleavage site and in the stem-loop on the expression of *uncC*. Derivatives of *E. coli* JM103 bearing the indicated plasmids were induced with 0.1 mM IPTG when A_{600} reached 0.1. Control (pHN1, N) received no IPTG. After 10 min and 1 hr of induction, cells were extracted with sample buffer containing SDS. **(Upper Panel)** The 1 hr induced samples were analyzed by SDS-PAGE. The two extreme lanes received 5 μg of purified F_1-ATPase as standards. Other lanes received proteins extracted from 100 μl of culture. The gel was stained with Commassie Brilliant Blue R-250. **(Lower Panel)** The 10 min induced samples were analyzed for β and ϵ contents by immunoblotting using ^{125}I-labeled monoclonal anti-β and anti-ϵ. The two extreme lanes received 0.45 μg of purified F_1-ATPase. Other lanes received proteins extracted from the cells in 50 μl of culture. **(B) Time course of *uncDC* expression from pHN30 (Thr→Pro).** *E. coli* strain carrying pHN30 was grown to early exponential phase and IPTG was added to final concentration of 0.1 mM to induce the expression. Aliquots were removed at various time intervals after addition of IPTG. Proteins from equal number of cells were subjected to Western blot analysis as described above. (Note: To reduce the signal for β relative to ϵ, a red plastic film was kept between the area where β is on the membrane and the intensifying screen, as discussed in the Materials and Methods).

A

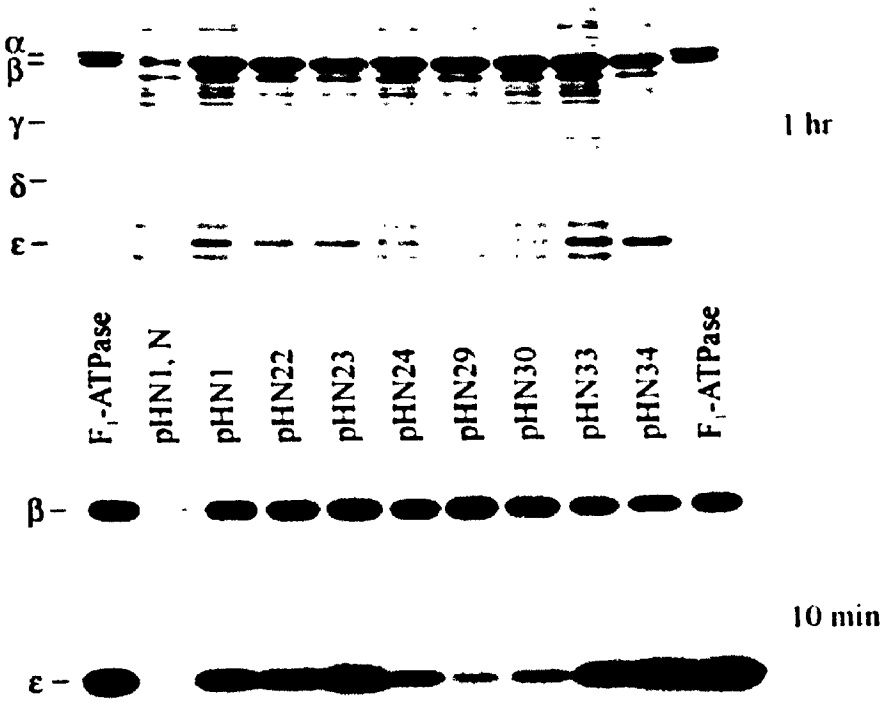
α=
β=
γ–
δ–
ε–
1 hr
F1-ATPase
pHN1, N
pHN1
pHN22
pHN23
pHN24
pHN29
pHN30
pHN33
pHN34
F1-ATPase
β–
10 min
ε–

B

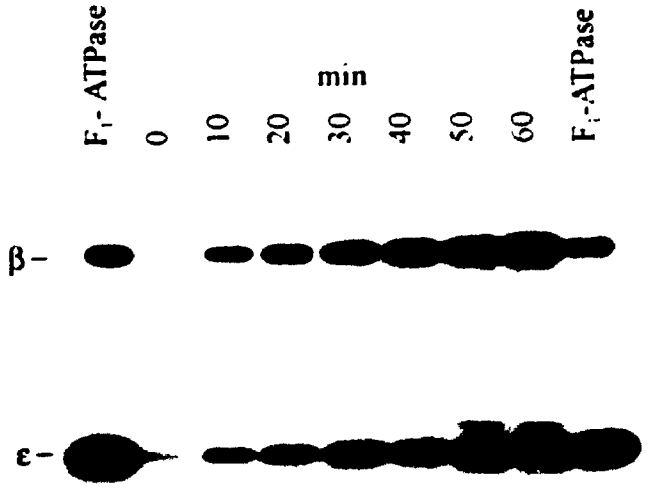
F1- ATPase
min
0
10
20
30
40
50
60
F1-ATPase
β–
ε–

the gels to identify β and ϵ. As can be seen, the expression of β in pHN1 and its derivatives was similar, but variation in the levels of the ϵ was apparent on both gels. In particular, the ϵ content decreased substantially in pHN24, pHN29 and pHN30. The two mutations designed to destabilize the stem-loop (pHN33, pHN34) showed an increase in the ϵ content, the latter having a more dramatic effect.

The observed variation in ϵ expression in these mutants cannot be due to differences in mRNA levels as Northern blot analysis showed similar amounts of *uncDC* mRNA (Fig. 4.2 and Fig. 4.5). Mutants which showed reduced *uncC* expression (pHN24, pHN29 and pHN30) had proline introduced at Thr-4. It could be argued that proline may introduce drastic changes in the structure causing the protein to be unstable. To determine if this is the case cells carrying pHN30 were induced with IPTG, proteins were extracted at various time points after the induction and analyzed by Western blotting as indicated above (Fig. 4.6B). It was apparent that as the time of induction went up the level of ϵ, as well as β, increased. If the low level of ϵ was due to protein instability, rather than slow synthesis, one would expect the levels of the protein to rise rapidly to a steady state level. This result implies that introduction of proline is not the cause of reduction. Rather, a change in the structure of the mRNA might be responsible for the observed affect (see discussion). One may also wonder if reduction in the levels of ϵ in pHN24, pHN29 and pHN30 was due to the introduction of proline causing changes in the epitope for the antibody. However, this could not be the case since the epitope for ϵ-4 has been mapped in the C-terminal half of ϵ (Skakoon and Dunn, 1993b) whereas this mutation was near the N-terminus. Also, the reduction was apparent in the SDS-

PAGE analysis in which the gel was stained with Commassie Blue. The stem-loop destabilizing mutants which showed increased ϵ levels did not change the amino acid sequence of the protein. The double mutant (pHN34) introduced an infrequently utilized UUA codon for leucine, but the levels of ϵ were higher rather than lower.

(Iv) Effects of Mutations on Expression of *uncC* in an *rne*$^-$ Strain

One may wonder if the effects seen above are due to any changes in the processing (since some mutations reduced cleavage) or if they are because the translation efficiency has changed. To investigate these possibilities, I made use of a strain which is deficient in the RNase E activity at higher temperature. If the effects were due to a change in the processing then in an *rne*$^-$ strain there should be no change in the expression because the processing does not occur. On the other hand if the effects are not related to processing then one should see the same effects of the mutations on the expression of *uncC* in *rne*$^+$ and *rne*$^-$ strains.

The three mutant plasmids, pHN30, pHN33 and pHN34, along with the wild type pHN1, were transformed into *rne*$^+$ and *rne*$^-$ strains. The RNase E in the temperature sensitive strain was inactivated by growing the cells at 43°C for 30 min. Proteins were extracted after 10 min of induction and analyzed by Western blotting using ^{125}I-labeled monoclonal antibodies against β and ϵ (Fig. 4.7A). As can be seen in the *rne*$^+$ strain grown at the permissive temperature (30°C) the levels of β subunit remained similar in all the plasmids, whereas the levels of ϵ varied as seen before. Namely, the expression was lower in pHN30, and higher in pHN33 and pHN34, compared to pHN1. At 30°C the levels of β expressed from the plasmids carried in

Figure 4.7 Comparison of β and ϵ expression from various plasmids in *E. coli* strains MG1693 (*rne*$^+$) and SK5665 (*rne*$^-$). Strains carrying the various derivatives of pHN1 were grown to early-log phase at 30°, shifted to 43° and grown at that temperature for 30 min to inactivate RNase E. IPTG was then added to a final concentration of 0.1 mM to induce expression. After 10 min of induction samples were taken for proteins and RNA extraction. (A) Western blot analysis of the protein samples from 50 μl of culture using anti-β and anti-ϵ. The upper panel shows the 30° samples and the bottom panel shows the 43° samples. (Note: To reduce the signal for β relative to ϵ, a red plastic film was kept between the area where β is on the membrane and the intensifying screen, as discussed in the Materials and Methods). (B) Northern blot analysis of RNA extracted from *rne*$^-$ grown at 30° (left panel) and 43° (right panel). Equal amounts of RNA (1 μg) were subjected to Northern blot analysis using *uncC*-specific probe. RNA in both panels were analyzed on the same gel but the right panel shows a shorter exposure.

A

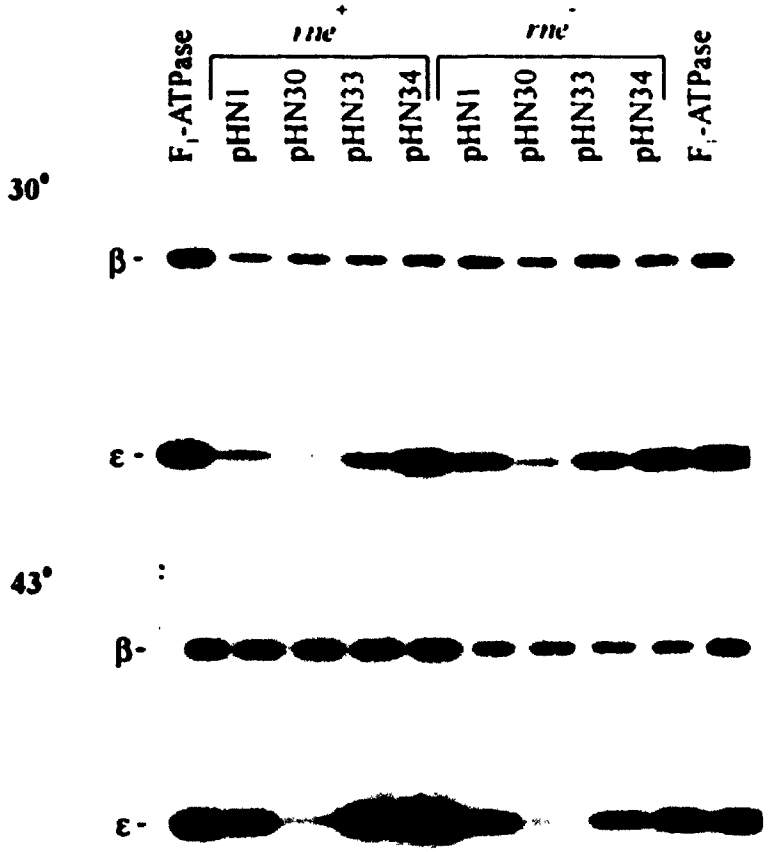
rne+
rne-
F1-ATPase
pHN1
pHN30
pHN33
pHN34
pHN1
pHN30
pHN33
pHN34
F1-ATPase
30°
β-
ε-
43°
β-
ε-

B

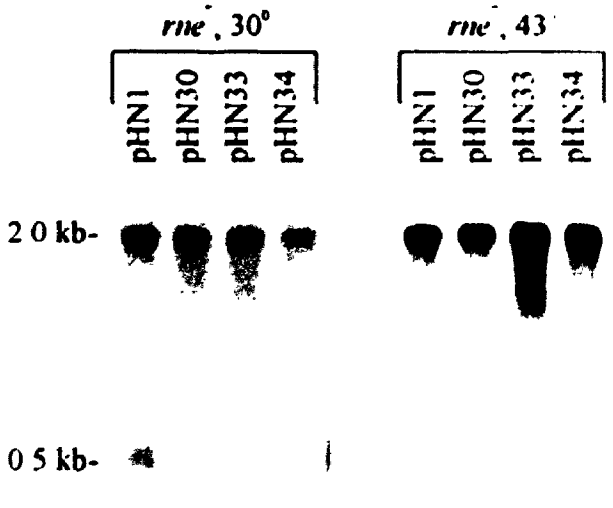
rne-, 30°
rne-, 43°
pHN1
pHN30
pHN33
pHN34
pHN1
pHN30
pHN33
pHN34
2.0 kb-
0.5 kb-

the *rne*$^-$ strain was also similar and ϵ levels varied as in the *rne*$^+$ strain, but the difference in the ϵ expression was in general smaller than that seen in the *rne*$^+$ strain. At the nonpermissive temperature (43°C) at which RNase is inactive a similar pattern in the expression of *uncC* was seen. This implied that it is not the activity of the enzyme that is responsible for the observed alteration in the *uncC* expression. The smaller difference in *rne*$^-$ compared to *rne*$^+$ could be a secondary affect of the RNase E inactivation. The expression of β and ϵ both went up in the *rne*$^+$ strain at 43°C. This could be due to removal of secondary structure at higher temperature. The increase in expression of the subunits was not seen in the *rne*$^-$ strain. This could be attributed to high competition for the translational machinery in the *rne*$^-$ strain since the inactivation of the enzyme is known to cause substantial increase in the total mRNA (Babitzke and Kushner, 1991, Mudd *et al.* 1990; Ono and Kuwano, 1979). From the above observations it can be concluded that the inhibition of cleavages at the normal site is not the cause of alteration in the apparent ϵ expression seen in the mutants.

Total RNA extracted from the *rne*$^-$ strain grown at 30°C and 43°C was analyzed by Northern blots using the *uncC*-specific probe (Fig. 4.7B) to confirm the *rne*-dependent processing of the mutant *uncDC* transcripts. At 30°C, the levels of the full length message (2.0-kb) remained similar for all the plasmids and the levels of the processed species (0.5-kb) were reduced for the three mutants compared to pHN1. The processed species was not detected in any of the plasmids at the nonpermissive temperature. At the same time the levels of the full length *uncDC* transcript increased in the *rne*$^-$ strain compared to the *rne*$^+$ strain. Thus, the

processing of the *uncDC* mRNA containing the mutations still requires functional RNase E but as seen in the primer extension analysis the cleavage is made at a different site.

(v) Effect of the Spacing Between the *uncC* Ribosome Binding Site (RBS) and the Secondary Structure on Expression of ϵ

To determine the influence of the position of the mRNA secondary structure on ϵ expression, various manipulations were carried out to change the spacing between the RBS of *uncC* and the base of the stem-loop (Fig. 4.8A). The stem-loop was brought closer to the S-D sequence by deleting the codon AUG, encoding Met-3 of ϵ (pHN39). In the plasmid pHN40, C7174 and G7177 were mutated to U and A, respectively. This destabilized the structure and at the same time moved the rest of the structure further downstream from *uncC* RBS. The stem was tightened and the spacing was reduced by one base by mutating A7180 to G in pHN41. This allowed the substituted G to pair with C7118 and increased the ΔG° of the structure by 5.5 Kcal/mol as predicated by method of Freier *et al.* (1986). All the mutations were designed so that the amino acid sequence of ϵ was not altered and good codon usage was maintained. Computer analysis of the *uncC* mRNA sequence with the codon deleted did not reveal any change to the stability of the stem. The influence of these mutations on the expression of ϵ was assessed by Western blot analysis (Fig. 4.8B, upper panel) using anti-β and anti-ϵ. The levels of β expressed from all the constructs was similar. The ϵ levels in strains carrying the mutation that shortened the spacing by 1 base (pHN41) was somewhat reduced compared to pHN1. Deletion

Figure 4.8 Effect of altering the spacing between the *uncC* RBS and the stem on the expression of ϵ. (A) The derivatives of pHN1 containing the indicated mutations are shown. pHN39 contains the deletion of an AUG codon, shifting the stem-loop closer to the ribosome binding site. Mutations in pHN40 destabilize the stem, while that in pHN41 will strengthen the stem-loop by allowing base pairing between the substituted G and C7118. (B) Analysis of proteins and mRNA. **Upper panel,** Western blot analysis of the proteins extracted from (50 μl of culture) induced *E. coli* strain JM103 carrying the indicated plasmids using ^{125}I-labeled monoclonal anti-β and anti-ϵ (in the presence of 0.5 mL of β-6 hybridoma culture supernatant to reduce signal for β). **Lower panel,** Northern blot analysis of RNA samples (1 μg) using the *uncC*-specific probe. (pHN1, N) uninduced control.

A

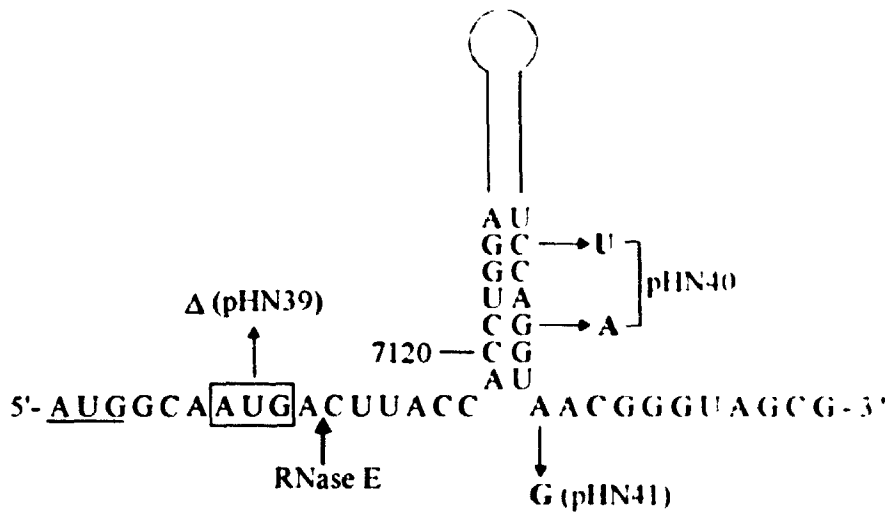
A U
G C → U
G C
U A
C G → A
C G
A U
pHN40
Δ (pHN39)
7120
5'- AUGGCA AUG ACUUACC AACGGGUAGCG - 3'
RNase E
G (pHN41)

B

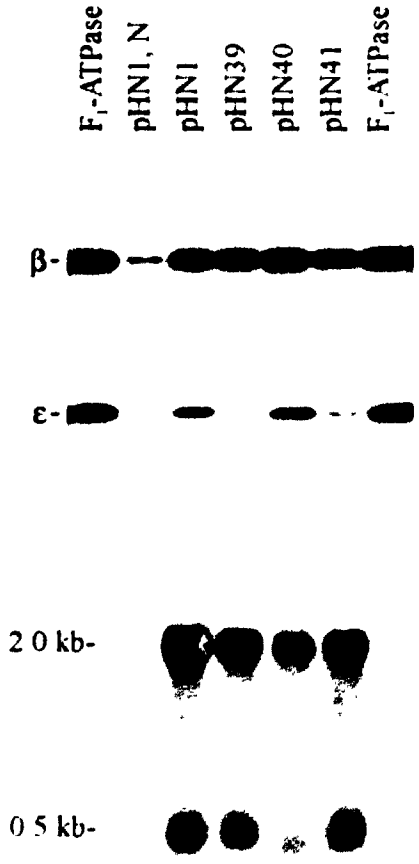
F1-ATPase
pHN1, N
pHN1
pHN39
pHN40
pHN41
F1-ATPase
β-
ε-
2 0 kb-
0 5 kb-

of 3 bases in pHN39 resulted in much lower expression of ϵ. The levels of ϵ increased in pHN40 slightly in comparison to pHN1. This was somewhat surprising since this mutation should open up the structure as same extent as pHN34 in which the structure was destabilized from the upstream side of the stem.

Northern blot analysis of the total mRNA from these derivatives of pHN1 demonstrated that cells bearing pHN39 and pHN41 had similar amounts of the full length and the processed messages as pHN1 (Fig. 4.8B, lower panel). pHN40 repeatedly showed lower amounts of *uncDC* mRNA. This might explain why the effect of this mutation in increasing ϵ expression is not as great as that seen in pHN34. However a potential problem with this explanation is that the levels of β remained similar. Alternatively, it is possible that the changes in pHN40 resulted in formation of some complex secondary structure. As in the case of the other stem loop mutants, the processed product was slightly smaller in pHN40. Primer extension revealed that the 5'-ends of the processed species in pHN40 was same as those seen in pHN33 and pHN34 (i.e T7173, see Fig. 4.3A and Fig. 4.4). The processed species in the other two mutants (pHN39 and pHN41) mapped in the region close to the normal site (Fig. 4.3A and 4.4).

In the above experiment it was demonstrated that shortening the distance between the start codon and the downstream stem reduced ϵ expression. I wanted to see if one can increase the expression by shifting the stem further downstream from the *uncC* RBS. For this purpose, the stem-loop was kept intact, but it was moved downstream by inserting a codon between the third and fourth codons as shown in Fig. 4.9A. Three insertions were made (pHN48-50) so that the predicated

Figure 4.9 (A) Derivatives of pHN1 containing insertions of a codon in *uncC*. The position of the insertion and codons inserted are shown. Plasmids pHN48-50 contain the indicated insertions and pHN51-53 also contain the A7180G mutation. **(B) Analysis of proteins and RNA. Upper panel,** Western blot analysis of the protein samples extracted from (50 μl of culture) *E. coli* strain carrying the derivatives of pHN1 after induction with IPTG using monoclonal anti-β and anti-ϵ (in the presence of 0.5 mL of β-6 hybridoma culture supernatant to reduce signal for β). **Lower panel,** Northern blot analysis of the RNA samples (1 μg) using *uncC*-specific probe. (pHN1, N) uninduced control.

A

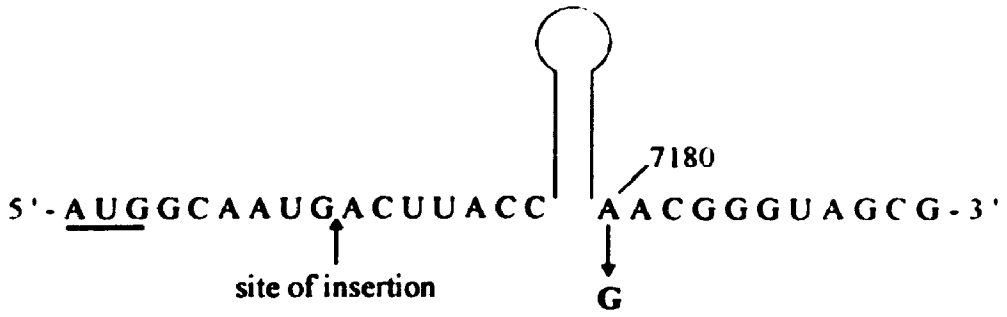

codon inserted	a.a	plasmid	plasmid with A7180G
ACU	Thr	pHN48	pHN51
UCA	Ser	pHN49	pHN52
UCU	Ser	pHN50	pHN53

B

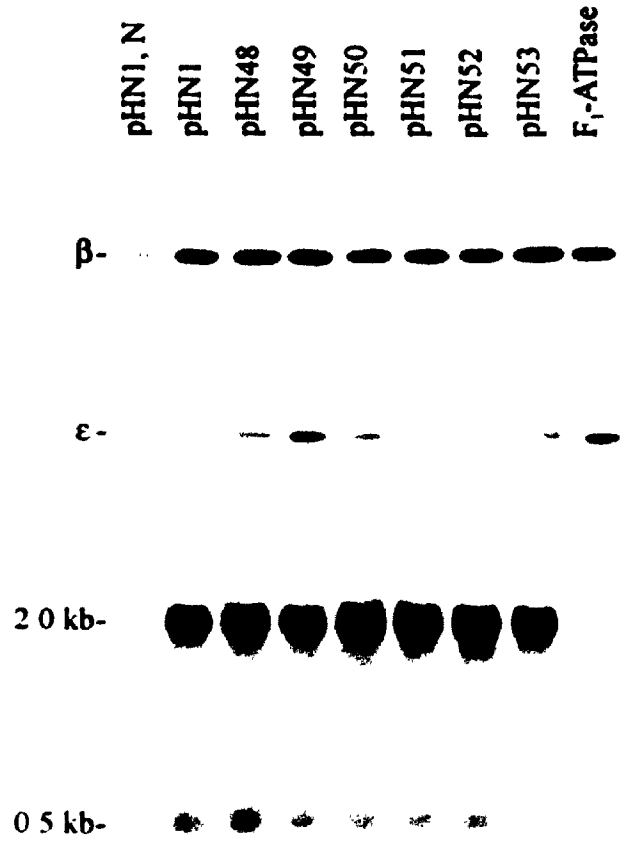

secondary structure did not change as determined by computer analysis. Each insertion was also combined with the A7180G mutation in a separate set of plasmids. The resulting hybrid plasmids (pHN51-53), also shown in Fig. 4.9A, would strengthen the stem and move it downstream by two bases compared to pHN1. Proteins expressed from all these constructs were analyzed by Western blot analysis (Fig. 4.9B, upper panel). It can be seen that the level of β was similar in all the constructs. In all the insertion constructs (pHN48-50) the ϵ levels went up significantly and in the insertion plus the A7180G mutations (pHN51-53) there was an apparent increase in the level of ϵ. The strengthening mutation (pHN41) by itself had reduced expression of ϵ (Fig. 4.8B) but shifting the strengthened stem by 2 bases downstream increased ϵ levels, suggesting that it is not the stability of the stem that is important in allowing efficient expression but rather the position.

To ensure that the increased expression in the insertion mutants was due to the higher levels of translation and not because of changes in the mRNA stability, RNA was isolated from strains carrying the mutant plasmids and hybridized to *uncC*-specific probe (Fig. 4.9B, lower panel). From the blot it is apparent that the mutations did not change the amount of *uncDC* mRNA (2.0-kb message). The levels of the processed message also remained similar in all the insertion mutants. The 5′ ends of the processed message were mapped to be at the same position as the wild type (Fig. 4.9B). However, some extra bands were seen in the analysis of the insertions plus the A7180G mutation. In particular the band at U7178 was intense. The origin of these bands is uncertain but they could be due to degradation of the mRNA samples.

(vi) Quantification of Relative Expression of ϵ in the pHN1 and pES2 derivatives

In order to get a more quantitative insight into the effects of the mutations of the expression of β and ϵ, proteins extracted from selected derivatives of pHN1 were analyzed by Western blotting. The mutations analyzed were pHN34 (C7121T, G7124A), pHN39 (deletion of AUG), pHN41 (A7180G), pHN49 (insertion of TCA) and pHN51 (insertion plus A7180G). Cells carrying these plasmids were induced with IPTG for 10 min followed by preparation of protein extracts in boiling SDS sample buffer. The same set of samples was analyzed on four gels to obtain an average. A typical blot is shown in Fig. 4.10A. The β and ϵ bands were cut from the gel and the activity was counted in a gamma counter as described in the Materials and Methods. Table 4.1 shows the average molar ratio of ϵ/β and the relative expression of ϵ in pHN1 and the mutant derivatives. Examination of the data suggests that there is a good correlation between the expression and the position of the stem-loop. In general, those mutations which brought the stem closer to the *uncC* RBS (pHN39, pHN41) had lower ϵ expression and a lower ϵ/β ratio. Those mutations which shifted the base of the stem away from the RBS (pHN34, pHN49 and pHN52) showed better expression of ϵ and a higher ϵ/β ratio.

The above comparison was done using plasmids which contained *uncDC*, thus in the presence of *uncD* translation. As mentioned in the introduction there are two independent stem-loops on either side of the RNase E site in *uncC* and the role of the upstream structure in limiting *uncC* expression was demonstrated by Dallmann and Dunn (1994). We wanted to see if translation of the *uncD* cistron in any way contributed to the above documented affects of the alteration in the downstream

Figure 4.10 (A) Samples of Western blots used for quantitation of β and ϵ expression from some selected mutant derivatives of pHN1. *E. coli* strain JM103 carrying the indicated plasmids was grown to A_{600} of 0.1, followed by induction of expression with 0.1 mM IPTG for 10 min. Protein samples were prepared and subjected to Western blot analysis using ^{125}I-labeled monoclonal anti-β and anti-ϵ, with 0.5 mL of β-6 hybridoma culture supernatant. Each lane received proteins extracted from 50 μl of culture. The molar amounts of purified F_1-ATPase standards are indicated. **(B) Samples of Western blots used to quantitate ϵ expression from derivatives of pES2, carried in *E. coli* strain MM294.** The blots were performed as above using anti-ϵ. Each lane received proteins extracted from 10 μl of culture. (pHN1, N) uninduced control.

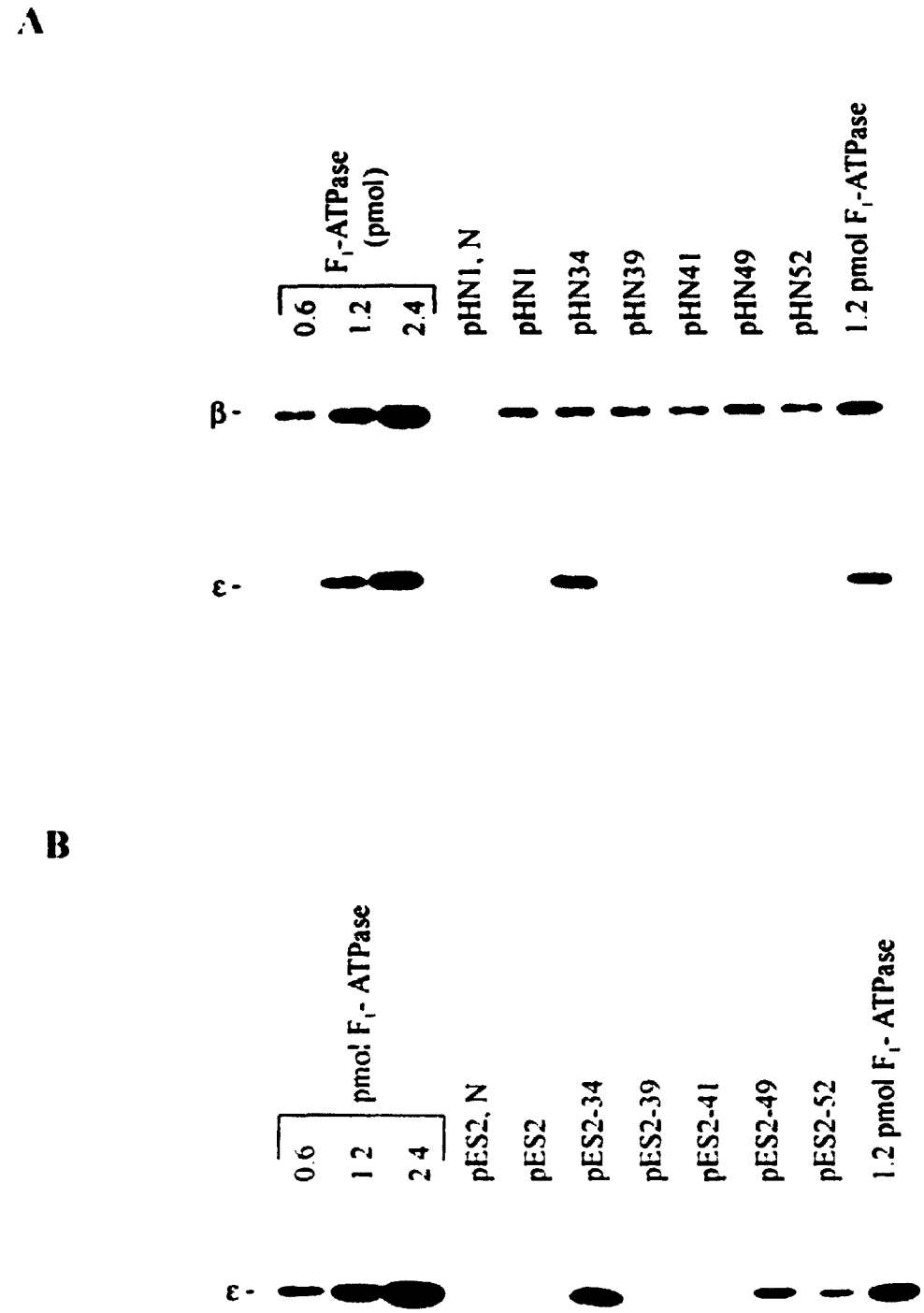
A
β-
ε-
0.6
1.2
2.4
F1-ATPase (pmol)
pHN1, N
pHN1
pHN34
pHN39
pHN41
pHN49
pHN52
1.2 pmol F1-ATPase
B
ε-
0.6
1.2
2.4
pmol F1- ATPase
pES2, N
pES2
pES2-34
pES2-39
pES2-41
pES2-49
pES2-52
1.2 pmol F1- ATPase

pHN1 Derivatives	ϵ/β	ϵ Expression Relative to pHN1	pES2 Derivative	ϵ Expression Relative to pES2
pHN1	0.24±0.05	1	pES2	1
pHN34	0.82±0.06	3.4±0.4	pES2-34	4.2±0.4
pHN39	0.11±0.02	0.46±0.04	pES2-39	0.45±0.08
pHN41	0.14±0.01	0.60±0.06	pES2-41	0.76±0.06
pHN49	0.33±0.03	1.38±0.16	pES2-49	1.56±0.10
pHN52	0.27±0.05	1.14±0.05	pES2-52	1.29±0.06

Table 4.1 Quantitation of Relative Expression of ϵ in pHN1 and pES2 Derivatives. Four sets of Western Blots were performed to quantitate amounts of β and ϵ expressed from pHN1 derivatives and pES2-like plasmids (a sample is shown in Fig. 4.10). The bands containing β and ϵ were excised from the blot and radioactivity was counted in a gamma counter as described in the Materials and Methods. In each case the molar amounts of β and ϵ were calculated from the purified F_1 standards. ϵ/β was calculated by taking the average of the molar ratios of ϵ to β from each gel for a given strain. Relative expression of ϵ was calculated by dividing the molar amount of ϵ in each strain with the amount of ϵ measured in a strain containing pHN1, followed by taking the average of all four gels.

structure on the expression of *uncC*. Therefore, the *uncC* from the derivatives of pHN1 was subcloned into pEX1 to give a set of plasmids which are similar to pES2, containing only the *uncC* gene. Thus, the mRNA transcribed from these plasmids would only have the downstream structure with the appropriate mutations. These plasmids were named according to pHN1 derivatives from which they were derived. As an example, pES2-34 is a mutant form of pES2 containing the same mutation that was present in pHN34.

The *uncC* expression in these plasmids was assessed as above and the results are shown in Fig. 4.10B. The relative expression of *uncC* is summarized in Table 4.1. The effects of the mutations on the expression of *uncC* were very similar to those seen in the pHN1 derivatives in terms of the relative expression of ϵ. These results indicated that the downstream structure modulates the *uncC* expression independent of the translation of the upstream *uncD* cistron.

4.4 DISCUSSION

The results presented in this chapter indicate a dual role for the secondary structure which is found in the early *uncC* coding region: (i) in the efficient processing by RNase E, and (ii) in regulating the synthesis of ϵ subunit.

RNase E Processing- As seen with many known substrates of RNase E, the site in *uncC* is in a single-stranded region and is adjacent to stable secondary structures (Fig. 4.1B). The importance of the sequence at the cleavage site was assessed by mutating the nearby nucleotides using site-directed mutagenesis. I

observed that the activity of the RNase E is tolerant to alteration at the actual cleavage site, by mutating the fourth codon of ϵ (ACU) by 1 or 2 bases. The single base changes (ACG, ACC, CCU) had no affect on the efficiency of cleavage, and a double mutation (CCG) resulted in somewhat reduced processing. It is interesting to note that changing bases at the site in some cases prevented cleavage at the normal site (C7113) but resulted in cleavages at new sites nearby (Fig. 4.4). These cleavage sites were similar to the consensus for RNase E (Ehretsmann *et al.*, 1992), and in the case of pHN30 (CCG) it was shown that the cleavage at the new site was still *rne*-dependent. Predicted secondary structure of the sequences with mutations (in pHN24, pHN29, and pHN30) revealed that the usual site in these mutants is sequestered in base pairing (Fig. 4.11). One can suggest that these mutations which apparently reduced the single strandedness inhibited processing at the usual site because the normal site may be sequestered in a secondary structure (Fig. 4.11). For example mutations CCC (pHN29) and CCG (pHN30) may alter the predicted mRNA secondary structure as shown in Fig. 4.11 and sequester the normal site in base pairing. Thus new sites were observed at different locations. It is interesting to see that the new sites are in the predicted single-stranded regions in most cases. The cleavage in pHN24 was in the predicted paired region, but the stability of this newly paired region was lower compared to the structures in the pHN29 or pHN30 transcripts. Ehretsmann *et al.* (1992) reported similar observations with RNase E-dependent processing of bacteriophage T4 mRNA. They hypothesised that RNase E binds to the stem-loop and while bound, it scans the upstream sequences until it finds the consensus before making the cleavage. Our results support their

Figure 4.11 Alternative secondary structures in the pHN24, pHN29 and pHN30 mRNA transcripts near the early *uncC* coding region. The stem-loop in pHN1 is on shown on the top for easy comparison. In each structure the *uncC* initiation codon is underlined and the mapped site of cleavage/s by RNase E is shown by arrow. The mutations in the pHN1 derivatives are indicated in bold.

pHN1:

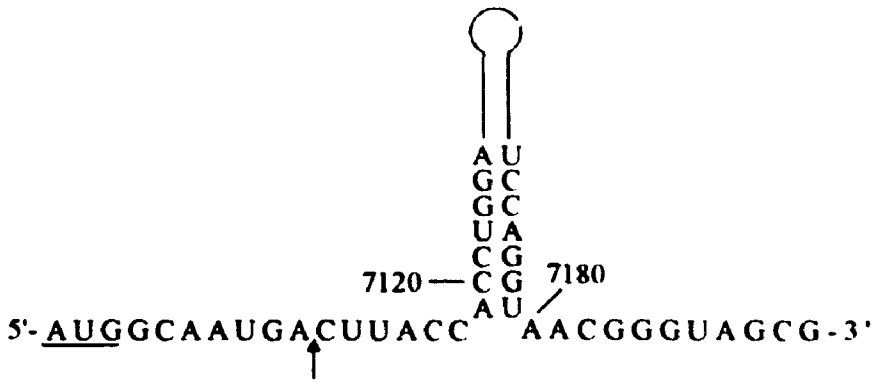

pHN24:

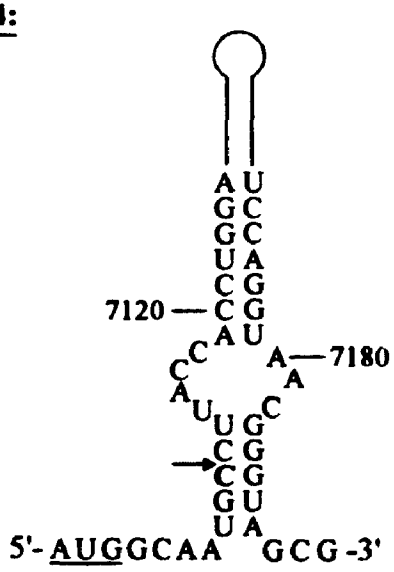

pHN29:

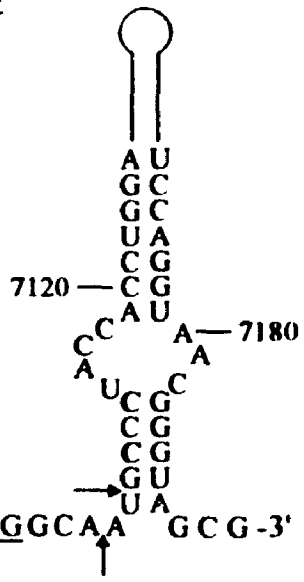

pHN30:

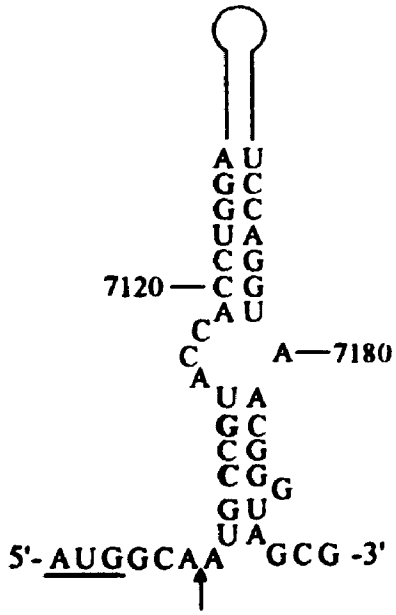

conclusions. Cormack and Mackie (1992) also reported that RNase E is more tolerant to the changes in the sequence at the site then to alteration of the secondary structure.

The importance of the downstream double-stranded RNA structure in efficient cleavage at C7113 was demonstrated by changing the stability of the structure. Mutations that destabilize the base of the stem-loop (pHN33, pHN34, and pHN40) completely eliminated cleavage by RNase E at the normal site. Mutating nucleotides in the base of the stem on either side resulted in inhibition of the cleavage at C7113 and introduction of a new site about 60 bases downstream of the usual site (at position T7173). This site is situated on the other side of the remaining portion of the stem-loop. Mutations in pHN34 and pHN40 should lower the stability of the stem by 10 Kcal/mol but the mutations are on opposite sides (i.e. destabilize the stem by breaking the base pairs from opposite sides). The fact that destabilizing the stem-loop by mutating bases on either side resulted in the same effect, namely inhibition of cleavage at C7113 and appearance of cleavage at T7173, provided a solid evidence in support for the presence of this partially mapped structure.

A few observations and implications about the appearance of the new site in the stem-loop destabilizing mutants should be considered. First, this site is either completely novel or normally a weaker site, but increased cleavage at this site is seen because the upstream site is not available. Secondly, it appeared that the cleavage at this site was less efficient because lower levels of processed products were seen. While there was no net increase in the full length message, it is possible that the cleavage is as efficient but that the processed product is less stable compared to the

normally processed species. One may suggest that the normal species is more stable because it still contains the secondary structure, as 5'-terminal stem-loop structures have been shown to stabilize some *E. coli* mRNA (Emory *et al.*, 1992, Bouvet and Belasco, 1992). Thirdly, this new cleavage is still dependent on functional RNase E since the processed species was not seen in an *rne*$^-$ strain. Ehretsmann *et al.* (1992) in their *in vivo* and *in vitro* analysis of the bacteriophage T4 mRNA processing by RNase E suggested that cleavages can not be made 3' of the structure. Cormack and Mackie (1992), however, showed that a structure 5' of the site is important in the RNase E-dependent processing of the *E. coli* 9S RNA.

Extensive deletion of the stem-loop (pES37 and pES137) also reduced the processing at the normal site supporting the notion that a stable structure is essential for RNase E action.

The results presented in this chapter combined with those seen in the previous chapter imply that the upstream *uncDC* structure is not critical for the cleavage at C7113. Studies of the previous chapter showed that messages which contained varying amount of the upstream *uncD* and complete *uncC* sequences were still processed normally. Some of these transcripts lacked a major part of the upstream *uncDC* secondary structure. Even the message transcribed from pES2, which only contains the *uncC* mRNA, was processed efficiently. Thus it seems that it is the presence of the downstream *uncC* stem-loop that is necessary for efficient RNase E processing. It also appears that RNase E cleavage is not affected by the rate of translation. The translation rates of pHN29 and pHN30 were lower compared to pHN1 while those of the pHN33 and pHN34 were higher, but the steady state levels

of the full length message did not change. It has been suggested previously that cleavages at sites located in translated regions could be sensitive to the density of the translating ribosomes (Klug and Cohen, 1991; Levinthal *et at.*, 1963; Petersen, 1992; Rapaport and Mackie, 1994; Yarchuk *et al.*, 1992). Thus, messages that are translated more efficiently should have poor cleavage and those that are poorly translated should be efficiently cleaved. However, this was not the case with *uncC*. The earlier work performed by Dallmann and Dunn (1994), using pHN1 derivatives, showed that introduction of stop codons upstream of the normal *uncD* stop codon in some cases resulted in lower expression of *uncC*. In the previous chapter I showed that these *uncDC* messages with stop codon mutations in *uncD* were processed normally. Thus, it provided addition evidence to suggest that the cleavage in *uncC* is not affected by the rate of translation. There is no correlation between efficiency and mRNA stability in *E. coli*. Some mRNA are stabilized by better translation whereas others showed no change in the stability (review by Petersen, 1992). Our results were in agreement with those of McCarthy and coworkers (McCarthy 1990, McCarthy *et al.*, 1991) who indicated that the stability of the *unc* mRNA does not correlate with the rate of translation.

In conclusion, these results support a proposed model for the requirements of RNase E action. Namely, the enzyme recognizes its substrate with relatively low sequence specificity, but in a single-stranded region adjacent to a stable secondary structure. Similar results were observed for the RNase E-dependent processing of T4 gene 32 mRNA (Ehretsmann *et al.*, 1992) and 9S RNA (Cormack and Mackie, 1992).

RNase E has a general role in the degradation of mRNAs and the results in this work show that this is the case. It seems that cleavage at C7173 is not so critical in the differential expression of β and ϵ because cleavage at the site results in inactivation of both genes as shown in the previous chapter. Secondly, some of the mutations either reduced or inhibited cleavage at C7113 but there was no corresponding increase in the levels of the full length message. It appears that if a cleavage at one site is inhibited then RNase E (or other enzyme) can still carry out the degradation by processing at an other site, which might normally be a weaker site. Thus it appears that this particular site is a major site of cleavage but it is not essential for the overall degradation of the *unc* mRNA, as thought earlier. However, it can be suggested that RNase E-dependent endonucleolytic processing is important in the overall decay of the *unc* mRNA, since inactivation of the enzyme leads to increased stability of the primary transcript.

***uncC* Expression-** The results presented here indicate that the position of the stem-loop in the *uncC* mRNA is critical in determining the level of expression of the ϵ subunit. The mutations which kept the structure intact but shifted the stem closer to the *uncC* RBS reduced *uncC* expression, whereas shifting the stem away from the RBS resulted in higher synthesis of ϵ. Deletion of a codon between the RBS and the base of the stem (pHN39) lowered *uncC* expression by 50% whereas insertion of a codon (pHN49) caused *uncC* expression to go up by 40%. Making the stem more stable and at the same time bringing it 1 base closer to the RBS (pHN41) reduced the expression of ϵ by 25%. The fact that the strengthening mutation lowered the

expression provided further support for the presence of the structure. One may argue that lower expression of *uncC* in the strengthening mutant is seen because the stronger stem is more efficient in reducing translation elongation. However, shifting this strengthened stem by two bases away from the RBS (pHN52) not only eliminated the apparent reduction but increased expression of *uncC* by 15% relative to pHN1. Thus it is not the stability of the stem that is a critical factor but the position of the stem-loop with respect to the *uncC* RBS that is important in determining the efficiency of *uncC* translation.

The double mutation that destabilized the stem (pHN34) will shift the rest of the structure about 9 bases downstream from the *uncC* RBS, assuming that the remaining structure is still formed. As expected this mutation had the greatest effect, causing the expression of *uncC* to go up 4-fold. The mutations on the other side of the stem (pHN40) were not as effective in increasing the expression of *uncC*, for reasons that are not obvious.

The mutations at the RNase E cleavage site which lowered the expression of *uncC* can also be explained by effects on RNA structure. Mutations carried in pHN24, pHN29 and pHN30 may have resulted in the formation of alternative structures as shown in Fig. 4.11. These structures extend the stem so that the base of the stem-loop is brought closer to the *uncC* RBS. This would be consistent with the reduced synthesis of ϵ. The expression of ϵ was better in pHN24 compared to pHN29 and pHN30. Interestingly, the alternative predicted structures in pHN24 is weaker than that in pHN29 and pHN30, consistent with the better efficiency of translation.

The observed differences in the *uncC* expression could not be attributed to the variation in the steady state levels of the message since there was not a significant change in the levels of the *uncDC* mRNA as determined by Northern blot analysis. One should note that in some mutants the amounts of the processed species were reduced but these species are not functional in translation. Finally, the fact that the level of β was similar implied that the changes specifically affected ϵ expression. We therefore believe that the differences in the translation initiation is a major contributing factor responsible for the observed variation in the *uncC* expression, rather than the mRNA stability.

There are two obvious ways in which the secondary structure in the early *uncC* coding region can modulate the expression of *uncC*. In the first mechanism, the structure being close to the start codon interferes with the binding of the ribosome and thus lowers *uncC* expression. In the second model, a translating ribosome pauses at the structure because of its high stability. It would have to unfold the structure before it can resume elongation. The evidence collected in this work favours the first mechanism.

A ribosome bound to its binding site occupies about 30 to 35 bases, including about 14-17 bases downstream of the first base of the initiation codon (Gold, 1988; Steitz, 1969). The structure in the *uncC* mRNA is 16 bases downstream from the initiation codon when the first nucleotide of the initiation codon is designated 1. It can be proposed that the base of the stem, being in the boundary of the region occupied by the ribosome, reduces accessibility of the TIR to ribosomes. The position of the stem relative to the RBS had a large affect on the efficiency of *uncC*

translation. Bringing the stem closer to the RBS by 3 bases reduced expression significantly, whereas shifting it away by 3 bases resulted in better expression. The computer analysis of the sequences around the stem did not predict any changes in the stability of the secondary structure which could account for the differences in translation efficiency. The most straightforward interpretation then is that the stem sterically hinders the binding of ribosomes to the RBS. The insertion of a codon permitted easier access of the ribosome to the S-D region and AUG codon. The opposite argument can be made in the case of the deleted codon. Thus, it appears that the stem modulates the rate at which a ribosome can bind to the *uncC* RBS.

The mechanism proposed above can explain a number of observations that were previously reported. Kuki *et al.* (1988) isolated a revertant of an *uncC* Shine-Dalgarno mutation which had wild type levels of ϵ. Strains carrying the S-D mutations in the *uncC* were not able to grow on a non-fermentable carbon source because the expression of ϵ was reduced drastically. The position of the second mutation G7123 (G mutated to A) in the revertant mapped in the base of the stem-loop in the *uncC* mRNA. This mutation should cause the base of the stem to unfold, moving the residual stem further from the RBS, and increasing the efficiency of *uncC* translation. Secondly, Schaefer *et al.* (1989), who conducted a toeprint analysis of *unc* genes, did not detect a toeprint for the *uncC* message. Toeprinting is often used to detect the position of the ribosome on mRNA by the ability of the complex containing ribosome, mRNA and tRNA to inhibit the extension of cDNA by reverse transcriptase (Hartz *et al.*, 1989, Gold, 1988). Thus, a toeprint signal reflects the efficiency of a ribosome binding site. For most messages a toeprint is observed at

14-16 bases from the first base of the start codon. Schaefer *et al.* (1989) suggested that the presence of a folded structure in the TIR could be responsible for the failure to get a toeprint. One could argue that *uncC* did not give a toeprint because the stem in *uncC* which is 16 bases from the first base of the start codon interferes with the ribosome binding. Finally, Skakoon and Dunn (1993b) also observed that strains containing *uncC* gene in which the bases that form the *uncC* secondary structure are deleted produced high amounts of the mutant ϵ. Their results are consistent with the model; such deletions remove the secondary structure, increasing the accessibility of the RBS to ribosomes.

Ringquist *et al.* (1993) reported that ribosomes can bind to a RBS even in the presence of a secondary structure within the complex and concluded that the mRNA track is sufficiently large to contain a stem-loop. This may seem contradictory to the model proposed here. Their studies, however, were performed *in vitro* using 30S ribosomes, tRNA and *in vitro* transcribed RNA and thus measuring binding at equilibrium rather than the rate of binding. Therefore, one can suggest that presence of such a structure could lower the rate at which a ribosome binds to the RBS.

There have been various studies indicating that secondary structures which sequester S-D region and/or initiation codons in base paired regions could block or reduce expression of bacterial genes (review by de Smit and Duin, 1990). This is attributed to the lower accessibility of the ribosome to the RBS. We know of no reported example where secondary structure downstream of the start codon could limit the access of ribosomes to the RBS. We showed that the stem in *uncC*, which is 16 bases downstream from the initiation codon, significantly reduces the efficiency

of *uncC* translation. The results reported here are novel in that they suggest that the presence of secondary structure even downstream of the initiation codon can restrict the binding of ribosome to RBS. This provides a mechanism for fine tuning the level of expression, while the secondary structures blocking S-D sequences provide a crude regulation.

Dallmann and Dunn (1994) suggested that a ribosome translating *uncD* opens the upstream *uncDC* secondary structure and provides an opportunity for the binding of a ribosome to the *uncC* RBS. The present studies suggest that during this opportunity the downstream structure restricts the binding of ribosome to the *uncC* RBS. Thus, here we have a situation where the upstream stem defines a period of time in which the S-D region is accessible and the downstream structure determines the efficiency with which a ribosome can bind in that time limit. Thus, the downstream stem provides a finer tuning in the expression of *uncC*. The effects of manipulating the downstream structure on the expression of *uncC* were the same in either *uncDC* or only *uncC* expression plasmids (Table 4.1) indicating that the downstream structure modulated the expression of *uncC* independent of the translation of *uncD*. This result also implies that there is no ribosomal reinitiation between *uncD* and *uncC*. Rather, the translation of the two genes is carried out by two separate ribosomes, in agreement with the two-ribosome model proposed by Dallmann and Dunn (1994).

Over the past 15 years much has been learned about post-transcriptional regulation of gene expression in procaryotes. The results presented in this chapter reveal an unexpected mechanism by which RNA secondary structures outside the

ribosome binding site can influence rates of protein synthesis by altering the efficiency of ribosome binding to the RBS.

The β and ϵ subunits, according to the subunit stoichiometry of the complex should be expressed in the ratio of 3 to 1. It can be suggested that the structure in the *uncC* may be an important contributor in the differential expression of *uncD* and *uncC*. The ϵ subunit is a noncompetitive inhibitor of the ATPase and is required for the efficient binding of the F_1 to F_0. To achieve the appropriate ratio the *uncC* expression should be lower than *uncD*. The results here show one way as to how this might be achieved.

In conclusion, the secondary structure in *uncC* is important in the efficient cleavage by RNase E and in providing the differential expression of the last two genes in the operon. The studies provide additional evidence for the involvement of the secondary structure in regulating the expression of *unc* genes. Finally, the results serve to point out that gene expression could be restricted by the presence of secondary structures that are in the early coding region, probably by providing steric hindrance to the entry of ribosomes.

CHAPTER 5

DEGRADATION OF *ESCHERICHIA COLI uncB* mRNA BY MULTIPLE ENDONUCLEOLYTIC CLEAVAGES

5.1 INTRODUCTION

The genes of the *Escherichia coli unc* operon which encode all the eight subunits of F_1F_0-ATP synthase are differentially expressed. The order of the genes in the operon is *uncIBEFHAGDC*, and the stoichiometry of the subunits in the complex is $ab_2c_{9-15}\alpha_3\beta_3\gamma\delta\epsilon$. As the subunits are produced in the proper relative amounts from a single polycistronic message, differential expression must arise from posttranscriptional mechanisms.

The major *unc* message detectable by Northern blot analysis of RNA extracted from *E. coli* has a size of about 6 kb, as opposed to the 7 kb length of the operon. We (Chapter 3; Patel and Dunn, 1992) and others (Schaefer *et al.*, 1989; McCarthy *et al.*, 1991) have shown that the 6-kb species lacks the expected 5′ end, which contains *uncIB*, while the 3′ end appears to be intact. Since the 7-kb species is ordinarily non-detectable, the removal of the 5′ end almost always occurs before transcription of the operon is complete. From these considerations it seems that the mRNA of the first two genes, *uncI* and *uncB*, must have shorter chemical half-lives than the rest of the message, and this might be expected to limit their expression relative to the later genes. Functional determinations of the half-lives of the mRNA of different genes by McCarthy's group (McCarthy *et al.*, 1991) revealed that the messages for the genes following *uncB* are more stable than that of *uncB* by a factor of greater than three. Lagoni *et al.* (1993), however, reported that the stabilities differ by a factor of less than two.

The detection of the chromosomally-encoded 7-kb species (Chapter 3) in temperature-sensitive RNase E mutants at the non-permissive temperature, indicated

that the removal of the 5′ end is dependent on functional RNase E (Patel and Dunn, 1992). Two potential processing sites located between *uncB* and *uncE* were identified by Gross (1991), using a hybrid message containing the *uncE* leader sequence. Cleavage of the intact *unc* transcript at these sites would directly inactivate neither of the messages, but it seems likely that the upstream *uncB* would be rapidly degraded by exonucleolytic attack.

In order to learn more about how *uncIB* is removed, and the significance of the two cleavage sites in the *uncE* leader, I have studied the degradation of the *uncBE* message in more normal contexts, using either *uncBE* mRNA expressed from a plasmid or *unc* mRNA expressed normally from the chromosome.

5.2 MATERIALS AND METHODS

(i) Enzymes and Chemicals

Sources of many enzymes and chemicals have been described in the previous Materials and Methods sections.

(ii) Bacterial strains

E. coli strains JM103, SK5006, MG1693, SK5665, and DK8 were described in Chapter 3.

(iii) Plasmid Construction

Recombinant DNA procedures were carried out by standard methods (Sambrook *et al.*, 1989). Plasmid pHN2 bearing the *unc* transcription terminator was

constructed by cloning the *Hind*III-linkered *Hinc*II-*Rsa*I fragment of pTK1(Patel *et al.*, 1990) into the *Hind*III site of pEX1 (Passador and Linn, 1989), a derivative of pKK223-3 (Brosius and Holy, 1984). The cloned insert contained 20 bases from the 3′ end of the *uncC* gene and the complete *unc* transcription terminator. The expression plasmid pHN4 was constructed by inserting the 1.1-kb *Pvu*II-*Dra*I fragment of pBJC706 (von Meyenburg *et al.*, 1984) into the *Sma*I site of pHN2. A schematic representation of pHN4 is shown in Figure 5.1. The plasmids pHN8, pHN9, and pHN11, which carried the inserts described below in the direction opposite to that of expression, were used for producing the antisense RNA for probing the 5′*uncB*, 3′*uncB*, and *uncE* regions, respectively (see Fig. 5.1). pHN8 contained the 0.2-kb *BamH*I-*Rsa*I fragment of the *uncB* (5′ *uncB*) gene cut from pHN4 cloned into pTZ18U(Mead *et al.*, 1986) using the *BamH*I and *Sma*I sites. pHN9 was constructed by cloning the 0.2-kb *BamH*I-*Rsa*I fragment (3 *uncB*) of pHN4 into the *BamH*I-*Sma*I sites of pTZ18U. pHN11 was created by cloning the 0.1-kb *Rsa*I fragment of pHN4 (5′ *uncE*) into the *Sma*I site of the pTZ18U. pHN15 was constructed by cloning the *Eco*RI-*Hind*III fragment of the pHN4 into pTZ18U for use as a template for the *in vitro* transcription of *uncBE* mRNA. Plasmid pHN3 which was used to prepare the *uncC*-specific riboprobe has been described in Chapter 2 (Patel and Dunn, 1992).

(iii) Bacterial Growth

Cells were grown at 37°C with shaking in Luria-Bertani broth unless otherwise indicated. Strains carrying plasmids were maintained in medium containing 40 μg of

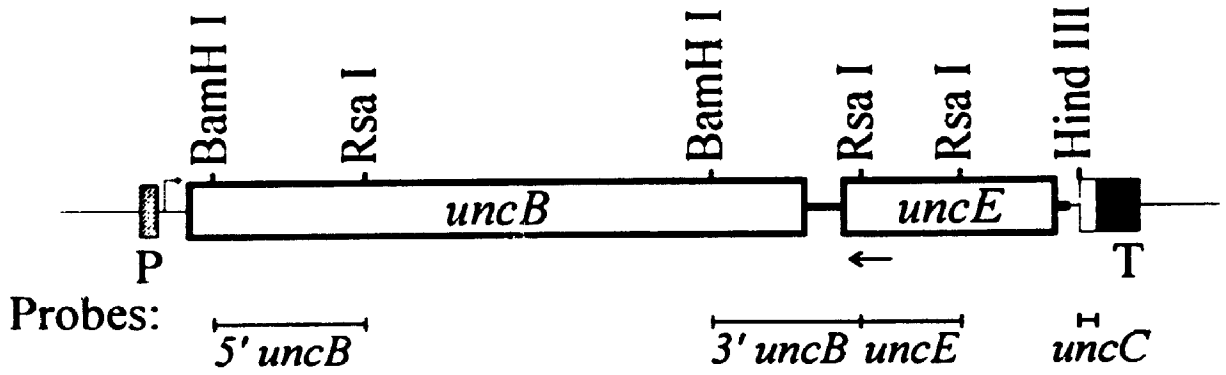

Figure 5.1 A scaled restriction map showing the expressed region of the plasmid pHN4 and the Northern hybridization probes. The *uncBE* fragment which was cloned into the *Sma*I site of the vector pEX1 is shown in thick boxes and lines. The inserted fragment lacked the first 70 bases of the *uncB* coding region, contained the complete *uncE* and 18 bases beyond the *uncE* termination codon. The last box denotes the *unc* transcription terminator which was cloned into the HindIII site of pEX1. The filled area represents the actual terminator sequences and the open area corresponds to the terminal *uncC* coding sequence which was carried through during the cloning manipulation. The cloning strategy left about 28 bases from the multiple cloning region of pEX1 between the two inserts. The restriction sites used to make the probes and the positions of the probes relative to sequence are shown. Abbreviations and symbols: P, *tac* promoter; T, *unc* transcriptional terminator; ←, position of the primer used in the extension analysis.

carbenicillin per ml. During early logarithmic growth IPTG was added to a concentration of 1 mM to induce expression. After 10 min of induction, samples were removed and RNA was extracted by the method of Mackie (1989). For the turnover studies, rifampin was added to a final concentration of 0.1 mg ml^{-1} after two min of induction and RNA was then extracted from samples taken at various times.

(iv) Temperature Shift Experiments

The temperature sensitive RNase E mutant strain and its wild type isogenic strain (carrying pHN4) were grown at 30°C to early log phase (A_{600}=0.2). Half of each culture was then shifted to 43°C and the other half kept at 30°C. After incubation for 30 min at the two temperatures, expression was induced by addition of IPTG to 1mM in strains carrying plasmids. RNA was extracted from samples taken after 10 min of induction.

(v) Northern Analysis

RNA samples were subjected to Northern blot analysis as described in Chapter 3. Pre-hybridization and hybridization with the appropriate probe were carried out at 55°C as described by Mackie (1986).

(vi) Labelling of Hybridization Probes

Antisense RNA transcribed *in vitro* using T7 RNA polymerase was used as a probe in the Northern analysis. pHN8, pHN9 and pHN11 which had been linearized with *Bam*HI were used to prepare the 5′ *uncB*-, 3′ *uncB*- and *uncE*-specific probes,

respectively (Fig. 5.1). The *uncC*-specific probe was prepared by *in vitro* transcription of pHN3 which had been linearized with *Nco*I. *In vitro* transcription was carried out as described in Chapter 3.

(vii) 5'-end Mapping of the Processed Transcripts by Primer Extension

A synthetic oligonucleotide primer, 5'-AGCAGATCCATATTCAGG-3', complementary to a region 9-27 bases into the *uncE* coding sequence, was radioactively end-labelled with [γ-^{32}P]ATP using T4 polynucleotide kinase as described by Sambrook *et al.* (1989). The primer extension and the analysis of the extension products were carried out according to the procedure described in Chapter 3.

5.3 RESULTS

(i) Northern Blot Analysis of *uncBE* mRNA

The positions of four complementary riboprobes used in Northern analysis are indicated in Fig. 5.1. Northern blot analysis of chromosomally-encoded RNA extracted from a wild type strain (SK5006), and an *unc* deletion strain (DK8) was performed using the four antisense RNA probes (Fig. 5.2A). The two RNA species seen in the *unc* deletion strain represent the 2.9 and 1.5-kb rRNA, respectively. These ribosomal RNAs are often recognized non-specifically due to their high abundance. As reported in Chapter 3 (Patel and Dunn, 1992), the 5'*uncB* probe did not hybridize to any detectable chromosomally-encoded *unc* transcript. The other three probes (3'*uncB*, *uncE* and *uncC*) recognized a major 6.0-kb chromosomally-

Figure 5.2 Northern blot analysis of *unc* mRNA using various antisense riboprobes.

(A) RNA was prepared from *E. coli* SK5006 (*unc*$^+$), DK8 (*unc*$^-$), and an induced *E. coli* strain JM103 carrying plasmid pHN4 as described in the Materials and Methods. RNA samples were separated on a 1.25% agarose gel after treatment with glyoxal, transferred to nylon membrane and probed with the indicated ^{32}P-labeled probes. The lanes labeled SK5006 and DK8 received 15 μg of total RNA and JM103/pHN4 lane received 1 μg of total RNA.

(B) Analysis of RNA transcribed from *E. coli* JM103 carrying pHN4. Equal amounts of total RNA (1 μg) from induced (I) and uninduced (N) cultures were size fractionated on a 6% polyacrylamide-8M urea gel, electroblotted to Zeta-probe membrane and hybridized to either *5'uncB* or *uncE* probe as described in the Materials and Methods. The full length message (A) and the processed transcripts (B-F) are indicated on the left. The two top bands seen in all the lanes correspond to the two large rRNA.

A

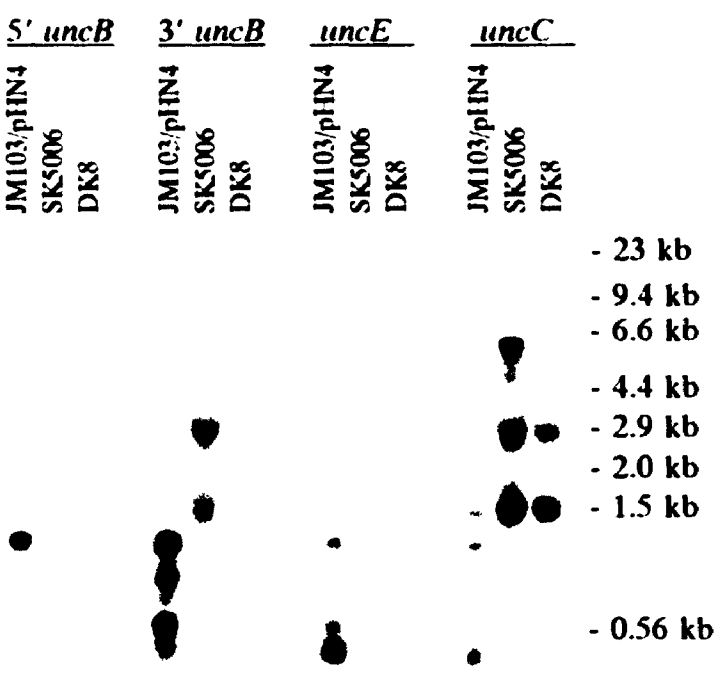
Probes:
5′ uncB
3′ uncB
uncE
uncC
JM103/pHN4
SK5006
DK8
- 23 kb
- 9.4 kb
- 6.6 kb
- 4.4 kb
- 2.9 kb
- 2.0 kb
- 1.5 kb
- 0.56 kb

B

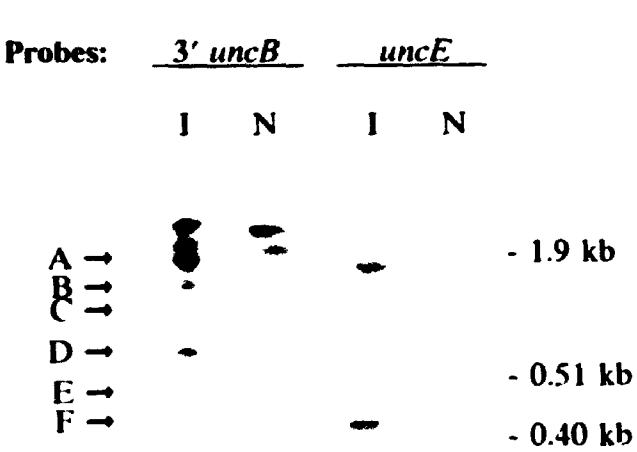
Probes:
3′ uncB
uncE
I
N
I
N
A
B
C
D
E
F
- 1.9 kb
- 0.51 kb
- 0.40 kb

encoded species which was previously shown to be a processed *unc* message missing the 5′ region of the full length transcript. The recognition of the 6.0-kb species by the 3′*uncB* probe implies that it probably contains the entire *uncE* coding sequence.

Studies of processing in the 5′-end of the natural *unc* transcript are limited in scope and difficult to carry out because of the constitutive expression, the large size of the RNA species and the relatively long time required for complete transcription. These difficulties were avoided using a plasmid pHN4 (Fig. 5.1), which carries most of the *uncB* coding sequence and the complete *uncE* gene, using the vector pEX1 (Passador and Linn, 1989), a derivative of pKK223-3 (Brosius and Holy, 1984) containing the $lacI^Q$ gene. In order to make the transcript stable against exonucleases the *unc* transcription terminator was cloned behind *uncBE*. The terminator insert carried about 20 bases from the 3′ end of the coding sequence of *uncC*, the last gene of the *unc* operon.

To further study the degradation of the 5′region of the *unc* message, RNA isolated from a strain carrying pHN4 was also analyzed (Fig. 5.2B, left lanes of each panel). The two top species of RNA seen in the induced samples are also present in the uninduced control and represent the two rRNA as discussed earlier. All four probes recognized the 1.2-kb full length transcript and the three probes at the 3′ end (3′*uncB*, *uncE*, *uncC*) also recognized various other breakdown products. To better resolve these breakdown products, the RNA species were separated on a denaturing polyacrylamide gel and probed with the 3′*uncB*- and *uncE*-specific probes (Fig. 5.2B). Both probes recognized the full length message (labeled A) and the same five breakdown species (labeled B-F). In contrast, only the full length transcript

hybridized to the 5'*uncB* probe (data not shown), indicating that the breakdown products had lost the 5' sequences. Since the appearance of the shorter mRNA species are dependent on induction they can be best explained as processing products of the full-length transcript by endonucleases.

These transcripts must be a nested set of fragments having a common 3' end since the probe directed to the terminator region (*uncC*) also recognized them (Fig. 5.2A). The estimated sizes of the full length message and the processed transcripts, and the position of the apparent cleavage sites with respect to the full length message are summarized in Fig. 5.3. The estimated size of the smallest species (F) is approximately 420 bases which should accommodate the intact *uncE* coding sequences. Also, species F is recognized by the 3' *uncB* probe which only extends about 20 bases into the early *uncE* coding region. Thus, all the cleavages giving rise to these species appear to be 5' to the *uncE* coding region.

As discussed earlier the species detected in these experiments have a common 3' end. One might expect that the cleavages would also produce fragments containing the original 5' end. For example, the 5' *uncB* probe should detect a species of 800 bases, corresponding to the 5' end of full length message which gave rise to species F. The apparent absence of such species implies that upon cleavage the upstream fragments are rapidly degraded by exonucleases, as usually happens in *E. coli* (Belasco and Higgins, 1988).

The intensity of each processed species depended on the probe used for the detection. For example the species D is recognized better by the 3'*uncB* probe compared to the *uncE* probe since it contains more sequences that would hybridize

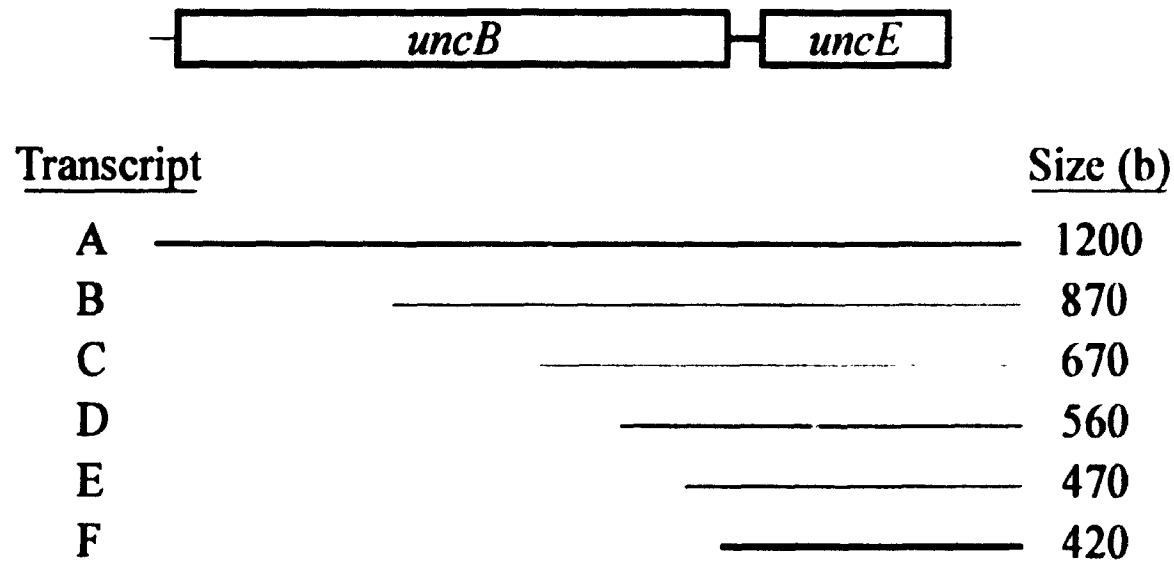

Figure 5.3 A diagrammatic representation of the transcripts observed in Fig. 5.2B using the *uncE* probe are shown to scale relative to the restriction map of pHN4. The thickness of the lines corresponds to the relative amount of each transcript as detected with the *uncE* probe. The species A is the primary full length transcript and B-F are the endonucleolytically processed products.

to the 3'*uncB* probe than *uncE* probe. The relative amounts of each species were estimated by the *uncE* probe since all the transcripts should have the complete sequences that would hybridize to the *uncE* probe. As can be seen among the processed products the species F is present in the highest amounts, with moderate levels of D and low levels of B, C and E. This implies that cleavages at the sites D and F are most efficient, or that the resultant species are relatively more stable.

(ii) Turnover of the pHN4-transcripts

In order to estimate the turnover rates of the pHN4 transcript, an exponentially growing culture of *E. coli* carrying the plasmid pHN4 was induced for just two minutes, then treated with rifampin to block further initiation of transcription, and total cellular RNA was isolated at intervals as described in the Materials and Methods. RNA was size-fractionated on a denaturing polyacrylamide gel and hybridized to the *3'uncB* probe (Fig. 5.4). At the point of rifampin addition (time 0), the full length transcript (A) gave the strongest signal. Within one minute one could see a decrease in the levels of the species A, B and C, whereas the smallest three species accumulated in that time period. After two minutes all the species disappeared except F, which remained strong through four minutes after rifampin addition. The complete conversion of the larger species to the smaller species F in less than two minutes indicates that processing in the *uncB* region is highly efficient.

Figure 5.4 Turnover analysis of mRNA species transcribed from the plasmid pHN4. *E. coli* JM103 bearing pHN4 was grown to early-log phase and induced as described in the Experimental Procedures. At 2 min after induction rifampin was added to block initiation of transcription and samples were collected for RNA extraction at the indicated time points. Northern blots of RNA samples were performed using the 3' *uncB* probe as described. All lanes received 1 μg of total RNA. N, non-induced sample.

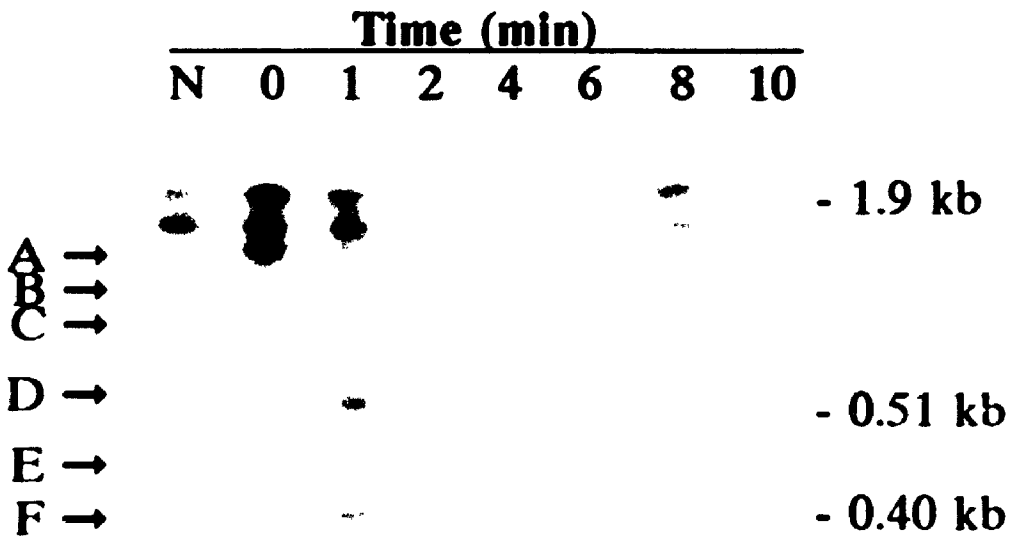
Time (min)
N 0 1 2 4 6 8 10
- 1.9 kb
A
B
C
D
E
F
- 0.51 kb
- 0.40 kb

(iii) Determination of the 5' Ends of the Processed Products

Primer extension was used to map the 5' termini of the processed species generated during the decay of the *uncBE* mRNA. A primer complementary to the mRNA sequence about 20 bases (Fig. 5.1) into the *uncE* gene was extended on RNA extracted from strains carrying pHN4 using moloney murine leukemia virus reverse transcriptase, and the products were electrophoresed alongside the product of dideoxynucleotide sequencing reactions on a sequencing gel (Fig. 5.5). The same sets of samples were run for different lengths of time to assign the positions of bands more precisely. As seen in the Northern blot analysis, six sets of bands are observed in the primer extension experiment. The sets are labeled so as to correspond with the species seen on the Northern blots. Notably, a number of different 5' ends can be identified for each of the bands seen in the Northern blot. The species corresponding to the two smallest bands run together in the Northern blot as the processed transcript F since the difference in size is small. While base T1789 is the prominent 5'end in set E, there are five equally abundant 5' ends in set D. In addition to the major species, various other minor bands were also detected by primer extension. The precise positions of the 5' termini of the processed species are indicated by triangles above the lines of sequence shown in Figure 5.6. The positions of species F cannot be read in Figure 5.5 but they were assigned in a separate experiment (data not shown). These two sites lie in the intercistronic region between the *uncB* and *uncE* coding regions and were previously reported by Gross (1991) to be RNase E-dependent cleavage sites using a hybrid plasmid-encoded RNA. Attempts to map the sites in region B more precisely using primers closer to

Figure 5.5 Primer extension analysis of RNA from uninduced(−) and induced (+) cultures of *E. coli* JM103 carrying the plasmid pHN4. A ^{32}P-labeled primer was used to prime cDNA synthesis, using total cellular RNA as template. The products were analyzed on a 6% polyacrylamide sequencing gel along with a pHN4-based dideoxy sequencing ladder. Bands or sets of bands corresponding to the species seen in the Northern analysis are labeled similarly. The same sets of samples were subjected to a shorter and a longer run to map the ends more precisely.


Long Run
TGCA+
Short Run
TGCA+
A
B
C
D
E
F
A
B
C
D

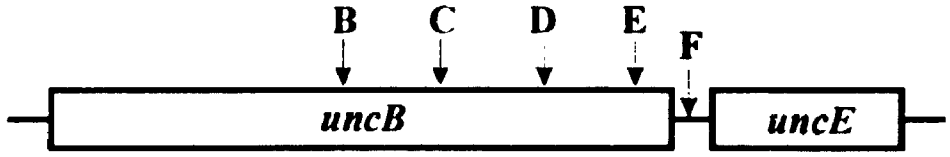

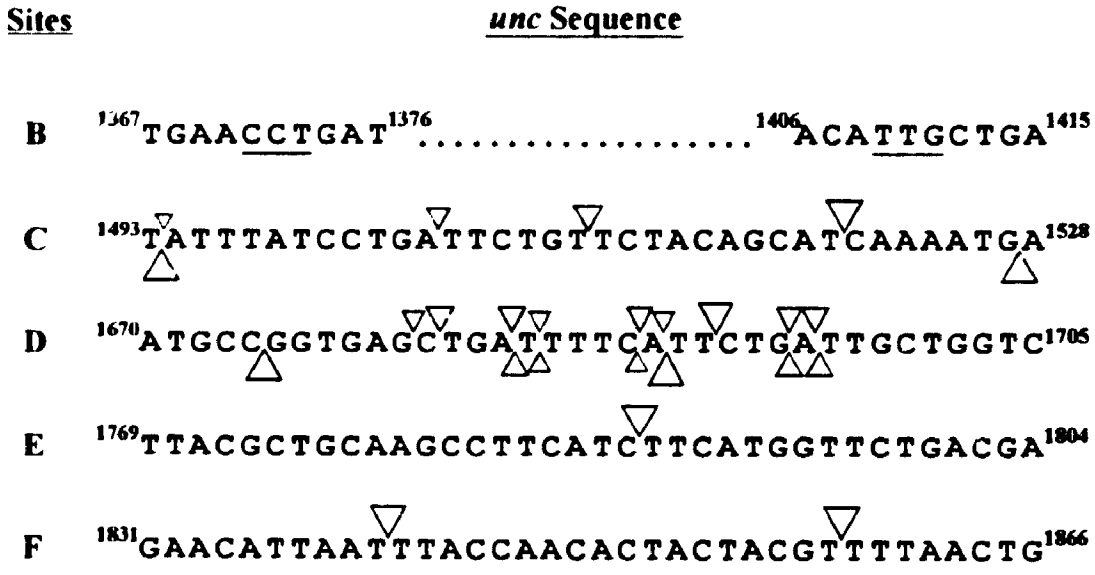

Figure 5.6 Nucleotide sequences of the *uncB* gene showing the positions of the observed cleavages. Only the sequences around the cleavage sites are shown and the bases are numbered as in Walker *et al.* (1984). The triangles above the sequences show the positions of cleavage in a wild type strain and the triangles shown below are the alternative sites that are observed in an RNase E-defective strain. The cleavages in E and F are missing in the *rne*$^-$ strain. The sizes of the triangles indicate the relative efficiency of cleavage in each group as observed in the primer extension analysis. The cleavage sites in B were within the underlined segments, but their exact positions were not determined.

the sites failed, possibly due to the presence of secondary structures or the relative instability of the message.

(iv) Processing of the *uncBE* mRNA in an RNase E-deficient Strain

In Chapter 3, I showed that the processing in the 5' end of the *unc* message was largely dependent on a functional RNase E (Patel and Dunn, 1992). Thus, RNA isolated from an RNase E mutant strain which showed reduced RNase E activity at the restrictive temperature was also analyzed. Primer extension products obtained by using RNA from *rne*$^+$ and *rne*$^-$ strains carrying the plasmid pHN4 using the aforementioned primer were run on a short polyacrylamide gel (Fig. 5.7). The levels of the full-length product (A) were greatly increased in the *rne*$^-$ mutant, especially at the nonpermissive temperature, confirming that degradation is dependent on RNase E. However, the cleavage products were still detected, except for product E, which was completely missing at 43°C. Thus some of the cleavage sites were clearly dependent on RNase E, but others were not.

To see if the chromosomally-encoded *unc* message is processed similarly, RNAs isolated from *rne*$^+$ and *rne*$^-$ strains were analyzed by primer extension and the products were separating on a sequencing gel (Fig. 5.8). The products obtained using chromosomally encoded *unc* mRNA are shown on the left of the sequencing ladder, and those obtained using plasmid-encoded mRNA are shown on the right. From this and related experiments the sites were mapped precisely, and the two sets of extension products were found to be highly similar, although the bands for the chromosomally-encoded message were relatively weak. As expected from Fig. 5.7,

Figure 5.7 Primer extension analysis of mRNA species transcribed from the plasmid pHN4 in various *E coli* strains. *E. coli* MG1693 (*rne*$^+$) and SK5665 (*rne*$^-$) bearing pHN4 were grown to early-log phase at 30°C, at which point half of each culture was shifted to 43°C to inactivate the mutant RNase E. After 30 min cultures were induced with IPTG for 10 min. RNA samples were prepared and primer extension was carried out as described in the Experimental Procedures. The products were separated on a small 6% polyacrylamide gel, which was then dried and exposed to x-ray film.

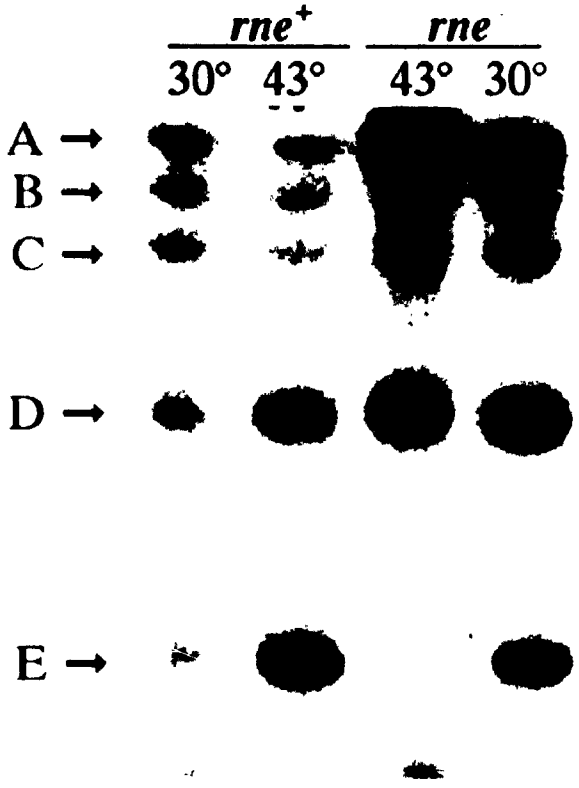
rne+
rne
30°
43°
43°
30°
A
B
C
D
E

Figure 5.8 Effect of the RNase E mutation on the processing. Comparison of the cleavages in chromosomally (left of the sequencing ladder) and plasmid encoded message (right of the sequencing ladder) in *rne*$^{+}$ and *rne*$^{-}$ strains. RNA from the indicated sources was used as a template to carry out primer extension analysis. The primer extension products were separated on a sequencing gel along with the pHN4 sequencing ladder. A control (lane labelled "in vitro RNA") in which the primer was extended on mRNA transcribed *in vitro* from pHN15 was used to determine reverse transcriptase stops that were due to secondary structure. I, induced; N, non-induced sample.


me, 43°
m, 30°
me, 43°
me, 30°
T
G
C
A
me, pIIN4, 30°, 1
me, pIIN4, 43°, 1
me, pIIN4, 30°, 1
me, pIIN4, 43°, 1
me, pIIN4, 43°, 1
me, pEN1, 43°, 1
in vitro, RNA
A
B
C
D
E

the bands corresponding to group E were missing in *rne*⁻ strains grown at the restrictive temperature irrespective of the source of RNA. The cleavages corresponding to species B, C, D were seen in all the conditions, but in some cases the precise positions of the cleavages were different if RNase E was inactive. The positions of the new sites are indicated in Figure 5.6 by triangles below the sequence. The appearance of the new sites was especially evident for group C, where the major cleavage at position C1521 in the wild type was replaced by a new cleavage at position A1528 and enhanced cleavage at position A1494 in the *rne*⁻ at 43°C. Also a new band at position G1675 (group D) was evident in the mutant at the nonpermissive temperature. Primer extension of RNA transcribed *in vitro* with T7 RNA polymerase (right hand lane, Fig 5.8) did not give any bands except the full length message implying the identified bands arose from new 5′ ends rather than from stops of reverse transcriptase due to RNA secondary structure.

5.4 DISCUSSION

RNase E, which was initially identified as an endonuclease that processes the rRNA primary transcripts to 5S rRNA (Misra and Apirion, 1979), now appears to be the most important endonuclease in bacterial mRNA degradation. It cleaves RNAs in single-stranded regions with a broadly defined consensus sequence of (G/A)AUU(A/U) and requires a double-stranded structure adjacent to the target site (Ehretsmann *et al.*, 1992b; Mackie, 1992).

The results indicate that the *uncBE* message is processed endonucleolytically, resulting in the formation of five stable transcripts, all having common 3′ ends and

various 5′ termini, extending in the *uncB* coding sequences. The turnover studies suggested that all the larger intermediates of the processing are further cleaved to give the smallest product (species F) in a relatively short time. The smallest species which contained functional *uncE* was relatively stable. The 5′ ends of the first four products were mapped in the coding region of the *uncB*, and the 5′ ends of the smallest species were mapped to the positions previously reported by Gross (1991) (in the intercistronic region between *uncB* and *uncE*). The chromosomally-encoded message was also found to be cleaved at same sites as in the plasmid-encoded message.

It appears that the major enzyme involved in the processing of *uncB* mRNA is RNase E as the full-length transcripts were much more abundant in the *rne*⁻ strain at 43°C. The sequences at the cleavage sites shown in Figure 5.6 are rich in A-T which has a tendency to be in a single-stranded region. It is also interesting to note that there is a good agreement between the RNase E consensus and the observed sites. The sites corresponding to E and F were clearly dependent on a functional RNase E. Cleavages at other sites still occurred to some extent in the RNase E-defective strain but the actual positions were different in some cases. Naturally, one wonders if these residual and alternative sites are dependent on RNase E, or if they imply that other endonucleases are also involved. It seems likely that the cleavages are seen here because of the much higher levels of the substrate mRNA (i.e., species A) that are present in the *rne*⁻ mutant at 43°C. Relatively inefficient cleavages become apparent under these condition because they have a much greater chance to occur, and the resultant species are more stable. It may be that another RNase can

slowly cleave in the same single-stranded regions, but at slightly different sites. The alternative sites seen in some cases support this notion. Alternatively, a trace of RNase E activity might be expected in the temperature-sensitive mutant, if, for example, the newly synthesized enzyme was active for a brief period before denaturation. It is also possible that the mutant form of RNase E has an altered specificity. Whichever the case, it must be emphasized that the major degradation pathway was dependent on RNase E, as indicated by the much higher levels of the full-length transcript in the *rne*$^-$ strain.

Results of the present study imply that degradation of *uncB* occurs through a series of endonucleolytic cleavages which are completed in less than two minutes. This speed is consistent with the processing nearly always preceding completion of transcription of the operon, which should require two to three minutes. The cleavage sites are present in groups located throughout *uncB*, with about 100 bases between the groups. The most 3′ of the groups (group F) consists of the two sites previously identified by Gross (1991) in the sequence between *uncB* and *uncE*. The probes did not detect any shorter species of mRNA from the plasmid-encoded *uncBE* message, suggesting that processing does not occur within the *uncE* coding sequence. The turnover study, also conducted with the plasmid-encoded *uncBE* message, showed that the cleavages in group F are the final cuts performed on messages rather than being initial steps in the decay of the upstream message. At this point, it is not clear whether the cleavages occur in a fixed order (*e.g.* 5′ to 3′), or if they occur randomly; either mechanism could give the pattern seen in Fig. 3. What is certain, however, is that the *uncB* message has a great potential for rapid decay.

Interestingly, a possible processing site has also been identified in the first gene, *uncI* (Schaeffer *et al.*, 1989).

uncE is the most highly expressed gene of the *unc* operon, consistent with the high stoichiometry of its product, subunit *c*, in the ATP synthase holoenzyme. Thus, it is the most efficiently translated *unc* cistron and its mRNA would be expected to be stable. The results presented here support this prediction. The *uncC* probe which was directed to the most 3' region of the transcript does not detect any other transcript smaller than F (longer exposer of the blots did not reveal any additional bands), suggesting that *uncE* is not cleaved internally into smaller fragments. McCarthy and co-workers (McCarthy *et al.*, 1985) have shown that *uncE* is expressed very strongly when it is preceded by the entire *uncB-uncE* intercistronic region, and that this high expression is almost entirely dependent on the 45 bases upstream from the Shine-Dalgarno sequence, rather than just the Shine-Dalgarno sequence itself. This intercistronic region is rich in A and T and it has been suggested that its unfolded structure is important in allowing ribosomes access to the *uncE* translation initiation region (Schauder and McCarthy, 1989). It may be significant that this sequence also includes the RNase E sites of group F. Cleavage at these sites might activate translation, as the Shine-Dalgarno sequence is left intact but removal of upstream message could make the translation initiation region more accessible to ribosomes. To date there is no direct evidence regarding the individual translational activities of the intact and processed forms.

In contrast, *uncB* is poorly expressed, and only a single copy of its product, the *a* subunit, is present in the enzyme. Limitation of the amount of subunit *a* produced

is essential, as this polypeptide is toxic if overexpressed (Eya *et al.*, 1989). Our observation of the rapid degradation of *uncB* mRNA by endonucleolytic cleavage at multiple sites provides a straightforward mechanism of degradation of this message. Whether the greater physical stability of *uncE* indicates a similarly greater functional stability is, however, not necessarily the case. Lagoni *et al.* (1993) estimated functional half-lives of the *unc* genes from exponential decay curves obtained after inhibiting transcription initiation with rifampin. They reported that the functional half-life of *uncB* is only mildly shorter than that of *uncE*, suggesting that functional decay may precede physical degradation. Interestingly, however, examination of their data reveals that while exponential decay of the *uncB* message began immediately after addition of rifampin, the onset of exponential decay of the other functional units was delayed by more than two minutes. Some delay might be expected for sections near the 3′ end of the operon, due to the time required for nascent transcripts to be completed, but this delay was apparent even for *uncE*, which follows immediately after *uncB*. This delay makes the actual message lifetimes longer than would be estimated from decay constants based on the subsequent period of exponential decay. In contrast, McCarthy and co-workers (1991) reported that the functional half-life of *uncE* was greater than that of *uncB* by a factor of between 3 and 4. It appears that these workers based their estimates on the time required for the first half of the functional message to decay, rather than on the later period. While less mathematically rigorous, this approach seems more appropriate when the assumption of first-order decay is invalid.

The multiple RNase E sites provide an opportunity for the decay of *uncB* to

commence quickly after its transcription, and might also function in delaying the onset of degradation of the downstream message. It could be that exponential decay of *uncEFHAGDC* does not begin until RNase E has worked its way through the sites in *uncB* to reach the two sites of group F. From the turnover studies (Fig. 5.4), this would be expected to take about two minutes. Gross (1991) interpreted the stabilization of his hybrid message in an RNase E-defective strain to indicate that these cleavages are the initiating steps in the degradation of the downstream message. This potential mechanism of timing the decay of the downstream *unc* sequence could arise if cleavage of the sites in *uncB* were somehow ordered, *e.g.* if the enzyme was slowly progressive in an overall 5′ to 3′ direction, or if the group F sites become better substrates as the upstream sequence is removed.

The decay mechanism of the *uncB* message is similar to the decay of the *uncDC* message which was reported earlier (Chapter 3) in that in both cases the cleavages are introducing new 3′ ends to exonucleases followed by its rapid degradation. However, the major difference is that the *uncB* message had multiple cleavages unlike the only one seen in the initial coding region of the *uncC* message (Patel and Dunn, 1992).

In conclusion, it is clear that the multiple cleavages in the *uncB* ensure the rapid inactivation of the 5′ region of the *unc* message. The *uncE* message was shown to be relatively more stable ensuring efficient expression of *uncE* but how the processing affects the translation of *uncE* remains to be studied.

CHAPTER 6

SUMMARY

In bacteria, genes for proteins that interact functionally are often organized into polycistronic operons so that their transcription can be regulated. Post-transcriptional regulation of the expression of individual genes within a polycistronic operon can result in synthesis of different amounts of their gene products. The *E. coli unc* operon is an appealing system to study the mechanism of post-transcriptional control because its gene products interact both functionally and structurally, and are expressed according to the subunit requirements in the mature ATPase complex.

In this thesis, the attention was focused on the two important aspects of post-transcriptional regulation of genes in polycistronic operons; the segmental differences in the mRNA stability and the efficiency of translation initiation. In particular, mRNA processing and degradation of the two extreme ends of the *unc* mRNA, and the regulation of differential expression of the last two genes was investigated. A peripheral attempt has been made to study the structural determinants of mRNA degradation of *E. coli* which still remain unresolved.

Northern blotting and primer extension analysis have revealed that the two extreme ends of the *unc* mRNA are subjected to RNase E-dependent endonucleolytic processing. In Chapter 5, it was reported that the *uncB* mRNA is rapidly degraded by a series of endonucleolytic cleavages, some specific to RNase E. It was found that *uncIB*, the most 5′ region of the message, is always removed before the transcription of the operon is completed thus explaining the lack of the full length *unc* transcript in wild type strains. It emphasizes that in bacteria not only transcription and translation are coupled but the degradation of the mRNA is coupled as well. A selective and rapid decay of the *uncI* and *uncB* portion of the message most likely

contributes to the low expression of their gene products, the *i* and *a* subunits, respectively. The major 6.0-kb *unc* transcript contained the intact *uncE* cistron as evidenced by primer extension studies. There were no apparent processing sites in the *uncE* message. This cistron is the most highly expressed of all the *unc* genes. This high expression has been attributed to its unstructured translation initiation region (McCarthy *et al.*, 1985, Sahauder and McCarthy, 1989). It is possible that the removal of the *uncIB*, in particular the RNase E-dependent cleavages in the *uncBE* intergenic region, allows even better translation of *uncE*.

Ziemke and McCarthy (1992) have reported that the functional half-lives of the seven genes downstream of *uncB* (*uncEFHAGDE*) are similar and longer compared to *uncIB*. Subsequently, it has been suggested that the segmental differences in the stability of these genes do not contribute significantly to the differential expression of the genes downstream of *uncB*.

The 3′ end of the *unc* message is also processed by RNase E. My results have revealed that there is a major RNase E-dependent processing site in the early *uncC* coding region which functionally inactivates the *uncD* and *uncC* messages which are expressed in a 3 to 1 ratio. The stability of these messages do not contribute to this apparent difference in the expression since the RNase E-dependent cleavage leads to functional inactivation of both messages. An inhibition of the RNase E-dependent cleavage at the aforementioned site did not result in an increase of the full length message, as seen in Chapter 4. Rather, it was observed that inhibition of cleavage at that site resulted in cleavages at other sites, and that the cleavages were still dependent on functional RNase E. These results have two important implications.

First, they suggest that RNase E is the most important enzyme that degrades *unc* message. Secondly, they imply that mRNA degradation probably operates in multiple pathways such that if the normal degradative pathway is blocked an alternative pathway operates.

The site-directed mutagenesis studies suggest that the structure of the *uncDC* mRNA, rather than its stability, is an important factor in regulating the differential expression of the *uncD* and *uncC* genes. The importance of a secondary structure in the intercistronic region between *uncD* and *uncC* in determining the differential expression of these genes was well documented by our laboratory previously (Dallmann and Dunn, 1994). The studies in this thesis reveal that another secondary structure which is 16 bases downstream of the *uncC* initiation codon is also important in downregulating *uncC* expression relative to *uncD*. We propose that the downregulation of *uncC* by the stem-loop is achieved through a somewhat novel mechanism. A shortening of the distance between the stem-loop and the *uncC* RBS led to lower expression whereas shifting the stem away from the RBS enhanced *uncC* expression. Northern blot analysis clearly revealed no effect of stem-loop on the stability of the mRNA, thus strengthening the proposed hypothesis that the stem-loop limits the access of *uncC* RBS to ribosomes.

The importance of the structure of mRNA in its degradation was also indirectly investigated. The hairpin formed by the *unc* transcription terminator was found to stabilize the *uncC* message against exonucleolytic degradation. The expression of *uncC* was increased ten-fold when it was followed by the *unc* transcription terminator than by the pre-5S rRNA sequence and the *rrnB* terminator.

The decay studies attributed this effect to the stability of the message since the *uncC* mRNA with the *unc* terminator was found to be three times more stable. This stability has enabled our laboratory to design an efficient derivative of pKK223-3 (Brosius and Holy, 1984) containing the *unc* terminator which has been useful in overproducing large quantities of some of the F_1 ATPase subunits and other unrelated proteins.

In Chapter 4, the importance of stem-loop in *uncC* mRNA in allowing efficient processing by RNase E was also demonstrated. A stable secondary structure was found to be a prerequisite for cleavage by RNase and that the enzyme was more tolerant to the changes at the actual site. These results extended the findings by Ehretsmann *et al.* (1992) and Cormack and Mackie (1992) for the requirement for RNase E cleavage. The studies also revealed that unlike some *E. coli* messages (Petersen, 1992), translation of *unc* mRNA does not affect the stability of the message.

With respect to the *unc* mRNA degradation, my results best fit with a general model of mRNA degradation in *E. coli*. Most genes are inactivated by endonucleolytic cleavages either in the early coding sequences or just upstream so as to prevent binding of ribosomes (Belasco and Higgins, 1988). Endonucleolytic cleavages expose new 3′ ends which could be substrate for exonucleases. It was observed that the cleavage in *uncC* mRNA was upstream of a stable secondary structure, in the initial coding sequences. This cleavage may serve to expose the upstream *uncD* sequences to exonucleases which are otherwise blocked by the secondary structure and simultaneously inactivating *uncD* and *uncC*. The upstream

products of the processing in the *uncB* message were also rapidly degraded, thus establishing that these cleavages are exposing new 3′ ends to exonuclease.

unc mRNA degradation is an involved process which is still incompletely understood. In this work, however, it was shown that RNase E is a key enzyme in degradation of *unc* mRNA. I have identified a number of the sites cleaved by this enzyme in the 5′ and 3′ ends of the operon, and have assessed the role of the degradation in the differential expression of the unc genes. My results for *uncC* expression have identified a novel mechanism by which mRNA secondary structures significantly limit gene expression.

The overall regulation of *unc* genes is an intricate process, achieved through a combination of different mechanisms. The factors that are implicated in regulating the expression of *unc* genes can be summarized as follows. The expression of the first two genes of the operon is down regulated by their lower mRNA stability compared to other genes. In retrospect, the structure of the mRNA in the translation initiation region seems to be extensively involved in the regulation of the other genes. This is supported by ample evidence of involvement of the secondary structure in almost all the pairs of genes in the operon. The *uncE* gene, for example, is efficiently translated because of its TIR being free of any secondary structure. In addition, most of the genes, downstream from *uncE*, are coupled through secondary structures of mRNA involving the TIRs. Therefore, it appears that the structure of mRNA is very important in the relative expression of the *unc* genes.

It has to be borne in mind that almost all the findings to date involve the cis-acting elements. There is no reported involvement of any trans-acting factors, such as translation repressor proteins, antisense RNA or autoregulation, all of which are otherwise known to regulate expression of some genes in *E. coli* (Gold, 1988). Potential roles, if any, of the endonucleolytic processing in the central part of the operon in regulating the differential expression of *unc* genes, and its contribution to the overall *unc* mRNA degradation still remain to be elucidated.

REFERENCES

Abrahams, J. P., Lutter, R., Todd, R. J., Vanraaji, M. J., Leslie, A. G. W., and Walker, J. E. (1993) Inherent asymmetry of the structure of F_1-ATPase from bovine heart mitochondria at 6.5 angstrom resolution. *EMBO J.* **12**, 1775-1780.

Adhin, M. R., and van Duin, J. (1990) Scanning model for translational reinitiation in eubacteria. *J. Mol. Biol.* **213**, 811-818.

Anato, V. P., and Tinoco, Jr. (1992) Thermodynamic parameters for loop formation in RNA and DNA hairpin tetraloops. *Nucl. Acid. Res.* **20**, 819-824.

Apirion, D. (1978) Isolation, genetic mapping and some characterization of a mutation in *Escherichia coli* that affects the processing of ribonucleic acid. *Genetics* **90**, 659-671.

Apirion, D. and Watson, N. (1975) Mapping and characterization of a mutation in *Escherichia coli* that reduces the level of ribonuclease III specific for double-stranded ribonucleic acid. *J. Bacteriol.* **124**:317-324.

Arraiano, C.M., Yancey, S.D. and Kushner, S.R. (1988) Stabilization of discrete mRNA breakdown products in *ams pnp rnb* multiple mutants of *Escherichia coli* K-12. *J. Bacteriol.* **170**, 4625-4633.

Babitzke, P. and Kushner, S.R. (1991) The ams (altered mRNA stability) protein and ribonuclease E are encoded by the same structural gene of *Escherichia coli*. *Proc. Natl. Acad. Sci. USA* **88**, 1-5.

Baga, M., Giransson, M., Normack, S., and Uhlin B.E. (1988) Processed mRNA with differential stability in the regulation of *Escherichia coli* pilin gene expression. *Cell* **52**: 197-206.

Bardwell, J.C.A., Régnier, P., Chen, S-M., Nakamura, Y., Grunberg-Manago, M. and Court, D.L. (1989) Autoregulation of RNase III operon by mRNA processing. *EMBO J.* **8**, 3401-3407.

Belasco, J.G., and Higgins, C.F. (1988) Mechanisms of mRNA decay in bacteria: a perspective. *Gene* **72**: 15-23.

Belasco, J.G., Beatty, J.T., Adams, C.W., von Gabain, A. and Cohen, S.N. (1985) Differential expression of photosynthesis genes in *R. capsulata* results from segmental differences in stability within the polycistronic *rxc*A transcript. *Cell* **40**, 171-181.

Bouvet, P., and Belasco, J. G. (1992) Control of RNase E-mediated RNA degradation by 5'-terminal base pairing in *E. coli*. *Nature (London)* **360**, 488-491.

Boyer, P. D. (1989) A perspective of the binding change mechanism for ATP synthesis. *FASEB J.* **3**, 2164 - 2178.

Boyer, P. D. (1993) The binding change mechanism for ATP synthase - Some probabilities and possibilities. *Biochim. Biophys. Acta* **1140**, 215-250.

Brosius, J., Dull, T. J., Sleeter, D. D., and Noller, H. F. (1981) Gene organization and primary structure of a ribosomal RNA operon from *Escherichia coli*. *J. Mol. Biol.* **148**:107-127.

Brosius, J., and Holy, A. (1984) Regulation of ribosomal RNA promoters with a synthetic *lac* operator. *Proc Natl Acad Sci USA* **81**: 6929-6933.

Brusilow, W.S.A., Klionsky, D.J., and Simoni, R.D. (1982) Differential polypeptide synthesis of the proton-translocating ATPase of *Escherichia coli*. *J Bacteriol* **151**: 1363-1371.

Brusilow, W. S. A., Porter, A. C. G., and Simoni, R. D. (1983) Cloning and expression of *uncI*, the first gene of the *unc* operon of *Escherichia coli*. *J. Bacteriol.* **155**, 1265-1270.

Cannistraro, V. J., Subbarao, M. N., and Kennell, D. (1986) Specific endonucleolytic cleavages sites for decay of *Escherichia coli* mRNA. *J. Mol. Biol.* **192**, 257-274.

Carter, P. (1987) Improved oligonucleotide-directed mutagenesis using M13 vectors. *Methods Enzymol.* **154**, 382-403.

Cormack, R. S., and Mackie, G. A. (1992) Structural requirements for the processing of *Escherichia coli* 5 S ribosomal RNA by RNase E *in vitro*. *J. Mol. Biol.* 228, 1078-1090.

Cox , G. B., Webb, D., Hatch, L., Lightowlers, R., Munn, A., and Gibson, F. (1987). Altered translation of the *uncC* gene coding for the ϵ subunit of the F_1F_o-ATPase of *Escherichia coli*. *J. Bacteriol.* **169**, 2945-2949.

Cozens, A. L., and Walker, J. E. (1987) The organization and sequence of the genes for ATP synthase subunits in the cyanobacterium *Synechococcus* 6301. *J. Mol. Biol.* **194**, 359-383.

Cross, R. L., Cunningham, D., and Tamura, J. K. (1984) Binding change mechanism for ATP synthesis by oxidative phosphorylation and photophosphorylation. *Curr. Top. Cell. Regul.* **24**, 335-344.

Dallmann, H. G., and Dunn S. D. (1994) Translation through an *uncDC* mRNA secondary structure governs the level of *uncC* expression in *Escherichia coli*. *J. Bacterio.* **176**, 1242-1250.

Dallmann, H. G., Flynn, T. G., and Dunn, S. D. (1992) Determination of the 1-Ethyl-3-[(3-dimethylamino)propyl]-Carbodiimide (EDC) Induced Crosslink Between the β and ϵ Subunits of *Escherichia coli* F_1-ATPase *J. Biol. Chem.* **267**, 18953-18960.

de Smit, M. H., and van Duin, J. (1990) Control of prokaryotic translational initiation by mRNA secondary structure. *Prog. Nucl. Ac. Res. and Mol. Biol.* **38**, 1-35.

de Smit, M. H., and van Duin, J. (1994) Translational initiation on structures messengers: Another role for the Shine-Dalgarno interaction. *J. Mol. Biol.* 235, **173**-184.

Denhardt, D. T. (1966) A membrane-filter technique for the detection of complementary DNA. Biochem. Biophys. Res. Commun. **23:** 641.

Dennis, P. P., and Nomura, M. (1975) Regulation of the expression of ribosomal protein gene in *Escherichia coli. J. Mol. Biol.* **97**, 61-76.

Devereux, J., Haeberli, P., Smithies, O. (1984) A comprehensive set of sequence analysis programs for the VAX. *Nucleic Acids Res.* **12**, 387-395.

Donovan, W.P., and Kushner, S.R. (1986) Polynucleotide phosphorylase and ribonuclease II are required for cell viability and mRNA turnover in *Escherichia coli* K-12. *Proc Natl Acad Sci USA* **83:** 120-124.

Downie, J. A., Gibson, F., and Cox, G. B. (1979) Membrane adenosine triphosphatases of prokaryotic cell. *Annu. Rev. Biochem.* **48**, 103-131.

Dreyfus, M. (1988) What constitutes the signal for the initiation of protein synthesis on *Escherichia coli* mRNAs ? *J. Mol. Biol.* **204**, 79-94.

Dreyfus, G. and Satre, M. (1984) The ϵ subunit as an ATPase inhibitor of the F_1-ATPase in *Escherichia coli. Arch. Biochem. Biophys.* **229:**212-219.

Dunn, S. D. (1986a) Effects of the modification of transfer buffer composition and the renaturation of proteins in gels on the recognition of proteins on western blots by monoclonal antibodies. *Anal. Biochem.* **157**, 144-153.

Dunn, S. D. (1986b) Removal of the ϵ subunit from *Escherichia coli* F_1-ATPase using monoclonal anti-ϵ antibody affinity chromatography. *Anal. Biochem.* **159**, 35-42.

Dunn, S. D. (1992) The polar domain of the *b* subunit of *Escherichia coli* F_1F_o-ATPase forms an elongated dimer that interacts with the F_1 sector. *J. Biol. Chem.* **267**, 7630-7636.

Dunn, S. D., and Dallmann, H. G. (1990) An upstream *uncD* sequence modulates translation of *Escherichia coli uncC. J. Bacteriol.* **172**, 2782-2784.

Dunn, S. D., and Futai, M. (1980) Reconstitution of a functional coupling factor from the isolated subunits of *Escherichia coli* F_1-ATPase. *J. Biol. Chem.* **255**, 113-118.

Dunn, S. D., Tozer, R. G., Antczak, D. F., and Heppel, L. A. (1985) Monoclonal antibodies to *Escherichia coli* F_1-ATPase. Correlation of binding site location with interspecies cross-reactivity and effects on enzyme activity. *J. Biol. Chem.* **260**, 10418-10425.

Ehretsmann, C.P., Caprousis, A.J., and Krisch, H.M. (1992) Specificity of *Escherichia coli* endoribonuclease RNase E: *in vivo* and *in vitro* analysis of mutants in a bacteriophage

T4 mRNA processing site. *Genes Dev* **6**: 149-159.

Emory, S.A. and Belasco, J.G. (1990) The *ompA* 5' untranslated RNA segment functions in *Escherichia coli* as a growth-rate-regulated mRNA stabilizer whose activity is unrelated to translational efficiency. *J. Bacteriol.* **172**, 4472-4481.

Emory, S.A., Bouvet, P. and Belasco, J.G. (1992) A 5'-terminal stem-loop structure can stablize mRNA in *Escherichia coli. Genes Dev.* **6**, 135-148.

Eya, S., Maeda, M., Tomochika, K.-I., Kanemasa, Y., and Futai, M. (1989) Overproduction of truncated subunit *a* of H^+-ATPase causes growth inhibition of *Escherichia coli. J Bacteriol* **171:** 6853-6858.

Foster, D.L., and Fillingame, R.H. (1982) Stoichiometry of subunits in the H^+-ATPase complex of *Escherichia coli. J Biol Chem* **257:** 2009-2015.

Fraga, D., Hermolin, J., Oldenburg, M., Miller, M. J., and Fillingame, R. H. (1994) Arginine 41 of subunit *c* of *Escherichia coli* H^+-ATP synthase is essential in binding and coupling of F_1 to F_0. *J. Biol. Chem.* **269**, 7532-7537.

Fraker, P. J., and Speck, J. C. (1978) Protein and cell membrane iodinations with a sparingly soluble chloramide, 1,3,4,6-tetrachloro-3a,6a,-diphenylglycoluril. *Biochem. Biophys. Res. Commun.* **134**, 849-857.

Freier, S. M., Kierzek, R., Jaeger, J. A., Sugimoto, N., Caruthers, M. H., Neilson, T., and Turner, D. H. (1986) Improved free energy parameters for predictions of RNA duplex stability. *Proc. Natl. Acad. Sci. USA* **83**, 9373-9377.

Gay, N. J. (1984) Construction and characterizarion of an *Escherichia coli* strain with a *uncI* mutation. *J. Bacteriol.* **158**, 820-825.

Gerstel, B., and McCarthy, J. E. G. (1989) Independent and coupled translation initiation of *atp* genes in *Escherichia coli*: experiments using chromosomal and plasmid-borne *lacZ* fusions. *Mol. Micribiol.* **3**, 851-859.

Gibson, B. (1983) *Proc. R. Soc. Lodon Ser. B.* **215**, 1-18.

Gibson, F., Cox, G. B., Downie, J. A., and Radik, J. (1977) Partial diploids of *Escherichia coli* carrying normal and mutant alleles affecting oxidative phosphorylation. *Biochem. J.* **162**, 665-670.

Gold, L. (1988) Posttranscriptional regulatory mechanisms in *Escherichia coli. Ann. Rev. Biochem.* **57**, 199-233.

Goldblum, K., and Apirion, D. (1981) Inactivation of the ribonucleic acid-processing enzyme ribonucleic E blocks cell division. *J. Bacteriol.* **146**, 128-132.

Gotta, S. L., Miller, O. L., and French, S. L. (1991) rRNA transcription rate in *Escherichia coli. J. Bacteriol.* **173**, 6647-6649.

Gross, G. (1991) RNase E cleavage in the *atpE* leader region of *atpE/interferon-β* hybrid transcript in *Escherichia coli* causes enhanced rates of mRNA decay. *J Biol Chem* **266**: 17880-17884.

Gualerzi, C. O., and Pon, C. L. (1990) Initiation of mRNA translation in prokaryotes. *Biochemistry* **29**, 5881-5889.

Gunsalus, R.P., Brusilow, W.S.A., and Simoni, R.D. (1982) Gene order and gene-polypeptide relationships of the proton-translocation ATPase operon (*unc*) of *Escherichia coli*. *Proc. Natl. Acad. Sci. USA* **79**:320-324.

Hartz, D., McPheeters, D.S., Traut, R., and Gold L. (1988) Extention inhibition analysis of translation initiation complexes. *Met. Enzymol.* **164**, 419-425.

Hellmuth, K., Rex, G., Surin, B., Zinck, R., and McCarthy, J. E. G. (1991) Translational coupling varying in efficiency between different pairs of genes in the central region of the *atp* operon of *Escherichia coli*. *Mol.Microbiol.* **5**, 813-824.

Heus, H. A., and Pardi, A. (1990) Structural features that give rise to the unusual stability of RNA hairpins containing GNRA loops. *Science* **253**, 191-194.

Hwlfman, D.M. and Hughes, S. H.. (1987) Use of antibodies to screen cDNA expression libraries prepared in plasmid vectors. *Methods Enzymol.* **152**, 451-457.

Jacques, N., and Dreyfus, M. (1990) Translation initiation in *Escherichia coli*: old and new questions. *Mol. Microbiol.* **4**, 1063-1067.

Jones, H. M., Brajkovich, C. M., and Gunsalus, R. P. (1983) *In vivo* 5′ terminus and length of the mRNA for the proton-translocating ATPase (*unc*) operon of *Escherichia coli*. *J. Bacteriol.* **155**, 1279-1287.

Kanazawa, H., Kiyasu, T., Noumi, T., and Futai, M. (1984) Overproduction of subunit *a* of the F_0 component of proton-translocating ATPase inhibits growth of *Escherichia coli* cells. *J. Bateriol.* **158**, 300-306.

Kindler, P., Keil, T.U. and Hofschneider, P.H. (1973) Isolation and characterization of a ribonuclease III deficient mutant of *Escherichia coli*. *Mol. Gen. Genet.* **126**, 53-69.

Klionsky, D.J., Brusilow, W.S.A., and Simoni, R.D. (1984) *In vivo* evidence for the role of the ϵ subunit as an inhibitor of the proton-translocating ATPase of *Escherichia coli*. *J. Bacteriol.* **160**:1055-1060.

Klionsky, D. J., Skalnik, D. G., and Simoni, R. D. (1986) Differential translation of the genes encoding the proton translocating ATPase of *Escherichia coli*. *J. Biol. Chem.* **261**, 8069-8099.

Klug, G. and Cohen, S.N. (1991) Effects of translation on degradation of mRNA segments transcribed from the polycistronic *puf* operon of *Rhodobacter capsulatus*. *J. Bacteriol.* **173**, 1478-1484.

Kokoska, R. J., Blumer, K. J., and Steege, D.A. (1990) Phage f1 mRNA processing in *Escherichia coli*: search for the upstream products of endonuclease cleavage, requirement for the product of the altered mRNA stability (*ams*) locus. *Biochime* **72**, 803-811.

Kuki, M., Noumi, T., Maeda, M., Amemura, A., and Futai, M. (1988) Functional domains of ϵ subunit of *Escherichia coli* H^+-ATPase. *J. Biol. Chem.* **263**, 17437-17442.

Laemmli, U.K. (1970) Cleavage of structural proteins during the assembly of the head of bacteriophage T4. *Nature* (London) **227**:680-685.

Lagoni, O.R., von Meyenburg, K., and Michelsen, O. (1993) Limited differential mRNA inactivation in the *atp* (*unc*) operon of *Escherichia coli*. *J. Bacteriol* **175**: 5791-5797.

Lang, V., Gualerzi, C., and McCarthy, J. E. G. (1989) Ribosomal affinity and translational initiation in *Escherichia coli*. *J. Mol. Biol.* **210**, 659-663.

Lesage, P., Chiaruttini, C., Graffe, M., Dondon, J., Milet, M. and Springer, M. (1992) Messenger RNA secondary structure and translational coupling in the *Escherichia coli* operon encoding translational initiation factor IF3 and the ribosomal proteins, L35 and L20. *J. Mol. Biol.* **228**, 366-386.

Levinthal, C., Fon, D. P., Higa, A., and Zimmerman, R.A. (1963) The decay and protection of messanger RNA in bacteria. *Cold Spring Harbor Symp. Quant. Biol.* **28**, 183-190.

Loayza, D., Carpousis, A. J., and Krish, H. M. (1991) Gene 32 transcription and mRNA processing in T4-related bateriophage. *Mol. Microbiol.* **5**, 715-725.

Lundberg, U., von Gabain, A., and Melefors, O. (1990) Cleavages in the 5' region of the *ompA* and *bla* mRNA control stability : studies with an *E. coli* mutant altering mRNA stability and a novel endonuclease. *EMBO J.* **9**, 2731-2741.

Lundberg, U., Nilsson, G. and von Gabain, A. (1988) The differential stability of the 3A and *bla* mRNA at various growth rates is not correlated to the efficienty of translation. *Gene* **72**, 141-149.

Mackie, G.A. (1986) Structure of the DNA distal to the gene for ribosomal protein S20 in *Escherichia coli* K12: presence of a strong terminator and an ISI element. *Nucl Acids Res* **14**: 6965-6981.

Mackie, G.A. (1989) Stabilization of the 3' one-third of *Escherichia coli* ribosomal protein S20 mRNA in mutants lacking polynucleotide phosphorylase. *J Bacteriol* **171**:4112-4120.

Mackie, G. A. (1991) Specific endonucleolytic cleavage of the mRNA for the ribosomal protein S20 of *Escerichia coli* requires the product of the *ams* gene *in vivo* and *in vitro*. *J. Bacteriol.* **173**, 2488-2497.

Mackie, G. A. (1992) Secondary structure of the mRNA for ribosomal protein S20.

Implications for cleavage by ribonuclease E. *J Biol Chem* **267:** 1054-1061.

Mandel, M., and Higa, A. (1970) Calcium dependent bacteriophage DNA infection. *J. Mol. Biol.* **53**, 154-158.

McCarthy, J. E. G. (1988) Expression of the *unc* genes in *Escherichia coli*. *J. Bioenerg. Biomembr.* **20**, 19-39.

McCarthy, J. E. G. (1990) Post-transcriptional control in the polycistronic operon environment: studies of the *atp* operon of *Escherichia coli*. *Mol. Microbiol.* **4**, 1233-1240.

McCarthy, J. E. G., and Bokelmann, C. (1988) Determinants of translational initiation efficiency in the *atp* operon of *Escherichia coli*. *Mol. Microbiol.* **2**, 455-465.

McCarthy, J.E.G., Gerstel, B., Surin, B., Wiedemann, U. and Ziemke, P. (1991) Differential gene expression from the *Escherichia coli atp* operon mediated by segmental differences in mRNA stability. *Mol. Microbiol.* **5**, 2447-2458.

McCarthy, J. E. G. and Gualerzi, C. O. (1990) Translational control of prokaryotic gene expression. *Trends in Genetics* **6**, 78-85.

McCarthy, J.E.G., Schairer, H.U., and Sebald, W. (1985) Translation initiation frequency of the *atp* genes from *Escherichia coli*: identification of an intercistronic sequence that enhances translation. *EMBO J* **4**: 519-526.

McCarthy, J.E.G., Schauder, B., and Ziemke, P. (1988) Post-translational control in *Escherichia coli*: translation and degradation of the *atp* operon mRNA. *Gene* **72:** 131-139.

Me[illegible] D.A, Szczesna-Skorupa, E., and Kemper, E. (1986) Single-stranded DNA "blue" T7 promoter plasmids: a versatile tandem promoter system for cloning and protein engineering. *Protein Eng* **1**: 67-74.

Melefors, ö. and von Gabain, A. (1991) Genetic studies of cleavage-initiated mRNA decay and processing of ribosomal 9S RNA show that the *Escherichia coli arns* and *me* loci are the same. *Mol. Microbiol.* **5**, 857-864.

Meselson, M., and Yuan, R. (1968) DNA restriction enzyme from *E. coli*. *Nature (London)* 217, 1110-1114.

Messing, J., Crea, J., and Seeburg, P.H. (1981) A system for shotgun DNA sequencing. *Nucl Acids Res* **9**: 309-321.

Misra, T.K., and Apirion, D. (1979) RNase E, an RNA processing enzyme from *Escherichia coli*. *J. Biol. Chem.* **254**:11154-11159.

Mudd, E.A., Carpousis, A.J. and Krisch, H.M. (1990) *Escherichia coli* RNase E has a role in the decay of bacteriophage T4 mRNA. *Genes Dev.* **4**, 873-881.

Mudd, E.A., Krisch, H.M. and Higgins, C.F. (1990) RNase E, an endoribonuclease, has a general role in the chemical decay of the *Escherichia coli* mRNA: evidence that *me* and *ams* are the same genetic locus. *Mol. Microbiol.* **4**, 2127-2135.

Mudd, E.A., Prentki, P., Belin, D. and Krisch, H.M. (1988) Processing of unstable bacteriophage T4 gene 32 mRNAs into a stable species rquires *Escherichia coli* ribonuclease E. *EMBO J.* **7**, 3601-3607.

Newbury, S.F., Smith, N.H., and Higgins, C.F. (1987) Differential mRNA stability controls relative gene expression within a polycistronic operon. *Cell* **51**: 1131-1143.

Nielsen, J., Hansen, F. G., Hoppe, J., Friedl, P., and von Meyenberg, K. (1981) The nucleotide sequence of the *atp* genes coding for the F_0 subunits *a*, *b*, *c* and the F_1 subunit δ of the membrane-bound ATP synthase of *Escherichia coli*. *Mol. Gen. Genet.* **184**, 33-39.

Nilssin, G., Lundberg, U. and von Gabain, A. (1988) *In vivo* and *in vitro* identity of site specific cleavages in the 5′ non-coding region of *ompA* and *bla* mRNA in *Escherichia coli*. *EMBO J.* **7**, 2269-2275.

Nilsson, P. and Uhlin, B.F. (1991) Differential decay of a polycistronic *Escherichia coli* transcript is initiated by RNase E-dependent endonucleolytic processing. *Mol. Microbiol.* **5**, 1791-1799.

Ono, M. and Kuwano, M. (1979) A conditional lethal mutation in an *Escherichia coli* strain with a longer chemical lifetime of messenger RNA. *J. Mol. Biol.* **129**, 343-357.

Ono, M. and Kuwano, M. (1980) Chromosomal location of a gene for chemical longevity of messenger ribonucleic acid in a temperature-sensitive mutant of *Escherichia coli*. *J. Bacteriol.* **142**, 325-326.

Passador, L., and Linn, T. (1989) Autogenous regulation of the RNA polymerase β subunit of *Escherichia coli* occurs at the translational level *in vivo*. *J Bacteriol* **171**: 6234-6242.

Patel, A.M., Dallmann, H.G., Skakoon, E.N., Kapala, T.D., and Dunn, S.D. (1990) The *Escherichia coli unc* transcription terminator enhances expression of *uncC*, encoding the ϵ subunit of F_1-ATPase, from plasmids by stabilizing the transcript. *Mol Microbiol* **4**: 1941-1946.

Patel, A. M., and Dunn, S.D. (1992) RNase E-dependent cleavages in the 5′ and 3′ regions of the *Escherichia coli unc* mRNA. *J Bacteriol* **174**: 3541-3548.

Pati, S., DiSilvestre, D., and Brusilow, W. S. A. (1992) Regulation of the *Escherichia coli uncH* gene by mRNA secondary structure and translational coupling. *Mol. Microbiol.* **6**, 3559-3566.

Penefsky, H. S., and Cross, R. L. (1991) Structure and mechanism of F_0-F_1-ATP synthases and ATPases. *Adv. Enzymol.* **64**, 173-241.

Petersen, C. (1992) Control of functional mRNA stability in bacteria: multiple mechanisms of nucleolytic and non-nucleolytic inactivation. *Mol. Microbiol.* **6,** 277-282.

Porter, A. C. G., Brusilow, W. S. A., and Simoni, R. D. (1983) Promoter for the *unc* operon of *Escherichia coli*. *J. Bacteriol.* **155,** 1271-1278.

Rapaport, L. R., and Mackie, J. A. (1994) Influence of translational efficiency on the stability for ribosomal protein S 20 in *Escherichia coli*. *J. Bacteriol.* **176,** 992-998.

Regnier, P. and Grunberg-Manago, M. (1989) Cleavage by RNase III in the transcripts of the *metY-nusA-infB* operon of *Escherichia coli* releases the tRNA and initiates the decay of the downstream mRNA. *J. Mol. Biol.* **210,** 293-302.

Regnier, P., and Hajnsdorf, E. (1991) Decay of mRNA encoding ribosomal protein S 15 of *Escherichia coli* is initiated by an RNase E-dependent endonucleolytic cleavage that removes the 3' stabilizing stem and loop structure. *J. Mol. Biol.* **217,** 283-292.

Rex, G., Surin, B., Besse, G., Schneppe, B., and McCarthy, J. E. G. (1994) The mechanism of translational coupling in *Escherichia coli*. *J. Biol. Chem.* **269,** 18118-18127.

Ringquist, S., Shinedling, S., Barrick, D., Green, L., Brinkley, J., Stormo, D., and Gold, L. (1992) Translation initiation in *Escherichia coli*: Seuences within the ribosome binding site. *Mol. Microbiol.* **6,** 1219-1229.

Robertson, H.D. and Dunn, J.J. (1975) Ribonucleic acid processing activity of *Escherichia coli* ribonuclease III. *J. Biol. Chem.* **250,** 3050-3056.

Ross, G.W., and O'Callaghan, C.H. (1975) β-Lactamase Assays. *Methods Enzymol.* **43**:69-85.

Sambrook , J., Fritsch, E.F., and Maniatis, T. (1989) *Molecular cloning: a laboratory manual.* Cold Spring Harbor, New York: Cold spring Harbor Laboratory Press.

Sanger, F., Nicklen, S., and Coulson, A. R. (1977) DNA sequencing with chain-terminating inhibitors. *Proc. Nat. Acad. Sci. USA* **74,** 5463-5467.

SantaLucia, J., Kierzek, Jr. R., and Turner, D. H. (1992) Context dependence of hydrogen bond free energy releaved by substitutions in an RNA hairpin. *Science* **256,** 217-219.

Schaefer, E.M., Hartz, D., Gold, L., and Simoni, R.D. (1989) Ribosome-binding sites and RNA-processing sites in the transcript of the *Escherichia coli unc* operon. *J Bacteriol* **171:** 3901-3908.

Schauder, B., and McCarthy, J.E.G. (1989) The role of bases upstream of the Shine-Dalgarno region and in the coding sequence in the control of gene expression of *Escherichia coli*: translation and stability of mRNAs *in vivo*. *Gene* **78:** 59-72.

Schmidt, B. F., Berkhout, B., Overbeek, G. P., van Strien, A., and van Duin, J. (1987)

Determination of the RNA secondary structure that regulates lysis gene expression in bacteriophage MS2. *J. Mol. Biol.* **195**, 505-516.

Schneppe, B., Deckers-Hebestreit, G., McCarthy, J. E. G., and Altendorf, K. (1991) Translation of the first gene of the *Escherichia coli unc* operon. *J. Biol. Chem.* **266**, 21090-21098.

Schulz, V. P., and Reznikoff, W. S. (1990) *In vitro* secondary structure analysis of mRNA from *lacZ* translation initiation mutants. *J. Mol. biol.* **211**, 427-445.

Senior, A. E. (1988) ATP synthesis by oxidative phosphorylation. *Physiol. Rev.* **68**, 177-231.

Senior, A. E. (1992) Catalytic sites of *Escherichia coli* F_1-ATPase. *J. Bioenerg. Biomemb.* **24**, 479-484.

Shaw, G. (1994) Unpublished data (Pesrsannal Communication).

Shine, J., and Dalgarno, L. (1974) The 3'-terminal sequence of *Escherichia coli* 16 S ribosomal RNA: Complementarity to nonsense triplets and ribosome binding sites. *Proc. Nat. Acad. Sci., U. S. A.* **71**, 1342-1346.

Skakoon, E. N., and Dunn, S. D. (1993a) Location of conserved residue histidine-38 of the ϵ subunit of *Escherichia coli* ATP synthase. *Arch. Biochem. Biophys.* **302**, 272-278.

Skakoon, E. N., and Dunn, S. D. (1993b) Orientation of the ϵ subunit in *Escherichia coli* ATP synthase. *Arch. Biochem. Biophys.* **302**, 279-284.

Smith, J.B., and Sternweis, P.C. (1977) Purification of membrane attachment and inhibitory subunits of the proton translocating adenosine triphosphatase from *Escherichia coli. Biochemistry* **16**:306-311.

Sololon, K. A., and Brusilow, W.S.A. (1988) Effect of an *uncE* ribosome-binding site mutations on the synthesis and aseembly of the *Escherichia coli* proton-translocating ATPase. *J. Biol. Chem.* **263**, 5402-5407.

Steitz, J. A. (1969) Polypeptide chain initiation: nucleotide sequences of the three ribosome binding sites in bacteriophage R17 RNA. *Nature (London)* **224**, 957-964.

Sternweis, P.C. (1978) The ϵ subunit of *Escherichia coli* coupling factor 1 is required for its binding to the cytoplasmic membrane. *J. Biol. Chem.* **253**:3123-3128.

Sternweis, P.C., and Smith, J.B. (1980) Characterization of the Inhibitory (ϵ) subunit of the proton-translocating adenosine triphosphatase from *Escherichia coli. Biochemistry* **19**:526-531.

Tabor, S., and Richardson, C. C. (1985). A bacteriophage T7 RNA polymerase/ promoter system for controlled exclusive expression of specific genes. *Proc. Nat. Acad. Sci. USA* **82**, 1074-1078.

Takata, R., Izuhara, M. and Hori, K. (1989) Differential degradation of the *Escherichia coli* polynucleotide phosphorylase mRNA. *Nucleic Acids Res.* **17**, 7441-7451.

Tomcsányi, T. and Apirion, D. (1985) Processing enzyme ribonuclease E specifically cleaves RNA I: an inhibitor of primer formation in plasmid DNA synthesis. *J. Mol. Biol.* **185**, 713-720.

Vieira, J., and Messing, J. (1982) The pUC plasmids, an M13mp7-derived system for insertion mutagenesis and sequencing with synthetic universal primers. *Gene* **19**:259-268.

von Meyenburg, K., Jorgensen, B.B., and van Deurs, B. (1984) Physiological andmorphological effects of overproduction of membrane-bound ATP synthase in *Escherichia coli* K-12. *EMBO J* **3**: 1791-1797

Walker, J. E., Saraste, M., and Gay, N.J. (1984) The *Unc* operon. Nucleotide sequence, regulation and structure of ATP-synthase. *Biochim Biophys Acta* **768**: 164-200.

Walker, J.E., Fearnley, I.M., Todd, R.J. and Runswick, M.J. (1990) Structural aspects of proton-pumping ATPases. *Phil. Trans. R. Suc. Lonz. B.* **326**, 367-378.

Walker, J. E., Cozens, A. L., Dyer, M. R., Fearnly, I. M., Powell, S. J., Runswick, M. J. (1987) Genes for ATP synthases from bacteria, chloroplasts and mitochondria. *Bioenergetics: Structure and Function of energy transducing systems.* (eds. T. Ozawa and S. Papa) pp. 167-178, Japan Sci. Soc. Press, Tokyo/ Springer Verlag, Berlin.

Wikström, P. M., Lind, L. K., Berg, D. E., and Björk, G. R. (1992) Importance of mRNA folding and start codon accessibility in the expression of genes in a ribosomal protein operon of *Escherichia coli*. *J. Mol. Biol.* **224**, 949-966.

Woese, C. R., Winker, S., and Gutell, R. R. (1990) Architecture of ribosomal RNA: Constraints on the sequence of "tetra-loops". *Proc. Natl. Acad. Scie., U. S. A.* **87**, 8467-8471.

Yajnik, V., and Godson, G. N. (1993) Selective decay of *Escherichia coli dnaG* messanger RNA is initiated by RNase E. *J. Biol. Chem.* **268**, 13253-13260.

Yarchuk, O., Jacques, N., Guillerez, J., and Dreyfus, M. (1992) Interdependence of translation, transcription and mRNA degradation in the *lacZ* gene. *J. Mol. Biol.* **226**, 581-596.

Zuker, M., and Stiegler, P. (1981) Optimal computer folding of large RNA sequences using thermodynamics and auxiliary information. *Nucl. Acids. Res.* **9**, 133-148.

APPENDIX I : Nucleotide Sequence of uncD and uncC genes

Note: Bases are numbered according to Walker et al. (1984)
The uncD and uncC initiation codons are underlined

```
      5690        5700        5710        5720        5730        5740
       ↓           ↓           ↓           ↓           ↓           ↓
ATTTCGTAGAGGATTTAAGATGGCTACTGGAAAGATTGTCCAGGTAATCGGCGCCGTAGT
                    uncD

      5750        5760        5770        5780        5790        5800
       ↓           ↓           ↓           ↓           ↓           ↓
TGACGTCGAATTCCCTCAGGATGCCGTACCGCGCGTGTACGATGCTCTTGAGGTGCAAAA

      5810        5820        5830        5840        5850        5860
       ↓           ↓           ↓           ↓           ↓           ↓
TGGTAATGAGCGTCTGGTGCTGGAAGTTCAGCAGCAGCTCGGCGGCGGTATCGTACGTAC

      5870        5880        5890        5900        5910        5920
       ↓           ↓           ↓           ↓           ↓           ↓
CATCGCAATGCGTTCCTCCGACGGTCTGCGTCGCGGTCTGGATGTAAAAGACCTCGAACA

      5930        5940        5950        5960        5970        5980
       ↓           ↓           ↓           ↓           ↓           ↓
CCCGATTGAAGTCCCGGTAGGTAAAGCGACTCTGGGCCGTATCATGAACGTACTGGGTGA

      5990        6000        6010        6020        6030        6040
       ↓           ↓           ↓           ↓           ↓           ↓
ACCGGTCGACATGAAAGGCGAGATCGGTGAAGAAGAGCGTTGGGCGATTCACCGCGCAGC

      6050        6060        6070        6080        6090        6100
       ↓           ↓           ↓           ↓           ↓           ↓
ACCTTCCTACGAAGAGCTGTCAAACTCTCAGGAACTGCTGGAAACCGGTATCAAAGTTAT

      6110        6120        6130        6140        6150        6160
       ↓           ↓           ↓           ↓           ↓           ↓
CGACCTGATGTGTCCGTTCGCTAAGGGCGGTAAAGTTGGTCTGTTCGGTGGTGCGGGTGT

            6170        6180        6190        6200        6210        6220
             ↓           ↓           ↓           ↓           ↓           ↓
AGGTAAAACCGTAAACATGATGGAGCTCATTCGTAACATCGCGATCGAGCACTCCGGTTA

      6230        6240        6250        6260        6270        6280
       ↓           ↓           ↓           ↓           ↓           ↓
CTCTGTGTTTGCGGGCGTAGGTGAACGTACTCGTGAGGGTAACGACTTCTACCACGAAAT

      6290        6300        6310        6320        6330        6340
       ↓           ↓           ↓           ↓           ↓           ↓
GACCGACTCCAACGTTATCGACAAAGTATCCCTGGTGTATGGCCAGATGAACGAGCCGCC

      6350        6360        6370        6380        6390        6400
       ↓           ↓           ↓           ↓           ↓           ↓
GGGAAACCGTCTGCGCGTTCCTCTGACCGGTCTGACCATGGCTGAGAAATTCCGTGACGA

      6410        6420        6430        6440        6450        6460
       ↓           ↓           ↓           ↓           ↓           ↓
AGGTCGTGACGTTCTGCTGTTCGTTGACAACATCTATCGTTACACCCTGGCCGGTACGGA
```

```
      6470       6480       6490       6500       6510       6520
AGTATCCGCACTGCTGGGCCGTATGCCTTCAGCGGTAGGTTATCAGCCGACCCTGGCGGA

      6530       6540       6550       6560       6570       6580
AGAGATGGGCGTTCTGCAGGAACGTATCACCTCCACCAAAACTGGTTCTATCACCTCCGT

      6590       6600       6610       6620       6630       6640
ACAGGCAGTATACGTACCTGCGGATGACTTGACTGACCCGTCTCCGGCAACCACCTTTGC

      6650       6660       6670       6680       6690       6700
GCACCTTGACGCAACCGTGGTACTGAGCCGTCAGATCGCGTCTCTGGGTATCTACCCGGC

      6710       6720       6730       6740       6750       6760
CGTTGACCCGCTGGACTCCACCAGCCGTCAGCTGGACCCGCTGGTGGTTGGTCAGGAACA

      6770       6780       6790       6800       6810       6820
CTACGACACCGCGCGTGGCGTTCAGTCCATCCTGCAACGTTATCAGGAACTGAAAGACAT

      6830       6840       6850       6860       6870       6880
CATCGCCATCCTGGGTATGGATGAACTGTCTGAAGAAGACAAACTGGTGGTAGCGCGTGC

      6890       6900       6910       6920       6930       6940
TCGTAAGATCCAGCGCTTCCTGTCCCAGCCGTTCTTCGTGGCAGAAGTATTCACCGGTTC

      6950       6960       6970       6980       6990       7000
TCCGGGTAAATACGTCTCCCTGAAAGACACCATCCGTGGCTTTAAAGGCATCATGGAAGG

      7010       7020       7030       7040       7050       7060
CGAATACGATCACCTGCCGGAGCAGGCGTTCTACATGGTCGGTTCCATCGAAGAAGCTGT

      7070       7080       7090       7100       7110       7120
GGAAAAAGCCAAAAAACTTTAACGCCTTAATCGGAGGGTGATATGGCAATGACTTACCAC
                                        uncC

      7130       7140       7150       7160       7170       7180
CTGGACGTCGTCAGCGCAGAGCAACAAATGTTCTCTGGTCTGGTCGAGAAAATCCAGGTA

      7190       7200       7210       7220       7230       7240
ACGGGTAGCGAAGGTGAACTGGGGATCTACCCTGGCCACGCACCGCTGCTCACCGCCATT

      7250       7260       7270       7280       7290       7300
AAGCCTGGTATGATTCGCATCGTGAAACAGCACGGTCACGAAGAGTTTATCTATCTGTCT
```

```
        7310        7320        7330        7340        7350        7360
GGCGGCATTCTTGAAGTGCAGCCTGGCAACGTGACCGTTCTGGCCGACACCGCAATTCGC

        7370        7380        7390        7400        7410        7420
GGCCAGGATCTCGACGAAGCGCGAGCCATGGAAGCGAAACGTAAGGCTGAAGAGCACATT

        7430        7440        7450        7460        7470        7480
AGCAGCTCTCACGGCGACGTAGATTACGCTCAGGCGTCTGCGGTACTTGCCAAAGCGATC

        7490        7500        7510        7520        7530        7540
GCGCAGCTGCGCGTTATCGAGTTGACCAAAAAAGCGATGTAACACCGGCTTGAAAAGCAC

        7550        7560        7570        7580
AAAAGCCAGTCTGGAAACAGGCTGGCTTTTTTTTGCGCGT
```